Microwave-Assisted Pyrolysis for Biomass Recovery and Applications

PhD Thesis

Scarlett Allende Leiva (MSc)

August 2023

For the degree of Doctor of Philosophy

in the College of Science and Engineering

James Cook University.

Townsville.

Advisory panel: Mohan Jacob, Yang Liu, and Graham Brodie

ACKNOWLEDGEMENTS

I would like to acknowledge the support, supervision, and encouragement of my advisor panel members: Mohan Jacob, Yang Liu and Graham Brodie, as well as my research team colleagues for their engaging discussions, company and support.

I especially thank Mohan for his trust in my work and for allowing me to belong to his research group. His supervision was generous and supportive, always giving me the freedom to research and explore areas of my interest. Also, I am grateful to Yang Liu for the great assistance and training in the electrochemistry field.

I would like to thank Graham Brodie for the validation, resources, and supervision of optimising energy recovery experiments and reviewing and editing my work. Additionally, I am grateful to Paul Trayner, Wilmar Sugar Townsville, Australia for supplying the sugarcane bagasse biomass.

I acknowledge the financial support of the James Cook University Postgraduate Research Scholarship and Cooperative Research Centre for Developing Northern Australia top-up scholarship, which is part of the Australian Government's Cooperative Research Centre Program (CRCP).

Finally, I appreciate the care and strength my family and God gave throughout my PhD journey- Their unconditional love was my motivation to continue this path. Also, friends and colleagues for great discussions and time.

STATEMENT OF THE CONTRIBUTION OF OTHERS

Nature of Assistance	Contribution	Co-Contributors
Intellectual support	Editorial assistance, supervision, and project administration	The research journey of each chapter of this thesis was assisted and supervised by Prof. Mohan Jacob. Also, the work was supported by Prof Graham Brodie, Dr Yang Liu, and Assoc Prof Rabin Tuladhar.
	Fee offset.	The Australian government
Financial support	Stipend	James Cook University Postgraduate Research Scholarship Cooperative Research Centre for Developing Northern Australia, (CRCNA) top-up scholarship.
Data collection	Research Assistance	Collaboration of PhD students in the discussion of electrochemical data.

ABSTRACT

Agricultural waste disposal in landfills, depletion of fossil fuels, lack of energy sources and accelerated population growth have caused an urgent need to solve waste management, reduce environmental impacts, explore sustainable energy alternatives, and minimise dependence on non-renewable fuels. Bioenergy is a viable source of renewable energy that offers diverse conversion methods (combustion, gasification, pyrolysis, anaerobic digestion, and formation) and several useful products (ethanol, biodiesel, heat, electricity, char, etc.). However, selecting and exploring new technology for bioenergy generation is crucial to developing high by-product quality and value-added applications. Microwave pyrolysis as a biomass conversion method has attracted strong interest owing to quick biomass processing, the versatility in the use of feedstock, high energy efficiency and the diversity of by-product applications.

This work investigates the agro-industrial waste conversion for energy and sustainable applications using microwave-assisted pyrolysis. Four study approaches are included in this research spanning from the overview, yield optimisation, energy recovery and by-product applications. A technological review of the breakdown of agricultural biomass for energy application was carried out. This review focuses on bioenergy technologies, microwave principles, biomass nature analysis, yield and quality of by-products, by-product applications and microwave pyrolysis economic analysis. This investigation exhibited influencing factors that impact the quality and yield of the solid, liquid and gas by-products during the microwave pyrolysis of agricultural waste. Biomass nature (fibre composition, particle size, moisture content, ash content, etc.) and diverse combinations of operating pyrolysis conditions (microwave susceptor, reaction time and microwave power) were evaluated based on the yield, energy, and quality of by-products. It was found that biomass with high lignin content promotes the formation of solid material, and high cellulose and hemicellulose are favourable

for the generation of bio-oil and biogas. Feedstock with a high concentration of moisture content reported high bio-oil yield with a superior aqueous fraction in the functional groups, which affects its quality. The input power, treatment time, and type and quantity of microwave susceptor are critical for biochar and bio-oil production. High microwave power and high susceptor addition led to excess pyrolysis temperature, which generates temperatures beyond the optimal condition for solid and liquid production but induces syngas formation.

The subsequent phase of this investigation involved enhancing the energy efficiency of the microwave pyrolysis procedure applied to sugarcane bagasse biomass. The experimental procedure comprised exposing the feedstock to different combinations of microwave power, reaction time and microwave susceptor to optimise each by-product. The optimisation evaluated the yield and quality of biochar, bio-oil and biogas. Results showed that low power (1 kW), minimal microwave susceptor addition (10 %) and longer residence time (40 min) were favourable conditions for achieving a higher biochar yield due to the gradual thermal decomposition of the biomass. The optimal pyrolysis conditions for bio-oil production (25 wt%) were medium power of 2 kW, 30 mins and 10% susceptor addition. In contrast, high heating rates reached by high microwave power and susceptor generated secondary pyrolysis reactions that cause permanent gaseous formation (84 wt%), facilitating carbonization and reducing the biochar mass and bio-oil yield. Once the by-product was optimised, the high output energy (0.24 kWh) and global energy efficiency (13 %) were obtained.

Biochar-based electrodes are a sustainable alternative for the development of sensing materials from residues. Varied agricultural wastes were used as feedstocks for developing value-biochar products. The synthesis of nanostructured biochar-modified for the fabrication of electrochemical working electrodes has focused the attention of researchers due to provided advantages of fast, ultrasensitive, and selective determination of several analytes in different

research fields, e.g., environmental, food, water treatment, pharmaceutical and clinical analysis. However, preparing carbon material involves toxic chemicals, expensive materials (metal/ metal oxide), and time-consuming and complex synthetic steps. This work studied the fabrication of modified glassy carbon electrodes by using sugarcane bagasse (SCB) and pineapple peel as feedstock for paracetamol and nitrite detection by reducing the synthesis step and chemicals without affecting the electrochemical properties. The electrode generated from activated biochar pineapple peel ($ZnCl_2$ activated biochar/GCE) showed higher electron transfer kinetic properties (Rct=110 Ω) than the bare electrode (Rct=280 Ω) and achieved a limit of detection (LOD) of 0.97 µmol L^{-1} for $NaNO_2$ detection. The application of H_2SO_4 SCB-activated biochar on a GCE enhanced the paracetamol oxidation peak (from 6.2 µA to 17 µA) and electrocatalytic activity in the non-modified electrode. The electrochemical detection of paracetamol at SCB-activated biochar/GCE attained a limit of detection (LOD) of 2.5 µM. The findings demonstrated that traditional carbon materials could be replaced by modified biochar, which offers a sustainable alternative, reduced synthesis procedure, minimal chemical consumption, and high electrochemical sensor applicability.

TABLE OF CONTENTS

LIST OF TABLES

LIST OF FIGURES

NOMENCLATURE

(ε_r')	Dielectric constant
(ε')	Dielectric constant of the material
(ε_0)	Dielectric constant of free space
(ε_r'')	Dielectric loss factor
(ε'')	Dielectric loss of the material
(σ)	Conductivity of the material
(f)	Microwave frequency
$(\tan\delta e)$	Electric loss tangents
$(\tan\delta m)$	Magnetic loss tangents
(Q_g)	Heat generation per unit volume
(HR)	Heating rate of the material
(E)	Electric field
(H)	Magnetic field
(ρ_t)	Thermal conductivity
(C_p)	Specific heat
(ω, rad/s)	Angular frequency of the microwave field
(ε_o)	Permeability of free space
(κ")	Dielectric loss factor of the material
(τ)	Surface reflection coefficient of the material
(E_o, V/m)	Strength of the electromagnetic field at the surface of the material
(β)	Wave attenuation factor
(h, W/ m K)	Convective heat transfer coefficient at the surface of an object
(Ra_L)	Rayleigh number

(Pr)	Prandtl number
(k, W/m ºC)	Thermal conductivity of the fluid
(L, metres)	Length of the object being heated
(T_i, ºC)	Initial temperature of the material
(k_s, W/m ºC)	Thermal conductivity of the heated material
(α_s, m^2/s)	Thermal diffusivity of the heated material
(c, m/s)	Speed of light
(k')	Relative dielectric constant of the material

LIST OF PUBLICATIONS

In the development of this research the following journal publications were achieved:

- S. Allende, G. Brodie, and M. V. Jacob, "Breakdown of biomass for energy applications using microwave pyrolysis: A technological review," Environmental Research, vol. 226, p. 115619.

- S. Allende, G. Brodie, and M. V. Jacob. 2022. 'Energy recovery from sugarcane bagasse under varying microwave-assisted pyrolysis conditions', Bioresource Technology Reports, 20: 101283.

- S. Allende, Y. Liu, M. A. Zafar, and M. V. Jacob, "Nitrite sensor using activated biochar synthesised by microwave-assisted pyrolysis," Waste Disposal & Sustainable Energy, 2023/01/17 2023.

- S. Allende, Y. Liu, and M. V. Jacob, 'Electrochemical sensing of paracetamol based on sugarcane bagasse-activated biochar', in the journal Industrial Crops and Products, special issue: Lignocellulosic Biomass-derived Functional Materials (under review).

- S. Allende, Y. Liu, and M. V. Jacob, 'Sustainable Utilization of Food Waste: Microwave-Assisted Conversion into Graphene Oxide for Sustainable Sensor Applications' in the journal Materials Today Sustainability (under review).

CHAPTER 1

INTRODUCTION

1.1 Problem description

Waste management, lack of energy sources and greenhouse emissions represent significant concerns in the agricultural and energy sectors. The agricultural industry faces a continuous increase in waste generation associated with the fast-growing population (Koul et al., 2022). Biomass waste can be generated during the cultivation or processing of agro-industrial products, and its sub-classification consists of sugarcane bagasse, rice husk, de-oiled seed, fruit peel, etc. (Koul et al., 2022; Sinha et al., 2021). Agro-industrial waste produced globally is equivalent to 50 billion tonnes of oil, and around 23.7 million tonnes correspond to food residues generated daily (Allende et al., 2023b; Babu et al., 2022). The disposal of this waste into landfills involves a severe environmental issue due to greenhouse gas emissions (GHG) contributing to global warming (Babu et al., 2022; Sinha et al., 2021). The agricultural industry is responsible for producing ~ 19.9% of the total GHG, releasing carbon dioxide (CO_2), nitrous oxide (N_2O), and methane (CH_4) (Allende et al., 2022; Allende et al., 2023b; Babu et al., 2022). Around 25% of agricultural waste is burning, the rest of the waste management strategies are landfill, animal feed, composting, fertilizers, textile fibres, roof thatching, etc. (Babu et al., 2022; Koul et al., 2022). The proper utilisation of residues is beneficial to minimize the environmental impact, maximize the cost-effectiveness of management, and gain strategies for developing clean energy methods.

The gradual depletion of fossil fuels causes a serious issue for the dependence on energy resources, a crisis for industrial development, and a challenge for the energy sector (Babu et al., 2022; Gupta and Mondal, 2020; Moriarty, 2022). Hence, there is an urgent need to explore an eco-friendly and efficient technology to convert biomass waste into energy and value-added products. Bioenergy allows the conversion of biomass to energy by using two main mechanisms- biochemical and thermochemical processes. Biochemical conversion includes anaerobic digestion, alcoholic fermentation and photobiological hydrogen production, whose main products are biogas, bioethanol and biohydrogen (Lee et al., 2019). Processing biomass using the thermochemical method involves the generation of heat, electricity and fuels by the utilisation of production obtained from gasification (syngas- fuel cell, electricity), combustion (steam- turbine, heat/electricity), and pyrolysis (biochar, bio-oil and biogas) (Babu et al., 2022; Osman et al., 2021).

Pyrolysis technology comprises two subclassifications- conventional and microwave pyrolysis. The main difference between pyrolysis technologies is the heating method, microwave pyrolysis involves electromagnetic heating instead of convective (external fuel source), where the heated material is due to a volumetric absorption of electromagnetic energy (Ethaib et al., 2020; Santhoshkumar and Anand, 2019). Conventional pyrolysis transfers the heat by internal conduction from the environment (furnace/oven) to the material, but microwave pyrolysis transfers the energy internally from the hot spots in the material (Ethaib et al., 2020; Fodah et al., 2022). Depending on the dielectric properties of the feedstock is necessary the addition of a microwave susceptor to absorb the microwave energy and convert it into thermal energy, which is transferred to the biomass material (Suriapparao et al., 2021). Microwave pyrolysis has multiple benefits over other conversion methods, such as versatility for biomass processing, low waste pre-treatment requirement, superior distribution of the heating, rapid start-up and shutdown of system mechanism, higher heating rates, and better control of

parameters (microwave power, temperature, reaction time, etc.) over the target by-product (Allende et al., 2022; Singh et al., 2022; Suresh et al., 2021a).

The by-product properties and quality generated from microwave pyrolysis are associated with the nature of biomass, feedstock physicochemical properties, microwave system configuration, and pyrolysis operating conditions (Ethaib et al., 2020; Zhang et al., 2017c). The intrinsic properties of biomass, such as fibre composition, ultimate analysis, moisture, volatile matter, and ash content are vital to developing the quality and yield target by-product (Suresh et al., 2021a; Zhang et al., 2017c). Biomass with high lignin compound contributes to increased biochar production with high carbon content (energy value), and waste material with high volatile matter and moisture content is favourable for generating high bio-oil yield and biogas fraction (Amalina et al., 2022; Ge et al., 2021; Wu et al., 2023). The microwave system configuration normally comprises a chamber, microwave reactor, vacuum pump, nitrogen flow, condensers, power/ temperature controller, by-product collection points, and thermocouple (Wu et al., 2023; Zhou et al., 2018). The operating conditions can be adjusted depending on the applications and characteristics requested of the target by-products, considering the microwave susceptor addition ratio, input power, reaction time, nitrogen flow concentration, chamber shape, vacuum pressure, etc.

The correlation between the simultaneous optimisation of by-products and the biomass material and microwave operating conditions of agricultural waste has not been explored. These factors are essential for developing an appropriate by-product application. Biochar, bio-oil, and biogas have an optimised energy value and yield by using optimisation of a specific combination of microwave operating conditions, which allows obtaining high energy recovery. The use of the by-products is varied, e.g., bio-oil and biogas are used for electricity generation by applying engine/turbine or as fuel by converting liquid into biodiesel (Abdurrahman, 2020).

The study of biochar as a sustainable carbon material has gained interest due to the diversity of applications and environmental benefits- reduction of waste disposal and carbon sequestration potential. Biochar is an excellent alternative replacement for some carbon materials, like graphite, graphene oxide, etc (Allende et al., 2023b; Li et al., 2022f; Sant'Anna et al., 2020).

1.2 Research aims.

This research aims to evaluate the breakdown of agricultural waste using microwave pyrolysis for optimising energy recovery and study the application of biochar in recent advancements in electrochemical sensors. Mainly, the study includes the following objectives:

- Investigate the use of microwave-assisted pyrolysis as a conversion method for the processing of agricultural waste.
- Evaluate the influencing factors that affect the quality and yield of the solid, liquid and gas by-products during the microwave pyrolysis process.
- Optimisation of energy recovery from agricultural biomass under varying microwave-assisted pyrolysis conditions.
- Synthesis of carbon-rich material from the breakdown of diverse agricultural feedstocks and their application in the development of sustainable electrochemical sensors.

1.3 Thesis structure

Chapter 1: Introduction- Includes the description of the research background and its scopes. In addition, it introduces the aims of the project.

Chapter 2: Literature review- Consists of the research review about the breakdown of lignocellulosic biomass using microwave pyrolysis for energy recovery. The first part of the chapter considers the discussion about the different biomass conversion methods, including the study of microwave pyrolysis principles. The next objective of this work comprises evaluating the influencing factors that impact the yield and quality of biochar, bio-oil, and biogas. In this section, the yield, and the method of conventional and microwave pyrolysis were compared based on the yield, characterisation (quality) and energy value. The review also incorporates the applications of the by-products and economic analysis.

This chapter was published as S. Allende, G. Brodie, and M. V. Jacob, "Breakdown of biomass for energy applications using microwave pyrolysis: A technological review," Environmental Research, vol. 226, p. 115619.

Chapter 3: Energy recovery under varying microwave pyrolysis conditions- Involves the energy optimisation from the microwave pyrolysis of sugarcane bagasse under various operating conditions. The first stage of the research consists of the study of raw biomass physicochemical properties of sugarcane bagasse. The optimisation of biochar, bio-oil and biogas was based on a diverse combination of pyrolysis operating conditions. The quality and energy balance of the optimised by-products was investigated. Also, this work comprises the economic and carbon footprint analysis.

This chapter was published as Allende, Scarlett, Graham Brodie, and Mohan V. Jacob. 2022. 'Energy recovery from sugarcane bagasse under varying microwave-assisted pyrolysis conditions', Bioresource Technology Reports, 20: 101283.

Chapter 4: Paracetamol sensor using activated biochar- Investigates the synthesis of activated biomass-derived biochar as a metal-free sensor for paracetamol detection. The activated biochar was synthesized using sugarcane bagasse (SCB) as feedstock, which was exposed to a chemical activation (H_2SO_4) and post-thermochemical treatment achieved by microwave pyrolysis. The physicochemical properties of the carbon material were evaluated to use it as a biochar-based electrochemical sensor by drop casting in a glassy carbon electrode (GCE). The analytical performance of SCB-activated/GCE was investigated using the correlation of the current-time response to the analyte concentration. The properties of selectivity, stability and reproducibility were also studied.

This chapter is under review for being published as S. Allende, Y. Liu, and M. V. Jacob, 'Electrochemical sensing of paracetamol based on sugarcane bagasse-activated biochar', in the journal Industrial Crops and Products, special issue: Lignocellulosic Biomass-derived Functional Materials.

Chapter 5: Food waste biochar for electrochemical sensing of nitrite- Assess pyrolysed pineapple peel as a biochar-based sensor for nitrite detection. The study starts with synthesising and characterising $ZnCl_2$- activated biochar, e.g., ultimate analysis, BET surface area, Raman spectra, TGA and SEM/TEM. The modified glassy carbon electrode (GCE) was coated using active biochar from microwave pyrolysis by drop-casting technique. The electrochemical detection of nitrite on a modified electrode was evaluated using the current response to the nitrite addition ranging and limit of detection. Additionally, selectivity, stability, and reproducibility of $ZnCl_2$- activated biochar/GCE were investigated.

This chapter was published as S. Allende, Y. Liu, M. A. Zafar, and M. V. Jacob, "Nitrite sensor using activated biochar synthesised by microwave-assisted pyrolysis," Waste Disposal & Sustainable Energy, 2023/01/17 2023.

Chapter 6: Graphene oxide for high selective electrochemical detection of dopamine- Study the synthesis of a negatively charged carbon-based material obtained from the microwave pyrolysis conversion of banana peel (BP) waste into biochar-based graphene oxide (BBGO). The electrostatic interaction property of the material was assessed by its application on a modified carbon screen printed electrode (CSPE) for selective detection of dopamine (DA). The selectivity determination of dopamine was evaluated in the coexistence with interference molecules of ascorbic acid (AA) and uric acid (UA). The electrochemical analysis was carried out using electrochemical impedance spectra (EIS), cyclic voltammetry (CV), and differential pulse voltammetry (DPV).

This chapter is under review for being published by S. Allende, Y. Liu., M. A. Zafar, and M. V. Jacob, 'Sustainable Utilization of Food Waste: Microwave-Assisted Conversion into Graphene Oxide for Sustainable Sensor Applications' in the journal Materials Today Sustainability.

Chapter 7: Conclusion and recommendations- Reveals the highlights and discussion of the implications of this work, including suggestions for new research possibilities.

CHAPTER 2

2 LITERATURE REVIEW

Abstract

The agricultural industry faces a permanent increase in waste generation associated with the fast-growing population. Due to the environmental hazards, there is a paramount demand for generating electricity and value-added products from renewable sources. The selection of the conversion method is crucial to developing an eco-friendly, efficient, and economically viable energy application. This chapter investigates the influencing factors that affect the quality and yield of biochar, bio-oil, and biogas during the microwave pyrolysis process, evaluating the biomass nature and diverse combinations of operating conditions. The by-product yield depends on the intrinsic physicochemical properties of biomass. Feedstock with high lignin content is favourable for biochar production, and the breakdown of cellulose and hemicellulose leads to higher syngas formation. Biomass with high volatile matter concentration promotes the generation of bio-oil and biogas. The pyrolysis system's conditions of input power, microwave heating susceptor, vacuum, reaction temperature, and the processing chamber geometry were influence factors for optimising the energy recovery. Increased input power and microwave susceptor addition led to high heating rates, which were beneficial for biogas production, but the excess pyrolysis temperature induced a reduction of bio-oil yield.

Keywords: Biomass; Microwave pyrolysis; Energy; Biochar; Bio-oil; Biogas.

This chapter was published as S. Allende, G. Brodie, and M. V. Jacob, "Breakdown of biomass for energy applications using microwave pyrolysis: A technological review," Environmental Research, vol. 226, p. 115619.

2.1 Introduction.

Fossil fuel dependence, waste management, greenhouse emissions, and the disposal of several types of waste generated by individuals and industries are crucial issues in the electrical energy sector (Ferrari et al., 2022; Yu et al., 2022b). The conversion of waste into energy is of significant interest because it represents a sustainable and environmentally friendly way of managing waste and also, recovering the energy thereby contributing to the circular economy (Ferrari et al., 2022; Yu et al., 2022b; Zhao et al., 2022). Renewable energy development is vital to decrease greenhouse gas emissions and increase the reliability of the energy system and energy supply (Sun et al., 2022a). Microwave pyrolysis is an attractive method of bioenergy production that allows the replacement of fossil fuels in favour of clean energy applications, like fuel production (biodiesel), heat, electricity, chemicals and other commodities from biowaste materials (Siddique et al., 2022; Sun et al., 2022a). Lignocellulosic biomass used in bioenergy production is diverse (Yu et al., 2022b). These include agricultural waste, energy crops, forestry products, urban waste and industrial residue (Cai et al., 2021b; Duarah et al., 2022). Thus, bioenergy offers abundant feedstock to produce liquid, gas and solid fuels. Unlike other types of renewable energy, the bioenergy source supply is continuous (biomass) and hence is not affected by the intermittency of resources such as solar and wind energy (Li et al., 2022b; Liu et al., 2022).

Biomass waste can be converted into biofuels by two conversion processes, which are thermochemical and biochemical. These bioenergy methods have substantial dissimilarities associated with biomass feedstock, by-products, and applications (Shahbeig and Nosrati, 2020; Varjani et al., 2022). Combustion, gasification, and conventional or microwave pyrolysis are thermochemical conversion methods (Karpagam et al., 2021; Von Cossel et al., 2021). Biochemical conversion involves anaerobic digestion and microbial fermentation (García-Depraect et al., 2022; Karpagam et al., 2021). A biochemical process requires biomass pretreatment and is selective (microbes, enzymes and chemicals). However, thermochemical conversion is possible for practically any type of biomass without pretreatment (García-Depraect et al., 2022; Karpagam et al., 2021; Zhao et al., 2022). The thermochemical process has less reaction time and higher productivity than the biochemical technique due to its limited by-products (biological conversion) and long reaction rate (Sun et al., 2022a; Yu et al., 2022b). Figure 2.1 shows different energy conversion methods, where combustion conversion implies burning biomass in the presence of oxygen, intending to generate heat and power.

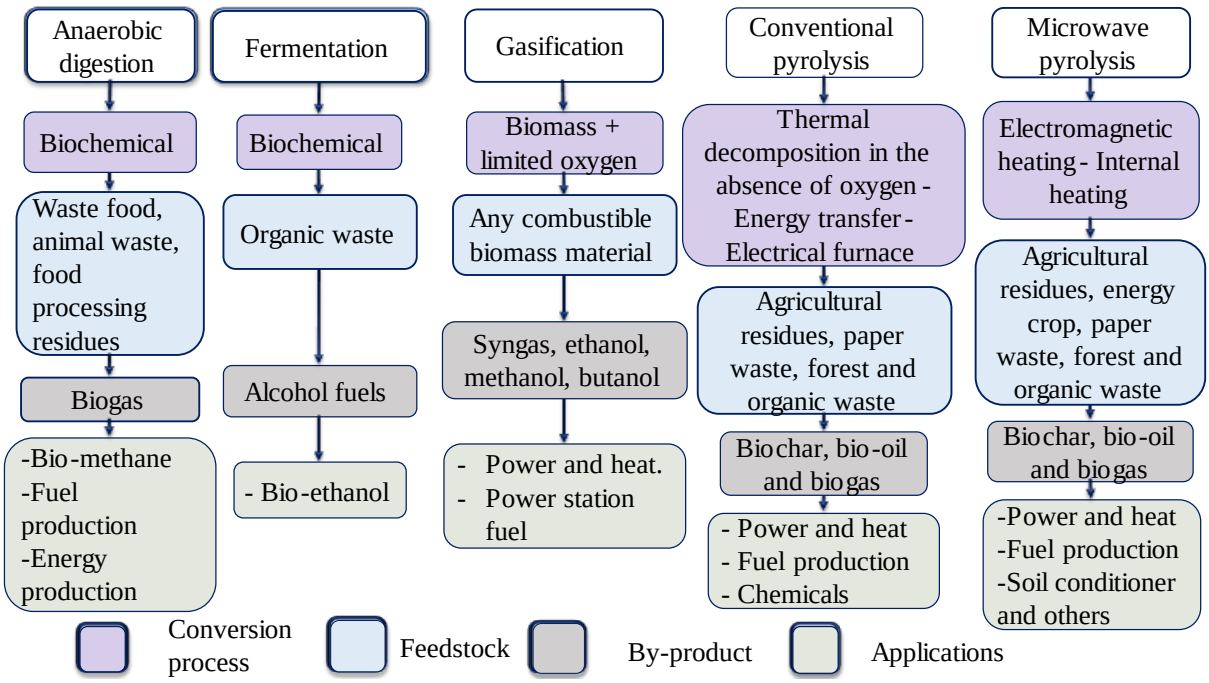

Figure 2.1: Biomass conversion process by bioenergy technology (Anca-Couce et al., 2021; Fodah et al., 2022; Hasan et al., 2021; Liu et al., 2022; Sun et al., 2022a).

Anaerobic digestion implicates microbial decomposition of organic biomass in an oxygen-free environment by applying an optimal temperature for the microorganism activity (Dhanya et al., 2020a; Liu et al., 2022; Zhu et al., 2021). The product obtained from the conversion process is mainly biogas (methane, carbon dioxide, water vapour and lesser concentration of hydrogen sulphide and hydrogen) (Dhanya et al., 2020a; Yu et al., 2022b). Fermentation is also a biochemical conversion process in the absence of oxygen, in which organic biomass is broken down by the action of enzymes (Pishvaee et al., 2021; Yu et al., 2022b). Biomass decomposition by fermentation involves a long process time, where the first step is sucrose conversion into fructose and glucose by hydrolysis enzymes (Ghosh et al., 2020; Yu et al., 2022b). Products obtained from the conversion process are alcohol fuels, such as ethanol and lactic acid (Gautam et al., 2019; Pishvaee et al., 2021).

The gasification method involves a high-temperature process that allows converting organic biomass into mainly syngas generation in a controlled oxygen environment for energy applications (Yu et al., 2022b; Zhang et al., 2019b). Conventional pyrolysis involves a convective heating method that occurs in the absence of an oxidizing agent, where the heating is transferred into the biomass through internal conduction from the surface of the biomass (Li et al., 2022e). The pyrolysis range temperature is between 400 ºC and 1200 ºC (Rajendran et al., 2019). Conventional heating is conducted using a batch furnace, auger reaction chamber or fixed bed reactor. In contrast, microwave pyrolysis technology is achieved by the thermal decomposition of biomass exposed to electromagnetic heating in the absence of oxygen (Hadiya et al., 2022; Wang et al., 2020d). The heating method is material-dependent (feedstock dielectric properties), in which microwave energy is transferred by the microwave susceptors (biochar or activated carbon) that absorb the microwave radiation and start to burn the biomass (Prathiba et al., 2018; Toscano Miranda et al., 2021). There are beneficial factors associated with the conversion process compared to conventional pyrolysis. For example, microwave heating provides quick start-up, higher heating rates and an efficient heating

distribution (Li et al., 2022e; Toscano Miranda et al., 2021; Zhang et al., 2022d). The microwave pyrolysis method is a promising alternative to energy generation due to its high heating efficiency, which can lead to higher yield and quality of the by-products, contributing to increased energy recovery efficiency of the conversion process (Hadiya et al., 2022; Li et al., 2022e; Zhang et al., 2022d). Consequently, the type of conversion method depends on the nature of the biomass, energy applications (the kind of energy obtained), economic factors, environmental standards, operating conditions of the conversion system, and others (Shahbeig and Nosrati, 2020; Toscano Miranda et al., 2021; Varjani et al., 2022).

2.2 Microwave pyrolysis technology.

The pyrolysis concept comprises the thermal degradation of the raw waste in inert atmospheric conditions (absence of oxygen) to obtain gas, liquid, and solid products (Foong et al., 2020; Ge et al., 2021; Rajendran et al., 2021). Microwave pyrolysis technology can include three stages. The first stage involves the evaporation of free moisture existing in the biomass. The second phase comprises dehydration, demethylation, and decarboxylation reactions related to the depolymerization and fragmentation process of lignocellulosic compounds. The final stage is secondary reactions associated with depolymerization and recondensation (Foong et al., 2020; Ge et al., 2021).

The pyrolysis process has three relevant factors associated with the pyrolysis operating settings and biomass conditions that depend on the residence time, heating rate, temperature, and particle size. The particle size of the sample impacts the intensity and distribution of the microwave irradiation, affecting the uniformity of the dielectric heating on the biomass. Small particle size is favourable to increasing the gaseous phase products (Li et al., 2022d; Suresh et al., 2021b). The slow pyrolysis process applies a low operating temperature and long solid

residence time (between 5 and 30 min) (Ethaib et al., 2020; Robinson et al., 2015; Suresh et al., 2021b; Yaning Zhang, 2017; Zhang et al., 2017a). These conditions produce limited bio-oil quality. Fast pyrolysis is commonly used for liquid fuel production due to the high heating rate and low solid residence time (Tomczyk et al., 2020a; Yaning Zhang, 2017). Furthermore, flash technology produces lower thermal stability and oil corrosiveness because of the short residence time and elevated heating rate and temperature (Suresh et al., 2021b; Yaning Zhang, 2017). The detail of the operating ranges is shown in Table 2.1.

Table 2.1. Operating parameters by pyrolysis process (Ethaib et al., 2020; Foong et al., 2020; Hasan et al., 2021; Kung et al., 2022).

Pyrolysis classification	Residence time (s)	Heating rate (ºK/s)	Particle size (mm)	Temperature (ºK)
Slow	450-550	0.1-1	5-50	550-950
Fast	0.5-10	10-200	<1	850-1250
Flash	<0.5	>1000	<0.2	1050-1300

Diverse studies reported the use of microwave pyrolysis for processing multiple types of waste materials. The configuration of the microwave system depends on biomass conversion, by-product target and energy application. Some work reveals the use of plastic and triglycerides as feedstock for maximising bio-oil production, considering a series of columns and condensers (Wan Mahari et al., 2022). Other research established the conversion of food waste into activated biochar by using microwave heating and CO_2 activation (Yek et al., 2020).

2.2.1 Microwave pyrolysis principles.

Microwave heating is a form of electromagnetic heating, involving the interaction of electromagnetic waves with ionic and dipolar molecules (Ge et al., 2021; Siddique et al., 2022; Yu et al., 2022a). Therefore, the heat is generated within the material rather than external to

the heated object, which is the opposite of conventional heating. Commercial microwave systems commonly operate at frequencies of 915 MHz and 2.45 GHz (Lam and Chase, 2012). Nevertheless, microwave heating requires an external microwave energy source to transfer energy to the content through a surface (Ethaib et al., 2020; Ge et al., 2021; Hadiya et al., 2022). Atomistic dynamic represents the interactions between microwave heating and the different materials (molecules) given by the components of electric and magnetic fields (electromagnetic waves). The heat is applied to the material producing either the translational motion of molecules or the vibration of lattice (phonons). These phonons are in a higher energy state (high-frequency motions) than the surrounding magnetic system, so there is an exchange of energy with the magnetic system— then magnons are excited with the use of high-frequency microwaves. The microwave's behaviour depends on different loss mechanisms, e.g., electric, conduction, hysteresis, and resonance. These mechanisms are subjected to material, microstructure, frequency, and temperature variables (Mishra and Sharma, 2016; Yoshikawa, 2020).

Microwaves have a wavelength range between 10^{-3} and 1 m and photon energy between 1.2 μeV and 1.2 meV. Microwaves are electromagnetic waves with perpendicular electric and magnetic fields, considering a frequency from 300 MHz to 300 GHz (Bartoli et al., 2019; Zamorano Ulloa et al., 2019). Microwave heating comprises two types of interactions between the material and the radiation. The most common interaction involves ion and dipole displacement by the wave's electric field; however, in some ferric materials, the wave magnetic field can interact with magnetic domains or induce eddy currents in the material. The most common interaction is with the electric field (Ge et al., 2021; Hadiya et al., 2022).

To fully understand the behaviour of feedstock material under microwave pyrolysis is crucial to study the volumetric absorption of electromagnetic energy in the heated material. The dissipated power in the feedstock reveals the main difference between conventional and microwave pyrolysis, which is to determine the heating profile (electromagnetic penetration depth) of the feedstock. Equations 1, 2, 3 and 4 (Bartoli et al., 2019) explain the interaction of electric and magnetic fields. Specifically, the relative dielectric constant (ε_r') associated with the dielectric constant of the material (ε') and the dielectric constant of free space (ε_0). The dielectric loss factor (ε_r'') is linked to the dielectric loss of the material (ε''), the conductivity of the material (σ), and the microwave frequency (f). The relative magnetic permittivity (μ_r') is the ratio of the magnetic permeability properties of the material (μ') and the magnetic permeability of the void (μ_o). The magnetic loss (μ_r'') comprises additional factors like the magnetic loss of the material (μ'') (Bartoli et al., 2019).

$$\varepsilon_r' = \varepsilon'/\varepsilon_0 \quad (1)$$

$$\varepsilon_r'' = (\varepsilon''/\varepsilon_o) + \left(\frac{\sigma}{2\pi f \varepsilon_o}\right) \quad (2)$$

$$\mu_r' = \mu'/\mu_o \quad (3)$$

$$\mu_r'' = (\mu'' + \mu_o) + \left(\frac{\sigma}{2\pi f \mu_o}\right) \quad (4)$$

Equations *5* (Bartoli et al., 2019) and *6* (Bartoli et al., 2019) describe the electric ($\tan\delta e$) and magnetic loss tangents ($\tan\delta m$), both of which represent absorption of the electromagnetic energy. Also, Equations *7* (Bartoli et al., 2019) and *8* (Bartoli et al., 2019) describe heat generation per unit volume (Q_g) and the heating rate of the material (HR), respectively, as the absorbed energy is converted to internal kinetic energy (i.e., heat) in the material. The electric field (E) and magnetic field (H), which are the mutually perpendicular fields of electromagnetic

radiation, are related. Furthermore, thermal conductivity (ρ_t) and specific heat (C_p) of the material are related to its heating rate calculation.

$$\tan \delta e = (\varepsilon''_r / \varepsilon'_r) \quad (5)$$

$$\tan \delta m = (\mu''_r / \mu'_r) \quad (6)$$

$$Q_g = \pi f \varepsilon'_o \varepsilon''_r |E|^2 + \pi f \mu'_o \mu''_r |H|^2 \quad (7)$$

$$HR = Q_g / \rho_t C_p \quad (8)$$

Electromagnetic heating depends on volumetric heating conditions. The dissipated microwave power in the material is an influencer of the thermal diffusion in the heated material (Brodie, 2008; Zamorano Ulloa et al., 2019). Equation *9* describes the involved factors in dissipated microwave power (Brodie, 2008). The factors associated with the dissipated power are; the angular frequency of the microwave field (ω, rad/s), the permeability of free space (ε_o), the dielectric loss factor of the material (κ"), the surface reflection coefficient of the material (τ), the strength of the electromagnetic field at the surface of the material (E_o, V/m), and the wave attenuation factor (β) (Brodie, 2008).

$$q = \frac{\omega \varepsilon_o \kappa'' \tau^2 E_o^2}{2} e^{-2\beta x} \quad (9)$$

The heat from the object, which interacts with the electromagnetic wave, will also be transferred to the surrounding environment by convection. The convective heat transfer coefficient at the surface of an object (h, W/ m K) is described by Equation 10 (Tomar, 2019; Welty.; et al., 2007). The convective heat transfer calculation involves; the Rayleigh number (Ra_L), Prandtl number (Pr), the thermal conductivity of the fluid (k, W/m ºC), and the characteristic length of the object being heated (L, metres) (Welty.; et al., 2007).

$$h = \frac{k}{L}\left\{0.825 + \frac{0.387\, Ra_L^{1/6}}{\left[1+\left(\frac{0.492}{Pr}\right)^{9/16}\right]^{8/27}}\right\}^2 \quad (10)$$

The temperature generated inside a semi-infinite material or a material that is many times larger than the penetration depth of the wave due to microwave heating can be calculated by Equation *12* (Brodie, 2008). The associated factors are the initial temperature of the material (T_i, ºC), distance from the surface into the core of the material (x, meters), the thermal conductivity of the heated material (k_s, W/m ºC), thermal diffusivity of the heated material (α_s, m^2/s), and heating time (t, seconds). The propagation factor is described in Equation *11* (Brodie, 2008; J. Tang, 2009), which includes the speed of light (c, m/s) and the relative dielectric constant of the material (k').

$$\beta = \frac{\omega}{c}\sqrt{\frac{\kappa'}{2}\left[\sqrt{1+\left(\frac{\kappa''}{\kappa'}\right)^2}-1\right]} \quad (11)$$

$$T = \frac{\omega \varepsilon_o \kappa'' \tau^2 E_o^2}{8 k_s \beta^2}\left(e^{4\alpha_s \beta^2 t}-1\right)\left[e^{-2\beta x}+\left(\frac{h}{k_s}+2\beta\right)x \cdot e^{\frac{-x^2}{4\alpha_s t}}\right]+T_i \quad (12)$$

2.2.2 Difference between conventional and microwave pyrolysis.

The difference between conventional and microwave pyrolysis lies in the heating method. Microwave heating is produced from internal sources, meaning that the heat is generated within the biomass, while conventional heating is from the external environment (Ethaib et al., 2020; Li et al., 2022e; Yu et al., 2022a). Figure 2.2 illustrates the heating mechanism of both technologies. Microwave heating transfers energy, through the interaction of the molecules (agitating dipolar molecules) within the biomass, in a much shorter reaction time than conventional heating (Yu et al., 2022a; Zhang et al., 2022b).

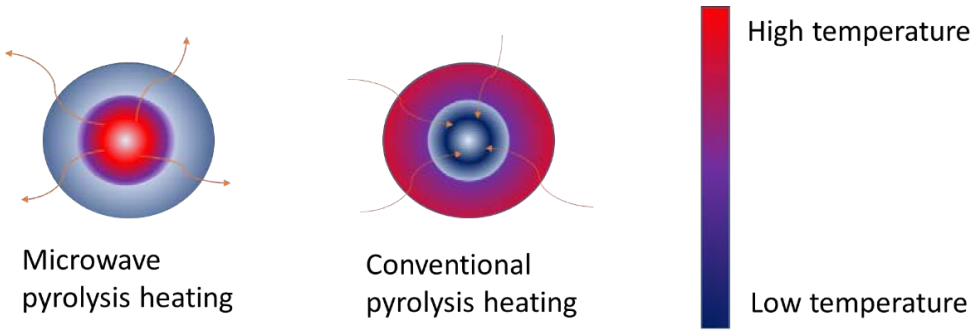

Figure 2.2. Comparison between heating mechanisms of microwave and conventional pyrolysis.

The electromagnetic energy is converted into heat by applying diverse microwave susceptors that absorb the microwave radiation and heat the biomass (Li et al., 2022e; Siddique et al., 2022). Another reason for adding microwave susceptor into the biomass is due to the low dielectric characteristics of the biomass feedstock (i.e., the dry biomass is relatively transparent to microwave radiation), which does not produce a heating effect by itself. Carbon material or water, which has much higher dielectric loss than dry biomass, can be added to the biomass to transform the microwave energy into heat (Ethaib et al., 2020; Li et al., 2022e; Nhuchhen et al., 2018; Siddique et al., 2022).

The advantages of microwave pyrolysis consist of the transfer of heat energy within the bulk of the material instead of heat transfer from outside to inside and the wide range of biomass materials that can be used (i.e., versatility in biomass processing) (Czajczyńska et al., 2017; Shukla et al., 2019; Yaning Zhang, 2017). For example, feedstocks can include agricultural biomass, plastics, tyre residues, and any other type of municipal solid waste. The precise and controlled heating method leads to the rapid and efficient start-up of the microwave system (Hadiya et al., 2022; Wu et al., 2022; Zhang et al., 2020). Microwave pyrolysis has instantaneous volumetric heating and uniform distribution in the energetic coupling. Subsequently, the microwave mechanism provides efficiency in the heating process, saving time, providing better heating distribution and controlling overheating (Hadiya et al., 2022; Siddique et al., 2022; Wu et al., 2022). Figure 2.3 shows a comparison of the pyrolysis technologies.

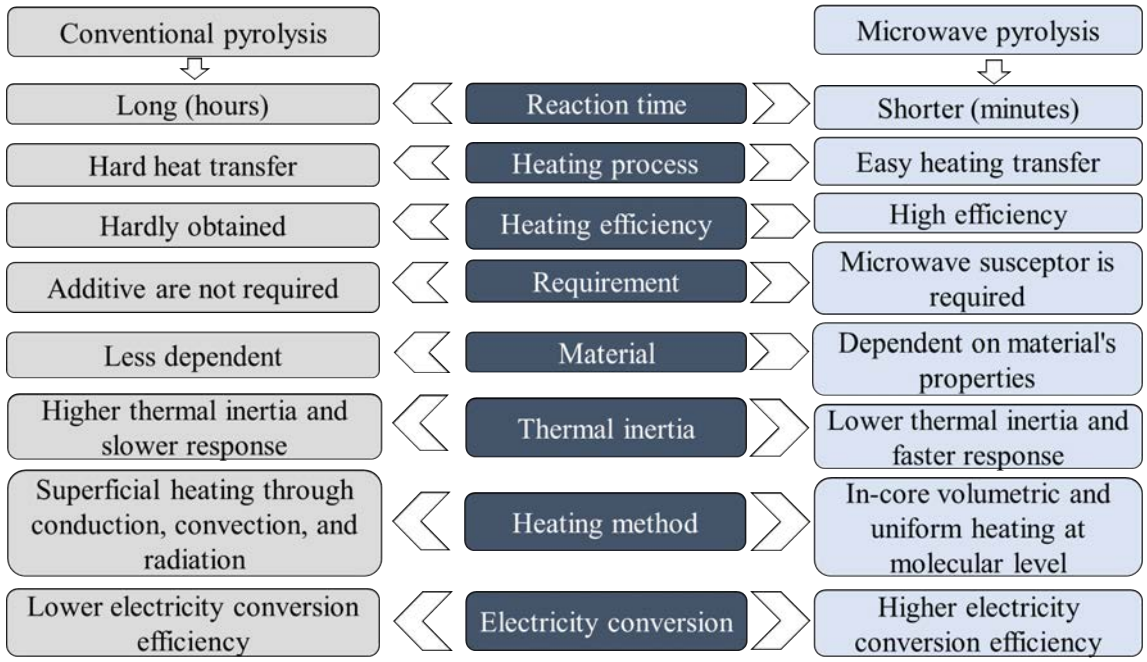

Figure 2.3. Difference between conventional and microwave pyrolysis technologies (Siddique et al., 2022; Toscano Miranda et al., 2021; Yaning Zhang, 2017; Zi et al., 2019a).

Microwave pyrolysis consists of dielectric heating, in which the absorption of microwave irradiation produces the migration and rotation of ionic and dipolar species, respectively. Then, the mixture of a microwave susceptor with a high dielectric loss factor into the biomass allows for improved heating rates and pyrolysis temperatures (Ellison et al., 2017; Hadiya et al., 2022; Nhuchhen et al., 2018; Yaning Zhang, 2017). Table 2.2 shows the dielectric properties of different microwave susceptors. Carbonaceous materials, like carbon, graphite and SiC, are the most common microwave susceptors used (Ellison et al., 2017; Zhang et al., 2020). The ratio of the microwave susceptor to raw feed stock is a relevant factor in terms of by-product yield. For instance, adding a higher microwave susceptor ratio can increase bio-oil production. But at the later stage of pyrolysis, rapid excess temperature leads to secondary reactions of the liquid products to form permanent gaseous products (Nhuchhen et al., 2018; Yaning Zhang, 2017).

Table 2.2. Dielectric loss tangent of diverse microwave susceptor materials (Ellison et al., 2017; Yaning Zhang, 2017; Zhang et al., 2017a; Zhang et al., 2020).

Material	**tanδ**
Water	0.15
SiC	0.37-1.05
Activated carbon	0.07-0.9
Biochar	0.2-1.04
Graphite	0.03-0.17
Carbon	0.28-0.38
Glycerol-water	0.3
Ethylene glycol	1

2.3 Biomass feedstock classification

Cellulose, hemicellulose and lignin are the three main components of biomass. The common term used to identify these three constituents is lignocellulosic (S.Bharathiraja et al., 2017). Cellulose has a crystalline structure and a molecular formula of $(C_6H_{12}O_6)n$ and exhibits exceptional resistance to acids and alkalis, but hemicellulose and lignin are amorphous

(Fermanelli et al., 2020). The lignin component comprises units of phenylpropane and its derivatives, which are bonded 3-dimensionally (Tawaf Ali et al., 2022). The hemicellulose interaction in the biomass is covalently bonded (ester bond) (Fermanelli et al., 2020). In the microwave pyrolysis process, the fibre constituents have different thermochemical stability. For instance, hemicellulose breakdown is faster (from 200°C to 300°C) than cellulose (from 300°C to 400°C). Nevertheless, lignin is the most heat-resistant due to its gradual decomposition (from 200 °C to 500 °C) (Fermanelli et al., 2020; Ge et al., 2021). In microwave pyrolysis, the thermochemical stability can also depend on the microwave power levels. For example, low power will produce a minor thermal degradation of the lignin component, obtaining biochar with a high heating value (Huang et al., 2016b; Tomczyk et al., 2020a).

Biomass fibre composition varies depending on its nature. The biomass components like lignin, cellulose, and hemicellulose are directly related to the pyrolysis by-product yield (Lin et al., 2015). For example, lignin and hemicellulose influence the cellulose characteristics during the pyrolysis conversion process but not vice versa. Mostly, bio-oil is obtained from the cellulose component, while biochar is derived from lignin (Burhenne et al., 2013; Lin et al., 2015; Tomczyk et al., 2020a). Furthermore, lignin content significantly impacts the carbonization and biochar properties due to its increased carbon and ash content (Tomczyk et al., 2020a).

The heating value of biochar is susceptible to the thermal decomposition of lignocellulosic compounds. The heating value of cellulose and hemicellulose is lower than lignin. Therefore, the gradual thermal breakdown of the lignin compound is beneficial for increasing the heating value of biochar (Chen et al., 2021; Ge et al., 2021; Li et al., 2016). Subjecting biomass with high lignin to pyrolysis technologies can improve bio-oil quality (heating value) due to the high heating value of the lignin compound and its steady thermal decomposition. However, there is an increase in its molecular weight and viscosity (Ge et al., 2021; Kan et al., 2016). Table 2.3

shows a compilation of the fibre composition of different biomass feedstocks. Cotton and banana peel has the highest cellulose (82.7%) and hemicellulose content (48.2%). The cellulose percentage suggests that paper is a suitable feedstock to produce a high bio-oil yield. In contrast, walnut shells have 52.3% lignin, which has the potential to generate a higher biochar yield.

Table 2.3. Fibre composition ranges of diverse lignocellulosic biomass.

	Lignin (%)	**Cellulose (%)**	**Hemicellulose (%)**	**Reference**
Olive husk	48.4	24	23.6	(Jahirul et al., 2012)
Tea waste	40	30.2	19.9	(Jahirul et al., 2012)
Walnut shell	52.3	25.6	22.7	(Jahirul et al., 2012)
Almond shell	20.4	50.7	28.9	(Jahirul et al., 2012)
Sunflower shell	17	48.4	34.6	(Jahirul et al., 2012)
Nutshell	35	27.5	27.5	(Jahirul et al., 2012)
Sugarcane bagasse	24.353	55.6	23.9	(Jayaprakash et al., 2022)
Pineapple leaf	5.35	70.55	18.73	(Jayaprakash et al., 2022)
Banana peel	5.55	60.25	48.2	(Jayaprakash et al., 2022)
Corncob	21	28	39	(Nozieana et al., 2021)
Rice husk	23	44	19	(Senthilkumar et al., 2021)
Coconut coir	41.23	36.62	0.15	(Dungani et al., 2015)
Rice straw	12.65	28.42	23.22	(Dungani et al., 2015)
Oil palm	19	65	-	(Hao et al., 2018)
Cotton	-	82.7	5.7	(Hao et al., 2018)
Kenaf	21.2	53.4	33.9	(Hao et al., 2018)
Bamboo	11.9	53.1	35	(Shi et al., 2020b)
Gumwood	14.4	62.4	23.2	(Shi et al., 2020b)
Pine	11.2	59.1	29.7	(Shi et al., 2020b)
Rosewood	24.1	62.9	13	(Shi et al., 2020b)

2.3.1 Biomass raw material properties

Usually, raw biomass needs preparation to be used in pyrolysis technology. The biomass's mechanical (physical) pre-analysis includes moisture content and particle size (Bu et al., 2016; Yaning Zhang, 2017). This latter variable involves cutting and grinding the feedstock until the required particle size is obtained; for example, for sugarcane bagasse, the required size of between 0.12 and 0.5 mm (Lin and Chen, 2015). The calculation of the water content biomass is another influencer factor on the yield and quality of the by-products (Ethaib et al., 2020; Ge et al., 2021; Li et al., 2022d). The following points explain the physicochemical parameters of the biomass.

2.3.2 Content of moisture and ash on the biomass

Moisture content is a vital property of biomass, upon which its heating value depends. The standard method for determining moisture involves heating a 1 gm biomass sample in a hot air oven at 110°C. The moisture content of the biomass can be calculated using Equation 13 (Basu, 2010).

$$\text{Moisture content } (\%\ \text{M}) = \frac{\text{w1}-\text{w2}}{\text{w3}} * 100 \quad (13)$$

$w1$: $Weight\ of\ the\ crucible\ \&\ the\ air-dried\ sample\ (g)$

$w2$: $Weight\ of\ the\ crucible\ \&\ oven\ dried\ sample\ (g)$

$w3$: $Weight\ of\ the\ air-dried\ sample\ (g)$

Once the moisture content is obtained, the ash percentage can be estimated by heating the oven-dried product at 575 °C until it attains constant weight (usually over 180 minutes). This value is the amount of inorganic material in the sample (Sluiter et al., 2008). In most cases, the weight of the residue represents the ash content of the biomass (Basu, 2010; Sluiter et al., 2008):

$$\text{Ash content (wt\%A)} = \frac{\text{Ash mass}}{\text{Initial mass}} * 100 \quad (14)$$

2.3.3 Volatile matter, fixed carbon, and high heating value

The high heating value (HHV) of the raw biomass is calculated based on the elemental content, such as carbon (C), hydrogen (H), and oxygen (O*). The O* value includes the rest of the elements, such as sulphur and nitrogen. The HHV represents the heat released at the end of the combustion process when water vapour is condensed (Sheng and Azevedo, 2005). Moreover, the low heating value (LHV) implies the formation of gaseous water during combustion (elimination of condensation heat of water) (Özyuğuran et al., 2018). Equations *17* (Sheng and Azevedo, 2005) and *18* (Özyuğuran et al., 2018) estimate the HHV (with more than 90% predictions) and LHV.

$$\text{HHV}\left(\frac{\text{MJ}}{\text{kg}}\right) = -1.3675 + 0.3137 * \text{C} + 0.7009 * \text{H} + 0.0318 * \text{O}^{*} \quad (15)$$

$$\text{LHV}\left(\frac{\text{MJ}}{\text{kg}}\right) = \text{HHV} - \left[\frac{18.015 * \text{H}}{2} + \%\text{Moisture}\right] * 5.85 \quad (16)$$

2.4 Physical and chemical classification of the biomass

The physical and chemical behaviour of the biomass feedstock depends on the previously discussed variables, such as fibre composition, volatile matter, the content of ash and moisture, etcetera (Ge et al., 2021; Li et al., 2022d). Notably, it is possible to get a higher biochar yield in a pyrolysis process when the biomass composition is high in lignin content due to the increased heating value, reaction temperature, and pollutants associated with the lignin presence (Ge et al., 2021; Su et al., 2022a). At the same time, influencing factors linked to the residue conditions can affect biomass product yield. These include density (kg/m^3), volatile matter (%), moisture, and ash content (%). For example, high fixed carbon represents a higher biochar yield with a minor portion of hydrogen, oxygen, nitrogen, and sulphur after subtracting the volatile matter, moisture and ash content in the biochar residue (Chen et al., 2015; K.Sarkar, 2015). Similarly, the volatile matter content is a vital parameter for combustion processes, producing high quantities of bio-oil and syngas during pyrolysis (Jahirul et al., 2012; Mierzwa-Hersztek et al., 2019)— the details are described in Figure 2.4.

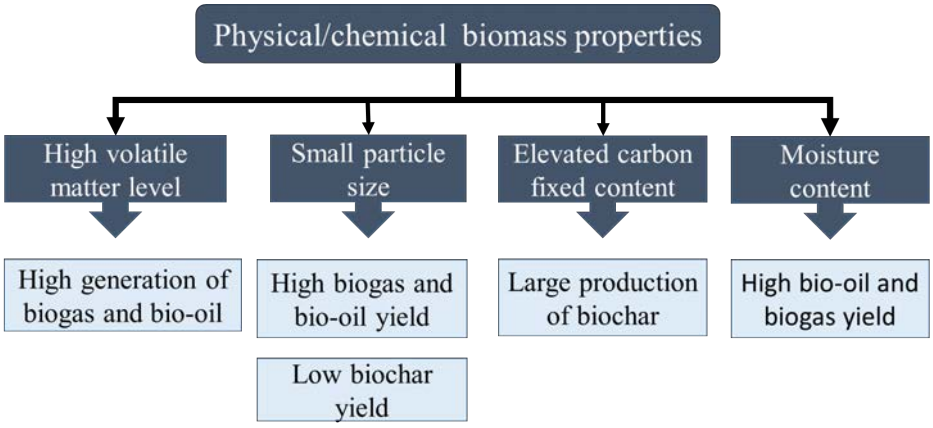

Figure 2.4. Factors influencing biomass product yield and generation (Ethaib et al., 2020; Ge et al., 2021; Leng et al., 2021; Su et al., 2022a; Yaning Zhang, 2017).

The yield and quality of the by-products are significantly affected by the moisture content of the raw biomass because of the presence of organic compounds. The water content in biomass exists in three forms; water vapour, bound water and a free liquid state (Li et al.,

2022d; Tomczyk et al., 2020a; Yaning Zhang, 2017). Biomass with a high moisture presence decreases the biochar formation but increases the bio-oil yield. Low water content is the optimal condition in biochar production, thereby heat energy and treatment time required during the pyrolysis process are less (Li et al., 2022d; Tomczyk et al., 2020a; Tripathi et al., 2016). High moisture in biomass produces a bio-oil with a higher aqueous fraction, lower viscosity and heating value (Ethaib et al., 2020; Yaning Zhang, 2017). On the other hand, since the water has high dielectric properties (high loss tangent factor, tanδ), dry lignocellulosic biomass requires a high percentage of microwave susceptor addition to absorbing the microwave energy due to its low electromagnetic absorbing properties (Supramono et al., 2015; Wu et al., 2019; Yaning Zhang, 2017; Zhang et al., 2017a).

The moisture in bio-oil comes from two sources; i) water in the biomass or ii) dehydration reactions generated during the microwave pyrolysis process. The water content of the bio-oil impacts the quality and yield of the bio-oil (Zhang et al., 2017b). High moisture content influences the heat transfer distribution during the conversion process. Moreover, water produces large quantities of condensate water in the liquid phase, generating a higher bio-oil yield, reducing its viscosity, and improving its combustion properties (Jahirul et al., 2012; Nomanbhay et al., 2017; Zhang et al., 2017b). Nonetheless, the high water content in bio-oil contributes to lower heating value, causing ignition delay and reducing combustion rate (Ethaib et al., 2020; Zhang et al., 2017b).

The raw biomass particle size will influence the yield of by-products using microwave-assisted pyrolysis; for example, a small size implies higher biogas and bio-oil generation. Conversely, larger particle sizes will contribute to higher biochar yield (Leng et al., 2021; Zaman et al., 2018). The main reason for this parameter is that the particle size determines the effect on the reaction time and temperature of the biomass. Small particles are conducive to shifting the

pyrolysis process to a lower temperature, generating a quick thermochemical conversion (Leng et al., 2021; Li et al., 2022d). Analogously, the size of the particle is directly related to the liquid yield; the larger the biomass particle, the lower the bio-oil production due to the incomplete decomposition of the kerogen (Nizamuddin et al., 2018).

Figure 2.5 displays a collection of different investigations associated with the physical ranges of some feedstock components, considering the volatile matter, fixed carbon, moisture, and ash content. Sugarcane bagasse and Arundo donax have high volatile matter content of around 86% and 83%, respectively. Nevertheless, bagasse, bamboo, and pine sources have the lowest moisture levels of between 2% to 4% of the content. Therefore, sugarcane bagasse has considerable potential for producing high-quantity biogas due to its volatile matter content. The high moisture content of wheat straw (16%) and peanut vine (11.58%) promote liquid formation (bio-oil) during microwave pyrolysis with a lower heating value due to the presence of water.

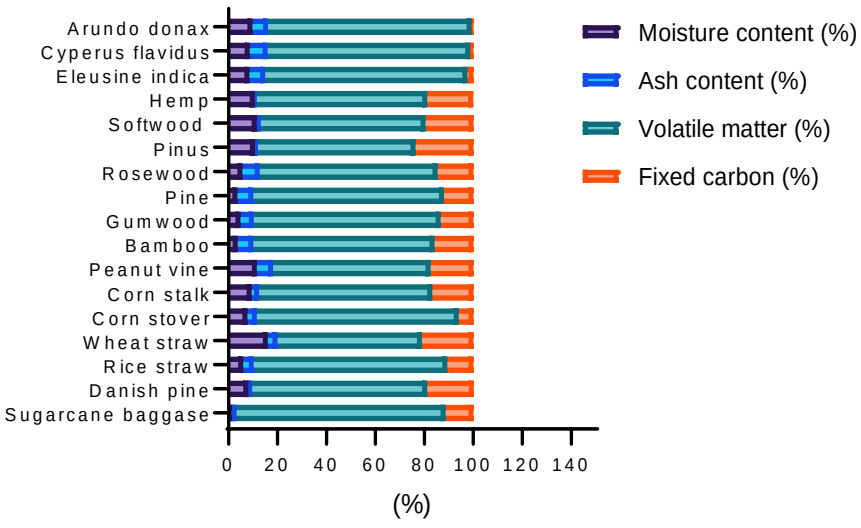

Figure 2.5. Biomass feedstock physical analysis (Cong et al., 2018; Huang et al., 2016a; J.Solar et al., 2016; Qu et al., 2011; Shi et al., 2020b; Singh, 2019; Wallace et al., 2019b).

The high calorific value of raw biomass denotes the energy content of the biomass, which is associated with the properties of the feedstock, such as elemental composition and ash content (Lo et al., 2017). Low heating value has been associated with the energy required to vaporise the water generated during fuel combustion. A high heating value considers the heat released in the combustion process, including vapour in the condensed state (Abhijeet et al., 2020). Table 2.4 shows studies of lignocellulosic feedstock characterisation, including the calorific value and elemental composition. A correlation possibly exists between the elemental composition of the raw biomass and the by-products obtained from microwave-assisted pyrolysis. For example, biochar yield is affected by a significant variation between elementary and average elemental composition. Also, a high hydrogen presence produces a higher moisture content. Similarly, the high carbon content of biomass generates more CO_2 production during the thermochemical conversion process (Abhijeet et al., 2020). Ash content represents a vital factor in the energy value of the biomass and by-products due to obstruction of the heat released during the burning of the biomass, causing a reduction in the fuel properties (Allen and Downie, 2020; Aller et al., 2017; Domingues et al., 2017; Rafiq et al., 2016).

Table 2.4. Heating value and elemental composition of raw lignocellulosic biomass.

Biomass	HHV (MJ/Kg)	LHV (MJ/Kg)	C (wt%)	H (wt%)	N (wt%)	O (wt%)	Reference
Rice straw	16.16	-	45.76	6.22	0.52	47.50	(Lo et al., 2017)
Rice straw	-	12.5	35.22	4.57	0.79	34.92	(Qu et al., 2011)
Rice husk	15.91	-	43.98	5.94	0.4	49.68	(Lo et al., 2017)
Corn Stover	16.82	-	44.92	5.77	0.98	41	(Cong et al., 2018)
Corn Stover	17.06	-	49.38	6.52	0.63	43.47	(Lo et al., 2017)
Pineapple peel	-	-	43.37	5.83	1.4	49.4	(Allende et al., 2023b)
Sugarcane bagasse	16.92	-	48.88	6.71	0.27	44.15	(Lo et al., 2017)

Sugarcane bagasse	17.32	13.83	41.93	5.47	0.21	53.39	(Allende et al., 2022)
Sugarcane peel	17.03	-	46.47	6.23	0.92	46.38	(Lo et al., 2017)
Waste coffee grounds	16.78	-	44.89	6.14	0.35	48.62	(Lo et al., 2017)
Bamboo leaves	15.75	-	39.98	5.81	1.12	53.09	(Lo et al., 2017)
Bamboo	-	6.9	49.9	6.5	6.0	37.0	(Shi et al., 2020b)
Bamboo	18.07	-	52	5.1	0.4	42.5	(Abhijeet et al., 2020)
Gumwood	-	6.7	48.9	6.5	3.5	0.6	(Shi et al., 2020b)
Pine	-	5.7	49.7	6.6	2.4	40.6	(Shi et al., 2020b)
Rosewood	-	6.2	54.9	6.6	0.5	37.4	(Shi et al., 2020b)
Coffee husk	18.5	-	46.41	6.33	2.66	44.51	(Setter et al., 2020)
Woody biomass	15.7	-	57.7	7.2	0.3	34.8	(J.Solar et al., 2016)
Kenaf	17.13	-	48.4	6.0	1.0	48.5	(Abhijeet et al., 2020)
Reed canary	18.72	-	49.4	42.7	6.3	1.5	(Abhijeet et al., 2020)
Miscanthus	18.06	-	49.2	44.2	6.0	1.0	(Abhijeet et al., 2020)
Switchgrass	18.54	-	49.7	6.1	0.7	43.4	(Abhijeet et al., 2020)
Cornstalk	-	13.6	39.24	4.92	0.81	42.52	(Qu et al., 2011)
Peanut vine	-	12.2	35.07	4.89	1.26	40.62	(Qu et al., 2011)

2.5 Microwave pyrolysis by-products analysis.

2.5.1 By-product yield calculation.

After completing the microwave pyrolysis procedure, the by-products can be analysed using the yield calculation of bio-oil, biochar and biogas. These values are defined in Equations 19, 20 and 21, respectively (Chen et al., 2008; Lin and Chen, 2015). Specifically, the yield factor is calculated by the ratio between the by-product weight obtained from the conversion process and the raw biomass weight.

$$\text{Liquid yield (wt\%)} = 100\,\frac{\text{weight of condensed gas}}{\text{weight of raw biomass}} \tag{17}$$

$$\text{Solid yield (wt\%)} = 100\,\frac{\text{weight of char residue}}{\text{weight of raw biomass}} \tag{18}$$

$$\text{Gas yield (wt\%)} = 100 - (\text{liquid yield} - \text{solid yield}) \tag{19}$$

$$\text{General yield (wt\%)} = \left(\frac{\text{biochar weight+ oil+gas}}{\text{biomass weight}}\right) * 100 \tag{20}$$

Alternatively, Equations 23, 24 and 25 show the calculation of by-product yields (Lo et al., 2017). The value establishes the relation between the fibre composition of biomass and product performance. The fibre analysis is crucial for determining comparative ranges between the predicted yields and the experimental data. These factors evaluate the effects of the operating parameters on the yield products.

$$\text{Solid yield (wt\%)} = -0.167\text{H} - 0.239\text{C} + 0.007\text{L} + 34 \tag{21}$$

$$\text{Liquid yield (wt\%)} = 0.185\text{H} - 0.076\text{C} + 0.272\text{L} + 34 \tag{22}$$

$$\text{Gas yield (wt\%)} = -0.018\text{H} + 0.315\text{C} - 0.280\text{L} + 31.9 \tag{23}$$

H: Hemicellulose content, wt%

C: Cellulose content, wt%

L: Lignin content, wt%

2.5.2 By-product yield analysis.

The operating conditions of the microwave system have a crucial effect on the biochar, bio-oil, and biogas yield. Some influencing factors are input power, microwave susceptor, vacuum pressure system, heating rates, nitrogen flow, and geometry of the processing chamber (Fang et al., 2021; Nizamuddin et al., 2018; Zhang et al., 2017a). For instance, high reaction temperatures and pyrolysis power produce low biochar yield but high biogas yield. A higher heating rate promotes the rapid formation of volatiles, causing secondary reactions of non-condensable gases and converting condensable vapours into permanent gaseous products (Dai et al., 2019; Ge et al., 2021; Nizamuddin et al., 2018; Shi et al., 2020b; Su et al., 2022a). A longer reaction time is beneficial for biochar and bio-oil yield. A prolonged thermochemical conversion and low power produce enough temperature to complete the pyrolysis process, reducing the secondary breakdown of organic vapours and increasing the release of volatiles for the formation of liquid components (Siddique et al., 2022; Toscano Miranda et al., 2021; Yaning Zhang, 2017).

Figure 2.6 shows the comparison of by-product yields between both technologies. In comparison to conventional pyrolysis, biogas yield is higher for microwaves. Microwave pyrolysis can reach high heating rates faster producing increased biomass devolatilization (promotes the biomass molecules interactions), higher breakdown of lignin structure (promotes CO formation), favoured the dehydrogenation reactions, and increase the secondary reactions of heavy intermediates and higher biogas fraction (Lin et al., 2022; Liu et al., 2021d; Macquarrie

et al., 2012; Shi et al., 2020b). However, as biogas increased, bio-oil yield decreased (18%) in microwave pyrolysis. This is associated with the secondary reactions of organic non-condensable gases and the devolatilization of biomass generated from the breakdown of intermediate vapours, converting them into syngas compounds (Shi et al., 2020b; Yaning Zhang, 2017). Biochar yield in microwave pyrolysis is slightly lower than in conventional pyrolysis due to the microwave heating method allowing higher thermal decomposition of the biomass compounds (Gabhane et al., 2020; Zhang et al., 2017a). Furthermore, a microwave reactor can reach a higher carbonization level than conventional pyrolysis, generating a higher graphitic char form (Macquarrie et al., 2012; Shi et al., 2020b).

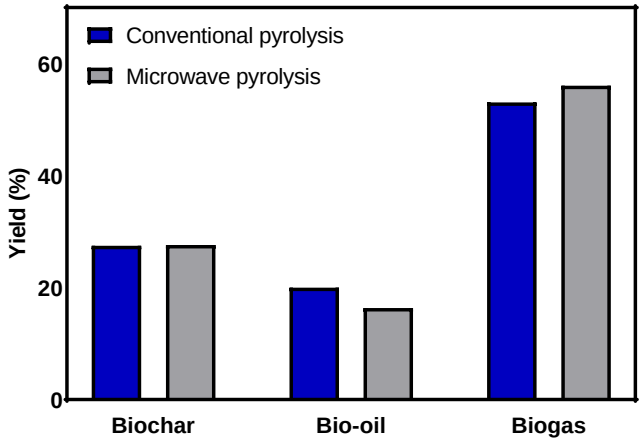

Figure 2.6. Comparison of by-product yield between conventional and microwave pyrolysis (Abdelsayed et al., 2019; Domínguez et al., 2007; Ferrera-Lorenzo et al., 2014; Halim and Swithenbank, 2016; K. Shi, 2013; Lin and Chen, 2015; Shi et al., 2020b; Wu et al., 2014).

Although the technology and operating conditions are relevant factors in the performance of the by-products, the nature of biomass is also another aspect to consider. The fibre composition of the biomass is influenced by diverse pyrolysis reactions, like depolymerization, dehydration, reformation, and depolymerization (Ansari et al., 2019). The bio-oil and biochar yield are correlated to cellulose and lignin components, respectively. The biomass fibre composition also affects the by-product quality and energy value (Lin et al., 2015; Tomczyk et al., 2020a). The devolatilization of cellulose and hemicellulose is favourable for increasing biochar energy value. In contrast, the devolatilization of lignin causes a decreased biochar

heating value, but increased biogas (Zhang et al., 2017a). Table 2.5 presents studies associated with by-product yields obtained in conventional and microwave pyrolysis using different biomass feedstocks and operating conditions. In microwave pyrolysis, the increase in temperature causes a decrease in biochar yield and an increase in biogas formation (Nhuchhen et al., 2018). For instance, the biochar yield generated from coffee hull biomass decreased by 4%, and biogas increased by 3%. The reason is that increased reaction temperature produces higher devolatilization and decomposition of the biomass, producing a significant mass loss, further volatile release, and gaseous products (Nhuchhen et al., 2018; Shi et al., 2020b). However, conventional pyrolysis generated a 33% higher bio-oil yield than microwave pyrolysis using coffee hull biomass. This increased yield fraction is due to the heating method of microwave pyrolysis promoting the conversion of liquid products into non-condensable gases (Jennita Jacqueline et al., 2022; S.Mutsengerere et al., 2019; Toscano Miranda et al., 2021; Yaning Zhang, 2017).

Table 2.5. By-product yield from conventional and microwave pyrolysis using different biomass.

Biomass	**Temp (ºC)**	**Time (min)**	**Conventional pyrolysis (wt%)**			**Microwave pyrolysis (wt%)**			**Reference**
			Char	**Oil**	**Gas**	**Char**	**Oil**	**Gas**	
Macroalgae	750	60	31	36	34	28	35	37	(Ferrera-Lorenzo et al., 2014)
Sugarcane bagasse	550	30	32	53	16	62	22	16	(Lin and Chen, 2015)
Coffee hulls	800	25	25	12	63	26	9	65	(Domínguez et al., 2007)
	1000	25	24	10	67	23	9	69	(Domínguez et al., 2007)

Bamboo	600	15	27	12	61	19	8	73	(Shi et al., 2020b)
Pine	800	15	14	8	77	18	4	79	(Shi et al., 2020b)
Gumwood	800	15	8	14	78	15	4	81	(Shi et al., 2020b)
Rosewood	700	15	12	10	78	22	6	72	(Shi et al., 2020b)
Wood pellets	800	16	23	17	61	22	26	52	(Halim and Swithenbank, 2016)
Rubberwood	800	16	22	14	70	21	19	60	(Halim and Swithenbank, 2016)
Wood sawdust	200	18	60	32	9	43	47	10	(Wu et al., 2014)
Gumwood	500	30	30	6	65	18	9	73	(K. Shi, 2013)
Pinewood + lignite coal	550		50	38	12	43	14	43	(Abdelsayed et al., 2019)

2.5.3 Biochar characterisation

The type of pyrolysis technology used influences the yield of biochar. It also influences the elemental composition and surface structure (Li et al., 2022e; Omar and Robinson, 2014; Riva et al., 2021; Sakhiya et al., 2020). For example, microwave pyrolysis produces biochar with a higher heating value than conventional pyrolysis due to the thermal breakdown of biomass compounds with low heating value (cellulose and hemicellulose), whose decomposition is established at the early stages of the pyrolysis reaction. In contrast, the lignin biomass compound has high thermo-resistant properties and a high heating value. Therefore, a gradual thermal decomposition of lignin is beneficial to reaching a high biochar energy value.

Since the heating value is based on the biochar elemental composition, microwave pyrolysis produces a low oxygen range and high carbon and hydrogen content (Fang et al., 2021; Ghesti et al., 2022; Su et al., 2022a; Wu et al., 2022). Some work report that biochar with high carbon content indicates that during biomass pyrolysis was produced the release of volatile matter and the elimination of oxygen-containing groups (Lim et al., 2022). Microwave heating promotes the formation of aromatic compounds and the coalification degree associated with low H/C and low O/C atomic ratios, improving the biochar energy potential (Liu et al., 2021d; Raheem et al., 2022). Table 2.6 shows the comparison of elemental composition and energy value between biochar produced from both pyrolysis technologies.

Table 2.6. Ultimate analysis of biochar generated from conventional and microwave pyrolysis (Brickler et al., 2021a; Halim and Swithenbank, 2016; Nzediegwu et al., 2021; Wu et al., 2014).

Element yield (wt%)	**Conventional pyrolysis**	**Microwave pyrolysis**
C	~43-87	~36-88
H	~1-6	~0.68-5.76
O	~11-46	~9.75-58
N	~0.3-5	~0.28-3.91
HHV (MJ/kg)	~33-38	~27.1-37.1

The surface morphology of biochar generated under the microwave pyrolysis process has higher quality and stability than conventional pyrolysis (Halim and Swithenbank, 2016). Microwave pyrolysis produces biochar with a higher surface area and pore volume, contrary to conventional pyrolysis, which generates biochar with no uniform pores, high cracks, and fissures (Halim and Swithenbank, 2016; M.Waqasa et al., 2018; Shin Ying Foong, 2020). The volumetric heating method of microwave pyrolysis promotes the formation of micropores by the rapid release of volatile matter (volatilization process) leading to clean pore production (Li et al., 2016; Wallace et al., 2019b). Table 2.7 shows an estimation of surface area and pore volume formation generated from conventional and microwave pyrolysis.

Table 2.7. Comparison of biochar surface area obtained from conventional and microwave pyrolysis (Halim and Swithenbank, 2016; Mašek et al., 2013; Mohamed et al., 2016; Nzediegwu et al., 2021).

	Conventional pyrolysis	Microwave pyrolysis
BET Surface Area Analysis (m^2/g)	~0.33-332.96	~1.14-377.56
Pore Volume Analysis (cm^3/g)	~0.049-1.44	~0.096-2.07

2.5.4 Bio-oil characterisation

Table 2.8 shows the bio-oil comparison of the ultimate analysis produced from both pyrolysis technologies. Conventional pyrolysis produces a higher bio-oil yield than microwave pyrolysis. However, microwave pyrolysis generates higher bio-oil quality, considering its heating value, elemental analysis, and chemical composition (Halim and Swithenbank, 2016; Huang et al., 2016b; Mohamed et al., 2016; Wu et al., 2014). For instance, bio-oil from microwave pyrolysis has higher carbon but lower oxygen levels. A low oxygen content indicates higher organic functional group decomposition with high oxygen contained. The deoxygenation reactions comprise phenol group reduction, higher stability, and higher heating values (HHV and LHV) (Suriapparao et al., 2020a; Zhao et al., 2021). Moreover, in microwave pyrolysis, the H/C and H/O ratios are slightly higher and lower than in conventional pyrolysis. A low H/C value represents higher aromatic functional groups (Ferrera-Lorenzo et al., 2014; Halim and Swithenbank, 2016). However, exceeding pyrolysis temperatures leads to the breakdown of aromatic groups, generating more aliphatic content (Halim and Swithenbank, 2016; Liu et al., 2021d; Nhuchhen et al., 2018).

Table 2.8. Estimation of bio-oil elemental analysis and the heating value obtained from conventional and microwave pyrolysis (Du et al., 2011; Ferrera-Lorenzo et al., 2014; Halim and Swithenbank, 2016; Nhuchhen et al., 2018; Suttibak et al., 2012).

Element yield (wt%)	Conventional pyrolysis	Microwave pyrolysis
C	~45-66	~21-63
H	~6-9	~6-11
O	~13-45	~20-70
N	~0.1-9.5	~0.01-9
H/C	~0.1-0.2	~0.1-0.38
H/O	~0.2-0.6	~0.11-0.32
HHV (MJ/kg)	~21.8-26	~10-28

Bio-oil functional groups are subject to pyrolysis technology and biomass nature. Conventional pyrolysis produces bio-oil with a higher phenol and alkane content, associated with the thermal decomposition of lignin compounds that promotes phenolic group formation (Ferrera-Lorenzo et al., 2014; Zhao et al., 2021). In contrast, microwave pyrolysis generates bio-oil with higher aromatic compounds due to higher cracking reactions of phenols leading to benzene conversion (Ghesti et al., 2022; Suriapparao et al., 2022a; Suriapparao et al., 2020b; Zhao et al., 2021). Moreover, the increased pyrolysis temperature (over 500 ºC) in a shorter reaction time induces the further breakdown of phenols, reducing phenol groups and increasing aromatic hydrocarbons content (Halim and Swithenbank, 2016; Khuenkaeo et al., 2021; Zhao et al., 2021). Alcohol and methylene content increases at elevated pyrolysis temperatures, but alkanes are decreased (Khuenkaeo et al., 2021; Liu et al., 2021d).

2.5.5 Biogas characterisation

The principal chemical composition of biogas from microwave pyrolysis is H_2 and CO; however, conventional pyrolysis is predominated by the generation of CH_4 and CO_2. Microwave heating promotes the breakdown of methoxy (lignin form) and biochar self-gasification, causing

increased CO and decreased CO_2 generation. The high heating rate reached during the microwave pyrolysis process contributes to large H_2 formation by the dehydrogenation and secondary reactions, which involves converting heavy intermediate compounds (condensable gases) into a permanent gaseous fraction (Lin et al., 2022; Lin et al., 2023; Sahoo and Remya, 2022; Shi et al., 2020b; Su et al., 2022a; Su et al., 2022b).

Table 2.9 shows the comparison of biogas yield between conventional and microwave pyrolysis techniques. Available data substantiates that conventional pyrolysis can produce 9% higher CO_2 than microwave heating. On the other hand, microwave pyrolysis exhibits a considerable increase in hydrogen (~ 19-52 Vol%) and syngas (~ 54-81 Vol%- CO, H_2, CO_2) generation than conventional heating. Increased pyrolysis temperature (600ºC to 900ºC) and prolonged residence time promote the breakdown of bio-oil (secondary reactions) and the volatile release from the biomass, causing more gaseous products (Ferrera-Lorenzo et al., 2014; Halim and Swithenbank, 2016; Liu et al., 2021d; Shi et al., 2020b). Then, higher syngas production makes microwave pyrolysis a better alternative for improving biogas heating value (Sharma et al., 2020; Su et al., 2022a; Su et al., 2022b).

Table 2.9. Gaseous fraction of microwave and conventional pyrolysis (Ferrera-Lorenzo et al., 2014; Halim and Swithenbank, 2016; Liu et al., 2021d; Shi et al., 2020b).

	Vol (%)	
Composition	**Conventional pyrolysis**	**Microwave pyrolysis**
CO_2	~3.2-36	~13-31
CH_4	~13-23	~1-15
CO	~18	~23-44
H_2	~0.8-24	~19-52
Syngas	~41-68	~54-81

2.6 Comparison and analysis of energy balance

The biochar calorific value (MJ/kg) can be studied by its ultimate analysis. Equation *26* (Qian et al., 2020) shows the relationship between the factors associated with carbon, hydrogen and oxygen content (%).

$$\mathrm{HHV(MJ/kg)} = 33.2\mathrm{C} + 176.6\mathrm{H} - 17.7\mathrm{O} + 0.702 \quad (24)$$

The high heating value (HHV) of bio-oil can be estimated by its elemental composition. The determination of the HHV is obtained by the correlation between the carbon, oxygen, sulfur and hydrogen content (%). The factors related are illustrated in Equation *27* (Riaz et al., 2016).

$$\mathrm{HHV(MJ/kg)} = (34\mathrm{C} + 124.3\mathrm{H} + 6.3\mathrm{N} + 19.3\mathrm{S} - 9.8\mathrm{O})/(100) \quad (25)$$

The relevance of the heating value of biogas released during pyrolysis is represented by the gas composition, mainly for the concentration of four gases: hydrogen (H_2), methane (CH_4), carbon monoxide (CO) and ethyne (C_2H_2). The lower heating value (LHV, MJ/m^3) of biogas is calculated by Equation 28 (Kazim, 2018; Moghadam et al., 2014).

$$\mathrm{LHV}\left(\frac{\mathrm{MJ}}{\mathrm{m3}}\right) = \frac{107.98\ \mathrm{H_2} + 126.36\ \mathrm{CO} + 358.18\ \mathrm{CH_4} + 56\ \mathrm{C_2H_2}}{1000} \quad (26)$$

Equation *34* shows the calculation of the by-product energy obtained through their heating value (HV, MJ/kg), the mass of the biomass sample (M, kg) and yields (%). Then, the total energy output achieved in the microwave pyrolysis process involves the energy value of biochar (Echar), bio-oil (Eoil) and biogas (Egas) (Jesus et al., 2018). The energy conversion efficiency can be obtained by Equation *31* (Suriapparao et al., 2015a), considering the ratio between the total energy achieved from the three by-products and the electrical consumption of the microwave pyrolysis system.

$$\text{By} - \text{product E(MJ)} = \text{HV}\left(\frac{\text{MJ}}{\text{kg}}\right) * \text{M (kg)} * \text{yield (\%)} \quad (27)$$

$$\text{Total output E (MJ)} = (\text{Echar} + \text{Eoil} + \text{Egas}) \quad (28)$$

$$\text{Energy recovered (\%)} = \frac{\text{Total output energy}}{\text{electrical consumption}} * 100 \quad (29)$$

Since the energy recovery of pyrolysis depends on the by-products and energy system consumption, microwave pyrolysis produces slightly higher output energy (Hansirisawat and Srinophakun, 2020; Shi et al., 2020b). Table 2.10 shows a compilation of energy by-products generated from both pyrolysis technologies. Studies demonstrated that microwave pyrolysis has output energy (~ 7.2-22.1 MJ) higher than conventional heating (~ 2%), considering the same total input energy by applying an identical pyrolysis temperature and reaction time. The biogas energy efficiency in microwave heating is ~ 16% higher than conventional pyrolysis. The increased total efficiency in microwave pyrolysis is attributed to its increased biogas energy value (high H_2 formation and low CO_2 content), reaching higher energy efficiency than conventional heating (Shi et al., 2020b; Su et al., 2022a; Zhou et al., 2021). Microwave heating achieves higher efficiency than slow pyrolysis due to low energy consumption during the biomass conversion process (Hansirisawat and Srinophakun, 2020; Shi et al., 2020b).

Table 2.10. Energy efficiency of conventional and microwave pyrolysis (Ferrera-Lorenzo et al., 2014; Shi et al., 2020b; Xiqiang Zhao, 2011).

	MJ	
	Conventional pyrolysis	**Microwave pyrolysis**
Char	~1.1-7.83	~1.3-7.1
Oil	~0.3-9.3	~0.19-8.6
Gas	~4.6-6.28	~5.6-7.3
Total output energy	~7.6-21.83	~7.2-22.1

2.7 Application of microwave pyrolysis by-products.

Other biomass conversion methods offer a limited application of by-products, mainly due to the restricted number of feedstock materials that can be processed and the target product obtained from the technology method. Microwave pyrolysis has several advantages over other bioenergy methods that involve the versatility of biomass uses and the simultaneous generation of char, oil and gas in shorter reaction time. Microwave pyrolysis generates biochar with a higher surface area than conventional heating, whose property is crucial for developing modified/ activated biochar (Allende et al., 2023b; Selvam S and Paramasivan, 2022). In terms of electricity generation, microwave pyrolysis provides two pathway mechanisms - by using biogas in a gas turbine or applying bio-oil upgraded in an engine. However, combustion, gasification and anaerobic digestion offer only one by-product to produce electricity by using steam, gas and biogas in the turbine, fuel cell and engine, respectively (Ifeanyi Michael Smarte et al., 2022).

The by-products generated from microwave pyrolysis of lignocellulosic biomass have diverse applications in the industrial sector (Su et al., 2022a; Xin et al., 2021; Xue et al., 2021; Zi et al., 2019a), as shown in Figure 2.7. Biochar products present higher mineral content and elemental carbon composition due to the nature of the original feed material (Mierzwa-Hersztek et al., 2019). Thus, biochar is an excellent resource for producing pellet conversion, activated carbon, soil conditioner, carbon nanofilaments, solid additives, and others (Shukla et al., 2019; Su et al., 2022a; Xin et al., 2021; Xue et al., 2021). Recent research reveals that biochar is an excellent additive that improves the properties of construction materials, especially mechanical strength and other relevant physical properties (Rossignolo et al., 2017). Interestingly, the integration of aluminium-siliceous material in concrete increases its strength, durability, performance, and porosity (Xu et al., 2019).

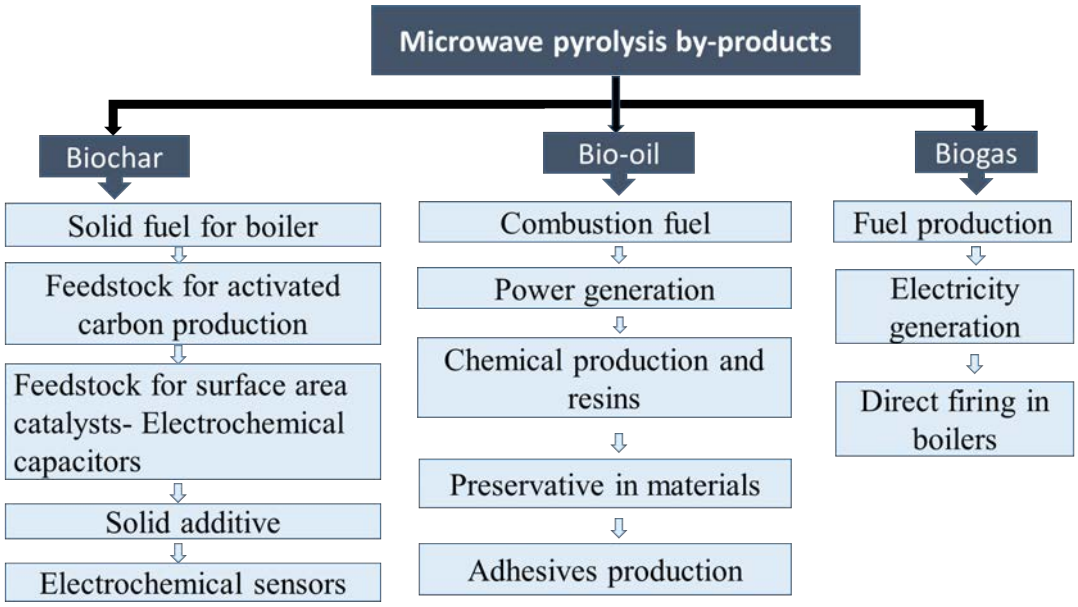

Figure 2.7. Applications of microwave pyrolysis by-products (Bu et al., 2016; Fernandez et al., 2011; Undri et al., 2011; Xu et al., 2019).

The electrochemical sensors development, based on biochar use, has gained relevance due to its significant electrocatalytic potential. The biochar activation consists of chemical activation before the pyrolysis process, considering biomass soaking into KOH, $ZnCl_2$, HNO_3 or H_2SO_4 (Cheng et al., 2017; Monticelli, 2020). The biomass chemical treatment and the pyrolysis process improve biochar porous structure, electron transfer, and ion insertion (Allende et al., 2023b). Once the biochar is pyrolysed, the modified biochar is applied in the electrode fabrication by drop-casting (in a carbon glassy carbon electrode) or carbon paste (Cheng et al., 2017; Monticelli, 2020; Sudha et al., 2019). The sustainable electrode can be used for different analytes detection, like dopamine, oxalic acid, nitrite, and uric acid (Monticelli, 2020; Sudha et al., 2019; Teo et al., 2019).

Some bio-oil uses comprise fuel combustion, power generation (stationary diesel engine), chemical production, transportation fuel, binders for pelletizing, etc. (Hu and Gholizadeh, 2020; Li et al., 2022c; Zeng et al., 2022). However, bio-oil often contains unstable chemical compounds that require upgrading for its application as fuel due to the viscosity and oxygen,

water, and nitrogen presence. Previous factors lead to bio-oil with low heating value and decreased thermal and chemical variability (Hussain et al., 2018; Li et al., 2021; Su et al., 2022a). The purification process involves the separation of the bio-oil from the raw product to obtain better quality and performance as a fuel (Bu et al., 2016; Su et al., 2022a). Some purification techniques are:

- The solvent addition (with a high heating value) in the bio-oil, causes a physical-chemical reaction between the solvent and the bio-oil components, increasing the heating value and decreasing viscosity. The standard solutions are ethyl acetate, acetone, methanol, and ethanol (Hu and Gholizadeh, 2020; Li et al., 2022c; Liu et al., 2014).

- Emulsification with other fuels, like diesel or biodiesel integration, improves ignition properties, although this represents some problems with heating values, corrosion and cetane number (Cai et al., 2021a). This last property indicates the ignition quality of diesel fuel (VenkataMohan et al., 2019).

- Esterification involves a reversible conversion, where it is possible to obtain methyl ester or biodiesel. The process entails the reaction between the bio-oil and alcohol (methanol or ethanol) in the presence of an acid catalyst (HZSM-5 or aluminium silicate) at a lower temperature than the boiling point of the alcohol (60 °C) (Hansen et al., 2020; Hu and Gholizadeh, 2020; Li et al., 2022c).

- Supercritical fluid means a fluid at pressure and temperature above a critical point that can dissolve the liquid. Some common solvents include ethanol, methanol and water (Bu et al., 2016).

- Hydrotreating reduces the concentration of oxygen, nitrogen, and sulphur in the form of water and H_2S (Hansen et al., 2020). This method requires removing the oxygen as water by adding hydrogen at high pressure in a catalytic process. Conventional catalysts are CoMo-based and NiMo-based, intended to remove O, N and S (Bu et al., 2016; Hansen et al., 2020; Huber et al., 2006; Kumar and Strezov, 2021). Hydrocracking is a method that uses high temperature (310°C -275°C) and pressure (10-20 MPa) in a catalytic cracking process in the presence of hydrogen gas, which involves the conversion of polymeric components into small fragments (Hansen et al., 2020; K.Tanneru and H.Steele, 2015; Li et al., 2022c; P.M.Mortensen et al., 2011).

- The extraction of valuable chemicals from the mixture also qualifies as an oil purification method. There are diverse separation processes, for example, through the absorption by acetone as a solvent, distillation techniques and fractionation of the oil (Bu et al., 2016; Li et al., 2022c).

Biogas application comprises combustible gas production, like hydrogen (H_2), acetylene (C_2H_2), methane (CH_4), ethylene (C_2H_4), ethane (C_2H_6), and carbon monoxide (CO) and some minority content of carbon dioxide and pollutants. The biogas produced from microwave pyrolysis had high hydrogen and carbon monoxide content, which allows the synthesis of gases, such as ammonia. As a result, biogas applications include the direct firing of boilers (without flue gas treatment), and gas turbines or engines for electricity generation (Abanades et al., 2022; Khan et al., 2021; Mulu et al., 2021). Fuel production is possible through steam reforming, which is the production of syngas (a reaction between hydrocarbon and water), whose objective is hydrogen generation (Bu et al., 2016; Mahari et al., 2018). Furthermore, microwave pyrolysis in a vacuum environment will generate more condensation volatiles, allowing bio-oil formation (Mahari et al., 2018).

2.8 Microwave pyrolysis economic analysis

Microwave pyrolysis development is crucial for sustainable benefits associated with energy independence, CO_2 mitigation, and the reduction of agricultural residues. Nevertheless, the economic factor of pyrolysis technology is challenging due to the highly competitive cost of fossil fuels (Inayat et al., 2022; Li et al., 2022d; Mulu et al., 2021). Additionally, multiple variable costs (V.C) are associated with financial viability and operating parameters, like technology method, biomass storage, plant size (operating scale), feedstock (represents 23-30% of the variable cost), maintenance (17-24% of the V.C), grinding (7-9% of the V.C), and transportation (5-7% of the V.C) (Hansirisawat and Srinophakun, 2020; Mullaney et al., 2002).

The economic analysis is determined considering the energy balance of the conversion process that involves the relationship between the energy consumed by the microwave pyrolysis and the energy generated from the by-products (biogas, bio-oil and biochar). Microwave energy demand depends on system conditions, for example, microwave vacuum pyrolysis or microwave pyrolysis process in a nitrogen environment. The energy consumption of both microwave pyrolysis conditions is obtained by Equations *32* and *33* (Lam et al., 2019a; Yang et al., 2018).

$$\mathrm{E}_{\mathrm{MP}_{\mathrm{system}}}(\mathrm{kWh}) = [\mathrm{A} + \mathrm{B} + \mathrm{C}]\mathrm{X}\ \mathrm{D} \tag{30}$$

$\mathrm{A} = Microwave\ power\ (W)$

$\mathrm{B} = Thermocouple\ (W)$

$\mathrm{C} = Vacuum\ power\ (W)$

$\mathrm{D} = Reaction\ time\ (hr)$

$$\mathrm{E}_{\mathrm{MP}_{\mathrm{system\_N2environment}}}(\mathrm{kWh}) = [\mathrm{A} + \mathrm{B}]\mathrm{X}\ \mathrm{D} \tag{31}$$

Microwave pyrolysis system design, biomass state, and optimal operating conditions are relevant to determine its techno-economic viability and efficiency. The optimal microwave pyrolysis system design decreases the microwave heating loss, improves the energy conversion process and enhances by-product quality and yield (Inayat et al., 2022; Lam et al., 2019a). For instance, using biogas as a fuel with high hydrogen content could be enough to self-supply the system (Xiqiang Zhao, 2011). Table 2.11 shows the operating cost comparison of both pyrolysis technologies. Biomass conversion based on small-scale microwave pyrolysis technology can be economically convenient (Beneroso et al., 2017; Wang et al., 2015). The economic viability lies in the low biomass cost, transportation, high returns (economic benefits for biomass producers), and accessible operating technology (Bu et al., 2016; Wang et al., 2015). Additional work is required to understand the economic viability of scaled-up systems, and the level of scaling achievable.

Table 2.11. Estimation of the techno-economic analysis of conventional and microwave pyrolysis (Badger et al., 2011; Lam et al., 2019a; Wang et al., 2015; Yahya et al., 2021).

	US $/yr	
Item	**Conventional pyrolysis**	**Microwave pyrolysis**
Capital costs		
Capital investment	110,000	208,000
Others cost	265,000	74,300
	375,000	**282,300**
Operating costs		
Feedstock	124,500-1,460,000	124,500-1,460,000
Electricity	38,880-104,869	8640
Labour cost	270,000	12,000
Maintenance	40,000-91551	10,000
Insurrance	39,539	4000
	1,239,439	**826,890**

2.9 Conclusion

This work revealed the influential parameters on the energy recovery of the breakdown of biomass using the microwave-assisted pyrolysis method. Microwave heating is a promising alternative for biomass conversion due to its high efficiency and fast heat transfer capacity. The energy conversion of biomass feedstock using microwave pyrolysis is a feasible method that allows excellent yield on the by-products. The conditions and nature of biomass, microwave power, microwave susceptor and reaction time are some influencing factors that are essential to determine the quality and yield of the bio-oil, biochar, and biogas. For instance, pre-treatment of the biomass, high water content, and particle size produce a higher bio-oil and biogas yield. The operating conditions of microwave pyrolysis, such as input power, heating rate, and microwave susceptor also influence the outcomes. By modifying these parameters to optimal ranges, the by-product yield can be optimised to obtain a higher energy production potential and improved elemental composition.

The optimisation of the by-products and their quality varied based on the operating conditions of the microwave pyrolysis system. High microwave susceptor addition and high microwave power cause more volatilization of larger molecules and the rapid release of small molecules, generating low biochar yield and non-uniform modification in its structure. Low temperature and longer reaction time are the optimal biochar conditions to obtain a higher BET surface area, adsorption efficiency and micropore volume. The combination of high power and microwave susceptor contributes to the thermal breakdown of heavy hydrocarbon and facilitates the formation of volatiles from the biomass, generating more gaseous fraction. Moderate microwave power and low microwave susceptor are beneficial for producing bio-oil with higher aromatic content. These factors are relevant to fully understanding the challenges that face energy recovery of a microwave pyrolysis system.

CHAPTER 3

3 ENERGY RECOVERY UNDER VARYING MICROWAVE PYROLYSIS CONDITIONS

Sugarcane bagasse is an abundant agricultural feedstock with valuable potential for clean energy generation. Literature review evidenced that microwave pyrolysis is an efficient technology for biomass conversion over the conventional pyrolysis method, which provides multiple sustainable benefits, e.g., reduction of greenhouse gas emissions, energy recovery and circular economy. However, the yield and quality of the by-products are subjected to intrinsic biomass properties and operating conditions. This chapter explores the energy optimisation of sugarcane bagasse considering different ranges of microwave power, susceptor addition and treatment time. Economic analysis and carbon footprint factors are also evaluated.

Abstract

Waste management and utilization of waste is a major global issue. This study investigated the influential parameters on the energy recovery from the sugarcane bagasse breakdown under microwave pyrolysis conditions. The by-product yield is optimised from 45 different combinations of microwave power, reaction time and microwave susceptor. The surface methodology, energy efficiency and by-product quality were studied. Low power, less microwave susceptor and longer residence time are the desirable conditions for high biochar yield due to the gradual thermal decomposition of the biomass and low heating rates. Higher microwave power and lower residence time obtained the highest bio-oil yield. The excess

pyrolysis temperature generated by the higher microwave power and higher microwave susceptor addition produces higher temperatures beyond the optimal conditions for bio-oil production. This phenomenon is relative to the self-gasification of the biochar during the high pyrolysis power, contributing to the formation of H_2, CO and CH_4.

Keywords: Microwave pyrolysis; Sugarcane bagasse; Biochar; Bio-oil; Biogas

This chapter was published as Allende, Scarlett, Graham Brodie, and Mohan V. Jacob. 2022. 'Energy recovery from sugarcane bagasse under varying microwave-assisted pyrolysis conditions', Bioresource Technology Reports, 20: 101283.

3.1 Introduction

Excessive use of non-renewable energy sources, depletion of fossil fuels and population growth cause a significant impact on climate change, air contamination and the economy (Daneshmandi et al., 2022; Ferrari et al., 2022). Fossil fuel combustion generates around 98% of human carbon dioxide emissions (Prasad and Ingle, 2019). On the other hand, the disposal of different types of waste produces significant greenhouse emissions, like methane and carbon dioxide gas, contributing to the rise in atmospheric temperature and global climate change (Liu et al., 2021c). Some biomass sources comprise agricultural waste, wood, animal and crop residues, food waste, municipal waste, algae, plastics, and cooking oil (Cai et al., 2021b; Lee et al., 2019; Wang et al., 2021b). Globally, 23.7 million tons of agroindustrial biomass is generated per day (Duque-Acevedo et al., 2020). Hence, the deficit of energy resources, high fossil fuel demand, and greenhouse gas (GHG) emissions make bioenergy a promising alternative for clean energy production (Daneshmandi et al., 2022; Mierzwa-Hersztek et al., 2019).

Bioenergy is acknowledged as a renewable and sustainable energy source due to the energy conversion of lignocellulosic biomass having a lower-carbon life cycle than fossil fuel, generating heat, electricity and fuels with low environmental hazards (Daneshmandi et al., 2022; Le Pera et al., 2022). Biomass can be converted to energy by two methods: thermochemical and biochemical processes. The thermochemical method comprises combustion, gasification, and conventional and microwave pyrolysis (Liu et al., 2022). Anaerobic digestion and microbial fermentation are biochemical conversion methods (Le Pera et al., 2022; Li et al., 2022b). The selection of biomass conversion method is crucial for synthesizing by-products and recovering energy (Lee et al., 2019; Li et al., 2022b). The nature of biomass is a relevant factor in choosing the appropriate energy conversion technology because of its structural and chemical composition. For example, the decomposition of

lignocellulosic biomass occurs faster in a thermochemical method than in a biological conversion due to the high heating efficiency (Arpia et al., 2021; Huang et al., 2016b). The fibre composition of lignocellulosic biomass is cellulose, hemicellulose, and lignin. The range of fibre compounds in these materials depends on the nature of the biomass. For example, sugarcane bagasse has higher cellulose content (46.55 wt%) than rice husk (30.42 wt%) (Huang et al., 2016b; Lo et al., 2017).

Conventional and microwave pyrolysis implies the thermochemical breakdown of the biomass in the absence of an oxidizing agent for producing biochar, bio-oil and biogas (Arpia et al., 2021). The main difference between microwave and conventional pyrolysis is the heating method; the microwave method involves volumetric heating, and conventional pyrolysis is conduction/convection heating (Selvam S and Paramasivan, 2022; Shukla et al., 2019). Conventional pyrolysis is achieved using a bath furnace with high thermal inertia and low electricity conversion efficiency (Arpia et al., 2021). Microwave-assisted pyrolysis has higher efficiency in the heating process because energy transfer is through the interaction of the molecules inside the biomass rather than by heat transfer from external sources ((Li et al., 2022a; Zi et al., 2019b). The advantages of microwave heating are shorter reaction time, better distribution and control over the heating, non-contact heating, and a quick start-up and stopping mechanism (Arpia et al., 2021; Yu et al., 2022a). However, microwave pyrolysis requires a microwave susceptor to absorb the electromagnetic radiation and start the energy transfer (Suriapparao et al., 2018).

Some types of biomass present poor dielectric heating properties, which involve lower absorption of microwave energy. In the case of dielectric loss tangent (tanδ) of polyethylene, polypropylene, fir plywood, wood polymer, sludge, and PVC are 0.0001, 0.0003, 0.01, 0.03 and 0.035, 0.0056, respectively (Zhang et al., 2017a; Zhang et al., 2017b).

Therefore, the addition of a microwave susceptor (M.S) is necessary to transform the electromagnetic energy into heat to be transferred to the biomass, allowing the pyrolysis reaction to initiate (Suriapparao et al., 2018; Zi et al., 2019b). The ratio of microwave susceptors, biomass feedstock volume and intrinsic biomass properties influence the heating rate of the conversion process and the biochar, bio-oil, and biogas yield. The high addition of microwave susceptor at an elevated reaction temperature can produce a secondary thermal breakdown of non-condensable volatiles into permanent gaseous compounds, increasing biogas yield but reducing bio-oil production (Shi et al., 2020a; Zhang et al., 2017a; Zhang et al., 2017b). Ranges of tanδ in diverse microwave susceptors are between 0.02 and 1.05 (Ellison et al., 2017; Zhang et al., 2017a; Zhang et al., 2017b). Representative absorber materials are SiC, activated carbon, biochar, graphite, glycerol, fly ash and water (Zhang et al., 2022b; Zhang et al., 2017a; Zhang et al., 2017b). The selection of a suitable microwave susceptor contributes to a significant difference in the heating rate, microwave assimilation capacity of bulk biomass, energy consumption (microwave energy system) and by-product quality (Selvam S and Paramasivan, 2022; Zhang et al., 2017a).

Several studies have reported the by-products optimisation of diverse biomass using microwave pyrolysis, e.g., horse manure (Mong et al., 2021), oil palm (Idris et al., 2022), plastic (Suriapparao et al., 2022b), corn cob (Quillope et al., 2021), flax shives (Ubiera et al., 2021), sugarcane bagasse (S and Paramasivan, 2021), bamboo, gumwood and pine (Shi et al., 2020a). However, most studies did not consider: (i) processing a higher biomass volume (over 50 g); (ii) evaluating the impact of the optimised by-product on global energy recovery; (iii) assessing operating parameters on the quality of the target by-product; (iv) integrating sustainable aspects (economic and environmental analysis) on global energy efficiency. These factors are relevant to investigate to fully understand the challenges that face energy recovery using a pilot-scale microwave system from the processing of sugarcane bagasse.

This study intended to investigate the influential parameters on the energy recovery of the breakdown of sugarcane bagasse under microwave pyrolytic conditions. The objectives of this research include: (i) identifying the optimal yield of by-products established by the experimental combination scenarios; (ii) evaluating the influential parameters on the characterization and quality of by-products; (iii) assessing the impact of the target by-product on the total energy output and global energy recovery; (iv) techno-economic estimation of microwave pyrolysis system based on diverse operational conditions; and (v) do the carbon footprint of the SCB processing.

3.2 Experiments and Methods.

3.2.1 Raw biomass material.

Sugarcane bagasse (Wilmar, Queensland) was used as feedstock in microwave pyrolysis. The water content of the biomass was determined by grounding the sample into smaller sizes (0.2–0.5 mm) until obtaining a representative feedstock. Then, the SCB was exposed to 110 °C in an oven until it attained constant weight (~2 h). The resulting moisture content was 10 wt%. Raw bagasse (wet condition) was used to determine proximate analysis. Table 3.12 shows the physicochemical properties of the raw biomass. The volatile matter, ash content and fixed carbon were 76 wt%, 4 wt% and 10 wt%, respectively. The high heating value (HHV) and low heating value (LHV) were estimated by the elemental composition of the biomass. The ultimate analysis indicates that carbon (41.93 wt%) and oxygen (53.39 wt%) are the most abundant elements in the sugarcane bagasse. The calculated HHV was 17.324 MJ/kg and LHV 13.863 MJ/kg. These values are relevant for the energy balance obtained from microwave pyrolysis.

Table 3.12. Physicochemical properties of raw sugarcane bagasse.

Biomass raw material properties, wt%	**Sugarcane bagasse**
Moisture content	9.9
Ash Content	4
Volatile matter	76
Fixed carbon	10
Elemental composition, wt%	
C	41.93
H	5.47
N	0.21
O	53.39
HHV, MJ/kg	17.324
LHV, MJ/kg	13.863

The microwave absorbance of sugarcane bagasse is represented by the loss tangent (tanδ), which is around 0.161 (Liyana et al., 2012). Biomass moisture content directly impacts the tanδ value due to the high microwave absorbance of water (tanδ = 0.12) (Zhang et al., 2017b). High moisture content can lead to a high tanδ value and increased bio-oil yield with an elevated aqueous fraction. Nevertheless, the moisture existing in the biomass is evaporated during the microwave conversion process, generating bio-oil with high aqueous fractions and low heating value (Ethaib et al., 2020; Giorcelli et al., 2021; Zhang et al., 2017a).

Thermal degradation of the fibre composition of sugarcane bagasse starts between 200 °C to 400 °C (Najeeb et al., 2021). Below 100 °C temperature, there is a mass loss associated with the moisture content of raw biomass (Gomes, 2018; Najeeb et al., 2021). Figure 3.8 shows the thermogravimetric curve of sugarcane bagasse used in the experiments. Studies in literature

show a steady and gradual degradation of biomass when the temperature and power are sufficient to initiate the decomposition of the lignin component, which is between 350 °C and 900 °C (Dai et al., 2020; Shi et al., 2020b; Zi et al., 2019a). However, the thermal breakdown of hemicellulose and cellulose is quicker than the lignin component, e.g., between 250 °C to 350 °C and 350 °C to 500 °C, respectively (Dai et al., 2020; Zi et al., 2019a). Therefore, using microwave pyrolysis, an optimal operating temperature of sugarcane bagasse is reported at over 400 °C.

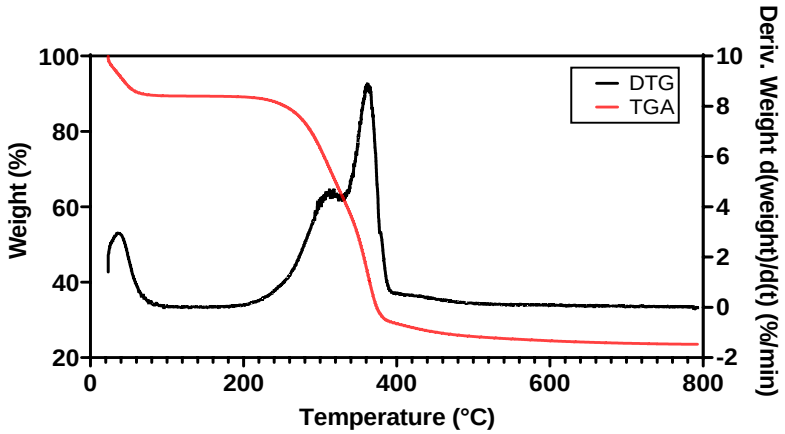

Figure 3.8. TGA and DTG of raw sugarcane bagasse

3.2.2 Microwave-assisted pyrolysis system and experimental procedure.

Figure 3.9 illustrates the microwave-assisted pyrolysis mechanism. The custom-made prototype was designed to process up to 5 kg of biomass (pilot-scale production). The system consists of a 3 kW microwave generator, an auto-tuner for impedance matching, a chamber where the biomass is pyrolysed, a vacuum pump, and various condensers for collecting biogas and bio-oil. Once the system is loaded with the biomass, the air is removed from the pyrolysis system using the rotary vacuum pump and purged with nitrogen gas. Between 5 and 6 $Lmin^{-1}$ of nitrogen gas was applied, preserving an inert atmosphere during experiments. The negative pressure generated inside the chamber is around 25 to 10 kPa. The vacuum pump allows extract gases from the reactor and then condenses them. Thus, more pyrolysis volatile

condensation is generated under a vacuum environment, contributing to oil production. Ranges of microwave power and treatment time were established using the controller.

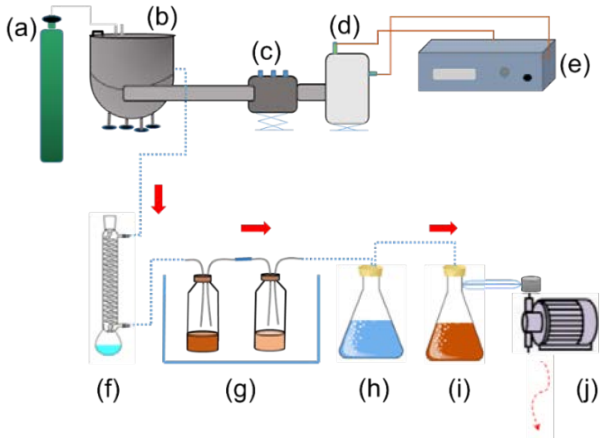

Figure 3.9. Components of microwave pyrolysis system. (a) nitrogen cylinder; (b) chamber; (c) tuner; (d) microwave generator; (e) controller; (f) condenser; (g) biogas flask in an ice bath, (h) biogas purification flask; (i) bio-oil flask; (j) vacuum pump.

- **Characterisation technique and optimisation**

The elemental analysis was collected using CHNS FlashSMART, scanning electron microscopy performance on JEOL 7001F SEM. Thermogravimetric analysis (TGA) of SCB, biochar and bio-oil was conducted by Netzsch STA 449F3 Jupiter Simultaneous Thermal Analyser. Then, biochar surface area was measured using a micromeritics 3-flex surface and porosity analyser. Bio-oil functional groups were achieved by the ATD-GC–MS system (Toluene D8 as an internal standard). Biogas compounds analysis was developed using Shimadzu GC 2030 gas chromatograph. The optimisation analysis was conducted by response surface methodology (RSM), and its statistical model was designed using DOE and ANOVA (Minitab).

- **Synthesis of by-products**

This research was established by the modification of operating conditions, e.g., microwave power (kW), microwave-heating susceptor (%), and residence time (min). To identify the maximum by-product yield and their global energy efficiency, the same setting range in experimental conditions was considered for all 45 experiments, which produced the by-products. The experimental design consisted of five microwave power ranges and three residence time and microwave susceptor additions. The SCB biochar generated from microwave pyrolysis was used as a microwave susceptor.

The input microwave power varied from 1 kW to 3 kW, increasing by 500 W in every experimental pyrolysis treatment. The residence times were 30, 40 and 50 min, and the microwave susceptor was 10 %, 15 % and 20 %. A representative by-product yield was reached by repeating the experimental procedure four times. Therefore, the performance of each combination corresponds to the average of four pyrolysis runs. The selection of the optimal yield was based on the maximum value performed in the optimisation process of the three by-products attained in the lowest energy consumption (multivariate analysis of variance), with the independent variables of microwave power, susceptor volume and treatment time. Table 3.13 describes the experimental design for the synthesis of by-products.

Table 3.13. Experimental microwave setup.

Microwave power (kW)	Microwave susceptor (%)	Reaction time (min)
1	10	30, 40 and 50
	15	
	20	
1.5	10	30, 40 and 50
	15	

	20	
2	10	30, 40 and 50
	15	
	20	
2.5	10	30, 40 and 50
	15	
	20	
3	10	30, 40 and 50
	15	
	20	

3.3 Result and Discussion.

3.3.1 Energy operational conditions.

Figure 3.10 shows the resulting yield over the variation of operating conditions. Microwave energy consumption was calculated considering the input microwave power and the reaction time of the conversion process. The electrical energy was estimated by the relationship between energy consumption and the microwave unit efficiency (80 %) (Shi et al., 2020c). Then, the total input energy calculation involves biomass energy value (13.86 MJ/kg), biomass sample weight and electrical energy. The highest input energy value is 3.4 kWh, which consumed electricity at 3 kW for 50 min (2.5 kWh energy consumption).

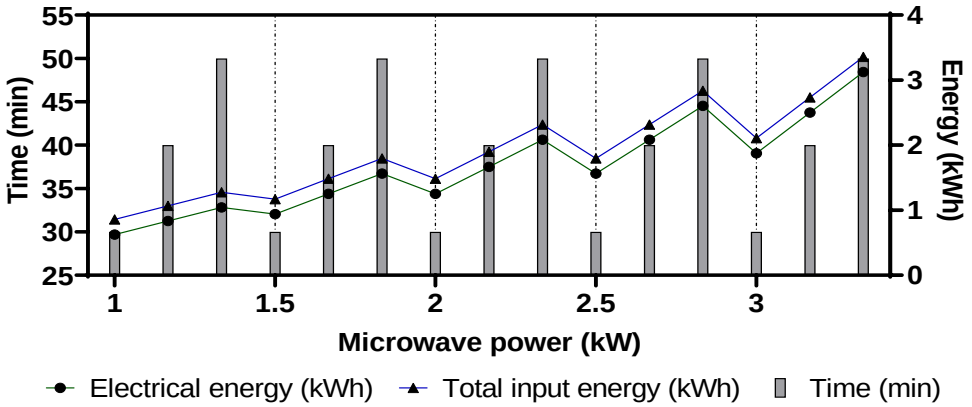

Figure 3.10. Operating conditions of microwave pyrolysis system.

3.3.2 By-products optimisation.

3.3.2.1 Biochar yield optimisation.

Figure 3.11 shows biochar optimisation, and Table 3.14 describes the general linear model from the microwave pyrolysis process. The highest biochar yield was 38.1 % at 1 kW for 40 min of treatment time and 10 % microwave susceptor. The second highest yield was 37.9.1 % at 1.5 kW for 30 min and 10 % susceptor content. Literature reports that low power decreased microwave susceptor addition and longer residence time are the desirable conditions to obtain a higher biochar yield due to the gradual thermal decomposition of the biomass and low heating rates (Idris et al., 2022; Shi et al., 2020a). This statement is confirmed by observing the biochar behaviour. When the reaction time was increased from 30 to 40 min at 1 kW, biochar yield increased by 43 %, considering a reduction of microwave susceptor from 20 % to 10 %. However, an excessive treatment time leads to the devolatilization of biomass and biochar by the excess pyrolysis temperature. Secondary pyrolysis reactions cause permanent gaseous formation, facilitating carbonization and reducing the biochar mass (Cong et al., 2018; Zhang et al., 2017a). For instance, when the residence time increased from 30 to 50 min, the biochar yield was reduced by 16 %, assuming a 20 % microwave susceptor and 1.5 kW.

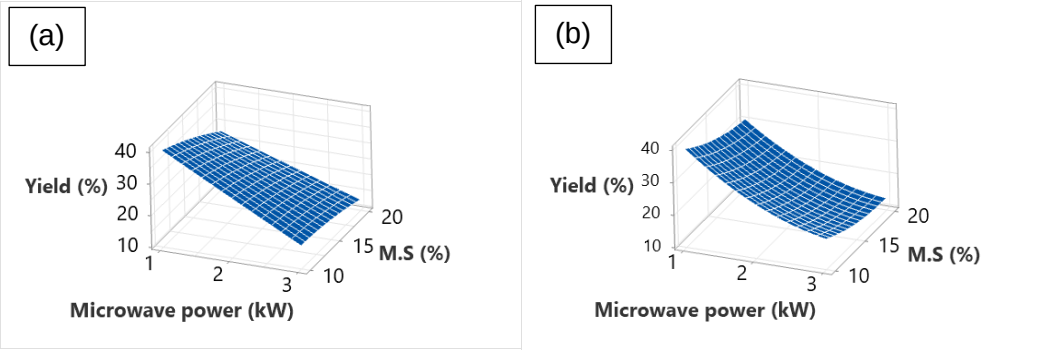

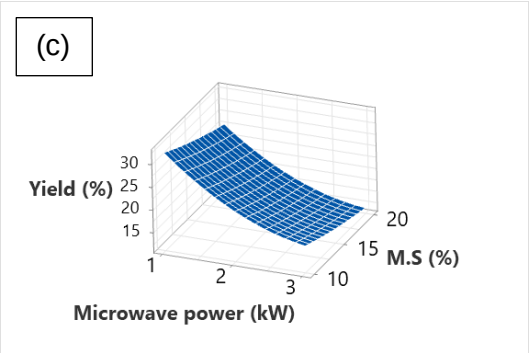

Figure 3.11. Response surface plot of biochar yield under (a) 30, (b) 40, and (c) 50 minutes of microwave pyrolysis.

Table 3.14. Regression equation of biochar yield versus reaction time, microwave power and microwave susceptor.

	R-sq (%)
B.C_Y(%)=22.685+1.906 *A*+ 0.757*B*- 2.663 *C* + 9.273 *D* + 5.133 *E*- 1.312 *F*- 5.765 *G*- 7.328 *H*+ 3.695 *I*- 0.267 *J* - 3.428 *K*	0.9406

A: Reaction time (min)_30; *B*: Reaction time (min)_40; *C:* Reaction time (min)_50; *D:* Microwave power (kW)_1.0; *E*: Microwave power (kW)_1.5; *F*: Microwave power (kW)_2.0; G: Microwave power (kW)_2.5; *H*: Microwave power (kW)_3.0; *I*: Microwave susceptor (%)_10; *J:* Microwave susceptor (%)_15; *K*: Microwave susceptor (%)_20.

Results evidence that a lower biochar yield was obtained at 3 kW at various residence times and 20 % susceptor, achieving between 11.9 and 13.67 wt%. High susceptor addition and increased microwave power produce low biochar yield. These operating conditions contribute to increased heating rates and facilitate the formation of volatiles from the bagasse and the thermal breakdown of heavy hydrocarbon, generating more liquid and gas compounds (Li et al., 2018; Sakhiya et al., 2020; Zhang et al., 2017a). However, higher M.S. addition and lower power (1–1.5 kW) induced better yield (49 % higher) than 3 kW. Regardless of the low pyrolysis power, higher susceptor addition enhances the microwave absorption and accelerates the biomass breakdown without exceeding the heating beyond the devolatilization of biochar (Agu

et al., 2022; Kadlimatti et al., 2019; Zhang et al., 2017a). This finding is validated by some studies reported in (S and Paramasivan, 2021; Zhang et al., 2017a).

The mass loss of feedstock is generated by two factors: water loss and organic matter decomposition. In the carbonization stage, the liquid and gaseous products are produced. Both yields depend on raw biomass properties, such as volatile matter and water content (Kosakowski et al., 2020). Moreover, inorganic substances and the moisture content in the biomass have a considerable impact on the quality and yield of biochar (Mierzwa-Hersztek et al., 2019). Biomass with high water content pyrolysed using high power causes higher energy release, enhancing the decomposition and depolymerization of lignocellulosic compounds. At the same time, higher input power advances the presence of moisture in the biochar pores, reducing its heating value (Shin Ying Foong, 2020; Zhang et al., 2017a).

3.3.2.2 Bio-oil yield optimisation.

Some studies reported that higher power and longer treatment time are optimal biomass treatments to achieve higher bio-oil yield (Suriapparao et al., 2015b). Nevertheless, maximum operational conditions were not always desirable parameters to obtain the highest bio-oil yield, which can lead to a critical secondary breakdown of oil components into non-condensable volatiles (Kadlimatti et al., 2019; S.Mutsengerere et al., 2019; Shi et al., 2020b). The results showed that the highest bio-oil yield was 25.37 wt% attained at 2 kW, 30 min of residence time and 10 % M.S. Bio-oil yield improved when more energy was released in the conversion process generating a breakdown of the organic bonds of SCB forming liquid products (condensable gases) (Y. Zhang et al., 2017). Then, 2 kW was enough microwave power to complete the pyrolysis process and reach the optimal bio-oil temperature (Yaning Zhang,

2017). Figure 3.12 shows bio-oil yields from the microwave-assisted conversion process, and its respective regression equation is described in Table 3.15.

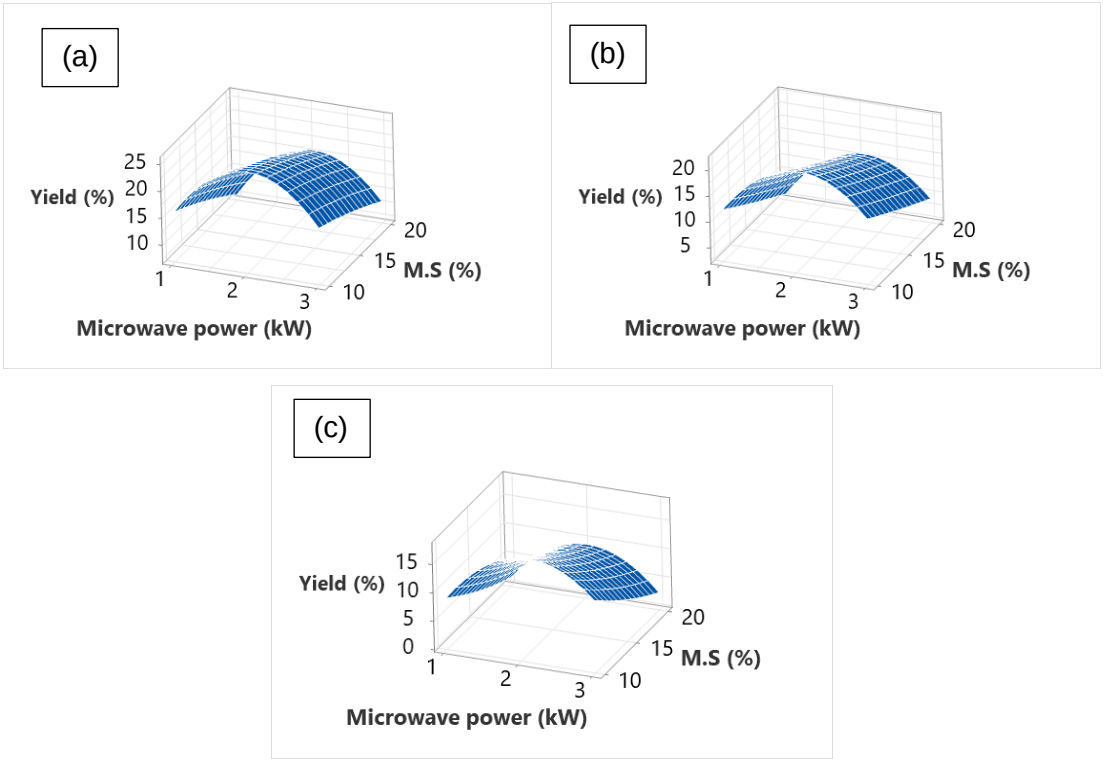

Figure 3.12. Response surface plot of bio-oil yield under (a) 30, (b) 40, and (c) 50 minutes of microwave pyrolysis.

Table 3.15. Regression equation of bio-oil yield versus reaction time, microwave power and microwave susceptor.

	R-sq (%)
B.O_Y(%)=13.450+3.946*A*-0.204*B*-3.742*C*-.512D+1.190*E*+5.331*F*+1.267*G*-2.276*H*+4.102*I*-0.082*J*-4.019*K*	0.9729

A: Reaction time (min)_30; *B*: Reaction time (min)_40; *C*: Reaction time (min)_50; *D*: Microwave power (kW)_1.0; *E*: Microwave power (kW)_1.5; *F*: Microwave power (kW)_2.0; *G*: Microwave power (kW)_2.5; *H*: Microwave power (kW)_3.0; *I*: Microwave susceptor (%)_10; *J*: Microwave susceptor (%)_15; *K*: Microwave susceptor (%)_20.

The increased input power and high susceptor improving the residence time to reach the heating rate, high pyrolysis temperature led to low bio-oil yield (Khelfa et al., 2020;

S.Mutsengerere et al., 2019; Y. Zhang et al., 2017). This asseveration can be confirmed by observing the variation of bio-oil performance from 2 kW to 3 kW, obtaining a reduction yield of 63 %. The excess pyrolysis temperature generated by the higher microwave power or/and microwave susceptor addition involves higher temperatures beyond the optimal condition for bio-oil production, reducing the solid and liquid products but increasing gas formation (Kadlimatti et al., 2019; Yaning Zhang, 2017). Therefore, there was a higher production of low molecular weight compounds due to the second breakdown of condensable vapours into syngas generation (Yaning Zhang, 2017).

The microwave susceptor produces oxygen migration from the condensable bio-oil to the non-condensable gases, inducing low bio-oil yield and high biogas production (Shi et al., 2020b). The resulting optimisation showed a bio-oil yield reduction of 49 % by increasing the susceptor from 10 % to 20 %, operating at 2 kW for 30 min. Moreover, an appropriate residence time is required to complete the microwave pyrolysis process and reach the optimal pyrolysis temperature, promoting the decomposition of biomass compounds (increased chemical reactions), like a breakdown of organic bonds of biomass to produce condensable gases. Increased residence time from 30 to 40 min and input power from 1 kW to 1.5 kW with a 10 % M.S. conducted to an increased bio-oil yield of 7 %. However, increasing the treatment time to 50 minutes caused a decreased bio-oil yield of 18 %. Longer pyrolysis time promotes organic volatile formation due to the devolatilization of biomass. An extended thermochemical decomposition reached higher pyrolysis temperatures than were desirable, causing non-condensable gas formation. Previous studies reported a critical temperature of over 550 °C (Kadlimatti et al., 2019; Lin and W.Chen, 2015). Hence, the optimal residence time for bio-oil production varied based on diverse factors associated with input power and the susceptor ratio (Y. Zhang et al., 2017).

The moisture content of the biomass used in the microwave pyrolysis process has a crucial impact on the yield and quality of the bio-oil (Ethaib et al., 2020). High moisture content can improve the bio-oil yield. However, a significant proportion of liquid products involves light oil with a high aqueous concentration, as water and hydro-soluble compounds (Ethaib et al., 2020; Giorcelli et al., 2021; Zhang et al., 2017a). The aqueous fraction in bio-oil can be generated by chemical reactions associated with the microwave pyrolysis process (Yaning Zhang, 2017). For example, the aqueous fraction can come from the thermal decomposition of lignocellulosic compounds, low molecular weight acids and aldehydes (Budarin et al., 2015). Bio-oil quality is affected by the presence of water due to its low heating value (Yaning Zhang, 2017).

3.3.2.3 Biogas yield optimisation.

Figure 3.13 shows the biogas yield distribution, and Table 3.16 indicates the general linear model of the biogas yield optimisation. The highest biogas yield was 84.43 wt% and 80.19 wt%. These yields were obtained at various operational parameters. The first optimisation was at 3 kW with a 20% microwave susceptor for 50 min, achieving 84.43 wt%. The second stage involved exposing the biomass to 3 kW with 20% M.S for 40 min, obtaining a 76.93 wt% biogas yield. Nonetheless, the lowest yield was 51.67 wt% at 2 kW with 15% microwave susceptor for 30 min.

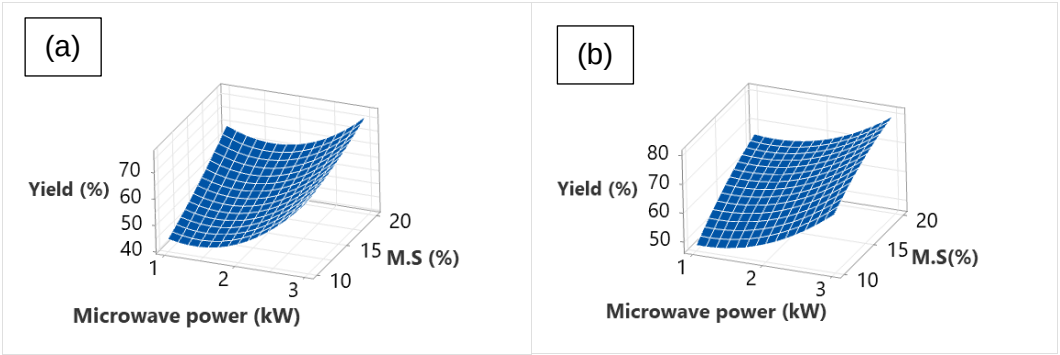

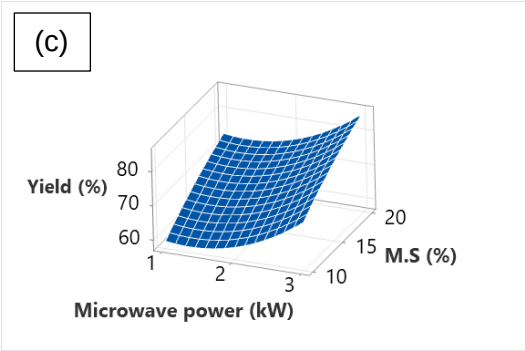

Figure 3.13. Response surface plot of biogas yield under (a) 30, (b) 40, and (c) 50 minutes of microwave pyrolysis.

Table 3.16. Regression equation of biogas yield versus reaction time, microwave power and microwave susceptor.

	R-sq (%)
B.G_Y(%)=63.865-5.852*A*-0.553*B*+6.406*C*-3.761*D*-6.323*E*-4.020*F* +4.498*G* +9.605*H*-7.796*I*+0.350*J*+7.447*K*	0.9729

A: Reaction time (min)_30; *B:* Reaction time (min)_40; *C*: Reaction time (min)_50; *D*: Microwave power (kW)_1.0; *E*: Microwave power (kW)_1.5; *F*: Microwave power (kW)_2.0; *G*: Microwave power (kW)_2.5; *H*: Microwave power (kW)_3.0; *I*: Microwave susceptor (%)_10; *J:* Microwave susceptor (%)_15; *K*: Microwave susceptor (%)_20.

The results show that time is a relevant factor in biogas yield, where the conversion process must be long enough to complete the biomass pyrolysis (Y. Zhang et al., 2017; Zhang et al., 2017a). Short treatment time and low power are not the optimal parameters to achieve a high by-product yield due to the impossibility of reaching the ideal pyrolysis temperature in a short time and the breakdown of lignocellulosic biomass compounds. In contrast, prolonged pyrolysis and high microwave power promote low molecular weight compounds, leading to secondary reactions, where condensable vapours generated in the chamber are decomposed into syngas components, increasing the biogas yield (Kadlimatti et al., 2019; Yaning Zhang, 2017). For example, the lowest biogas yield was increased by 14 % when residence time was prolonged from 30 to 50 min, considering treatment settings of 1.5 kW and 10 % susceptor.

The combination of high input power and high microwave susceptor content provokes an increased heating rate, facilitating biogas formation. High heat release induces the decomposition of heavy intermediate vapours into non-condensable gases (Kadlimatti et al., 2019; Supramono et al., 2015). The result shows that biogas yield increased by 40 % when the power increased from 1 kW to 3 kW, considering 10 % susceptor and 30 min of treatment time. Moreover, by increasing the susceptor concentration from 10 % to 20 %, the biogas yield increased by 34 wt% at 1 kW and 40 min of residence time. Another influencing factor was the moisture of the raw biomass, which promotes syngas production. Biomass water content contributes to microwave absorbance because of its high tanδ value of 0.12, generating a higher temperature increase rate in the early stage of the pyrolysis process related to water evaporation (Yaning Zhang, 2017). Therefore, the biomass moisture content can improve the volatilization process due to the breakdown of liquid products (secondary reactions), forming permanent gaseous compounds ((Yaning Zhang, 2017). In this case, the raw biomass applied in the experiments has no pre-drying pre-treatment.

3.3.3 By-products characterisation.

3.3.3.1 Biochar analysis.

To better understand the effect of the microwave pyrolysis process on the biochar quality, CHNS elemental analysis was undertaken. The microwave pyrolysis parameters and ultimate analysis are shown in Table 3.17. The results demonstrate that a high pyrolysis power produces biochar with high carbon content and low oxygen and nitrogen presence. This phenomenon is due to the high input power, which leads to more breakdown of chemical bonds, e.g., C—O and C—H (Shin Ying Foong, 2020; Wallace et al., 2019b). For example, the biochar generated at 2 kW, 10 % microwave susceptor and 30 min of pyrolysis resulted in the

highest carbon content (57 %) and the lowest oxygen concentration (39 %). Unlike the biochar produced at 2 kW power, 40 min reaction time and 20 % M.S. resulted in the lowest carbon content (27 %) and the highest oxygen presence (72 %). A higher concentration of microwave susceptor (20 %) produced higher heating rates, involving less water loss during biomass degradation. Then, a high pyrolysis temperature reached in a shorter reaction time forms more pores, trapping the moisture from the biochar (Shin Ying Foong, 2020; Tomczyk et al., 2020a).

The carbonization (O/C) and aromatization (H/C) degrees were reduced using high microwave power. The lowest H/C ratio (0.01) was reached at 2 kW input power, 40 min of reaction time and 20 % M.S. The scenario of 2 kW, 30 min pyrolysis time and 10 % microwave susceptor achieved the lowest O/C ratio (0.68). Previous studies have reported that the O/C and H/C ratios should be <0.4 and 0.6, respectively (Mierzwa-Hersztek et al., 2019). Reduction of the O/C and H/C ratio is associated with the high aromaticity properties and lower polarity of the biochar generated from the microwave pyrolysis conditions (Tomczyk et al., 2020a). Therefore, high microwave power promotes the carbon and thermal stability of biochar (M.Waqasa et al., 2018; Mierzwa-Hersztek et al., 2019).

Table 3.17. Ultimate analysis of biochar obtained at different operational conditions.

Microwave pyrolysis sample condition	**N%**	**C%**	**H%**	**O*%**	**H/C**	**O/C**	**LHV MJ/kg**
1.5 kW/30min/10%M.S	0.39	55.33	2.56	41.72	0.05	0.75	16.21
2 kW/30min/10%M.S	0.36	57.61	3	39.03	0.05	0.68	18.22
2 kW/30min/15%M.S	0.24	37.75	0.37	61.64	0.01	1.63	2.97
1 kW/30min/20%M.S	0.3	36.29	0.7	62.71	0.02	1.73	2.88
1 kW/40min/10%M.S	0.48	44.07	1.48	53.97	0.03	1.22	8.39
2 kW/40min/20%M.S	0.16	27.33	0.28	72.23	0.01	2.64	2.14

3 kW/30min/20%M.S	0.4	54.6	1.34	43.66	0.02	0.80	13.468

O*, oxygen was calculated employing the difference between the total percentage and all the remaining elements.

Apart from biochar yield, the variation of microwave power, reaction time, and microwave susceptor also affected the heating value of the biochar due to the thermal decomposition of lignocellulosic compounds (Huang et al., 2016b; Nizamuddin et al., 2018). The heating values of cellulose and hemicellulose are much lower than lignin. Therefore, the volatilization of those components in the biomass contributes to the biochar heating value. There is a higher thermal breakdown of cellulose and hemicellulose content at a low microwave power but not very much cracking of lignin components, thus increasing the biochar heating value (Huang et al., 2016b). Moreover, high oxygen content causes a significant reduction in the biochar heating value, affecting its quality as fuel (Nizamuddin et al., 2018). For example, the results show that the highest biochar LHV (18.22 MJ/kg) was obtained at 2 kW power, 30 min of pyrolysis and 10 % microwave susceptor, which also represents the highest carbon content (57.61 %) and the lowest oxygen concentration (39.03 %). However, 2.14 MJ/kg was the lowest heating value attained, representing only 27.23 % oxygen content.

Figure 3.14 and Figure 3.15 show the combustion and thermal performance of biochar generated from different microwave pyrolysis conditions. The decomposition stability is represented in the thermogravimetric analysis (TGA) and derivative thermogravimetry (DTG). The graph shows that biochar produced at higher microwave power (2 kW) presents less weight loss at the early stage (3 %), between 100 and 150 °C. However, low input power (1 kW) causes slightly higher weight loss (5 %). Moreover, higher power generates more weight loss at a later stage of the pyrolysis reaction than low power. A weight loss of 21 % and 24 % for the samples produced at 1.5 kW and 2 kW was observed at range temperatures of 350–750 °C, respectively. The mass loss increase at high temperatures was due to the thermal

decomposition of the lignin and inorganic compounds and the high moisture removal from the biochar at high pyrolysis power (Brickler et al., 2021b; Nizamuddin et al., 2018). Therefore, high pyrolysis temperatures cause more thermal stability of the biochar (Mohammed et al., 2015).

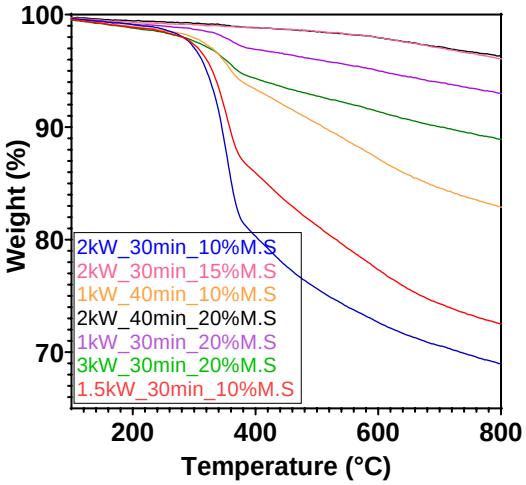

Figure 3.14. TGA curve of biochar generated at different microwave power, reaction time and microwave susceptor.

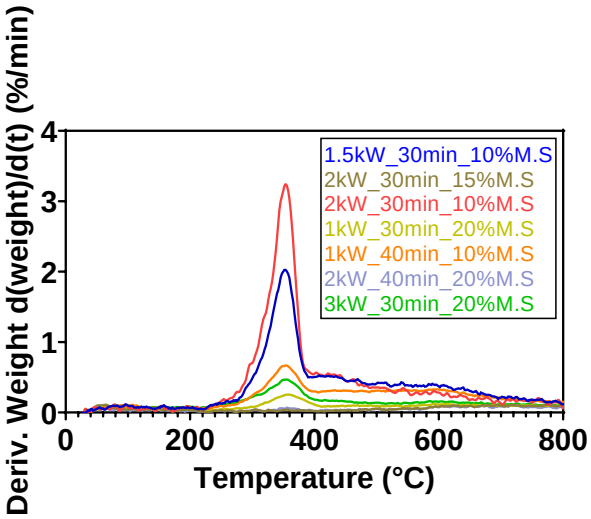

Figure 3.15. DTG curve of biochar generated at different microwave power, reaction time and microwave susceptor.

The DTG curve shows the difference in the thermal peak quantity of biochar. The first peak was obtained between 250 °C to 400 °C, which involves the degradation of cellulose and hemicellulose components. High microwave power promotes the volatilization of biochar,

which is associated with dehydrogenation and aromatization (Mohammed et al., 2015). For example, there was a 94.4 % difference in the thermal peak between the raw biomass and the biochar obtained at 3 kW, 30 min of pyrolysis and 20 % microwave susceptor. However, 2 kW and 10 % microwave susceptor achieved only 59 % volatilization.

The structural porosity and morphology of biochar generated from microwave pyrolysis have a higher surface area and pore volume (Leng et al., 2021). Figure 3.16 shows the SEM image of sugarcane bagasse biochar at different microwave operational conditions. Figure 3.16 (a) and (c) demonstrate that the biochar produced at high pyrolysis power presents lower pore breakdown due to the quick release of volatiles during the increased heating rates. The biochar samples generated at over 1.5 kW have a small pore size, higher pore volume, higher externally accessible surface area and higher mass loss (Brickler et al., 2021b; Nizamuddin et al., 2018; Tomczyk et al., 2020a; Wallace et al., 2019b). Moreover, high input power allows more energy production due to the breakdown of C-O bonds, generating the fragmentation, depolymerization, and decomposition of organic matter associated with lignocellulosic biomass (Shin Ying Foong, 2020). Figure 3.16 (b) reveals that low microwave power caused a gradual thermal decomposition of biomass, reducing the blocking of pore formation and decreasing the mass loss (Shin Ying Foong, 2020; Wallace et al., 2019b).

Table 3.18. BET data of biochar obtained at different operational conditions.

Analysis	**BCa**	**BCb**	**BCc**	**BCd**	**BCe**	**BCf**	**BCg**
Surface area (m^2/g)							
BET Surface Area	121.78	131.23	211.60	197.03	202.16	157.29	139.29
t-Plot micropore Area	65.03		140.46	126.38	136.56	94.36	67.94
t-Plot external surface area	56.76	14.65	71.13	70.65	65.60	62.92	71.34

BJH Adsorption cumulative surface area of pores	25.24	8.93	31.79	31.12	26.03	35.23	18.95
Pore volume (cm^3/g)							
t-Plot micropore volume	0.03	0.00	0.06	0.05	0.05	0.04	0.03
Total pore volume calculated <1.0228nm	0.04	0.00	0.07	0.06	0.07	0.05	0.04

BCa: Biochar generated at 1.5 kW/30min/10%M.S; BCb: Biochar generated at 2 kW/30min/10%M.S; BCc: Biochar generated at 2 kW/30min/15%M.S; BCd: Biochar generated at 1 kW/30min/20%M.S; BCe: Biochar generated at 1 kW/40min/10%M.S; BCf: Biochar generated at 2 kW/40min/20%M.S; BCg: Biochar generated at 3 kW/30min/20%M.S.

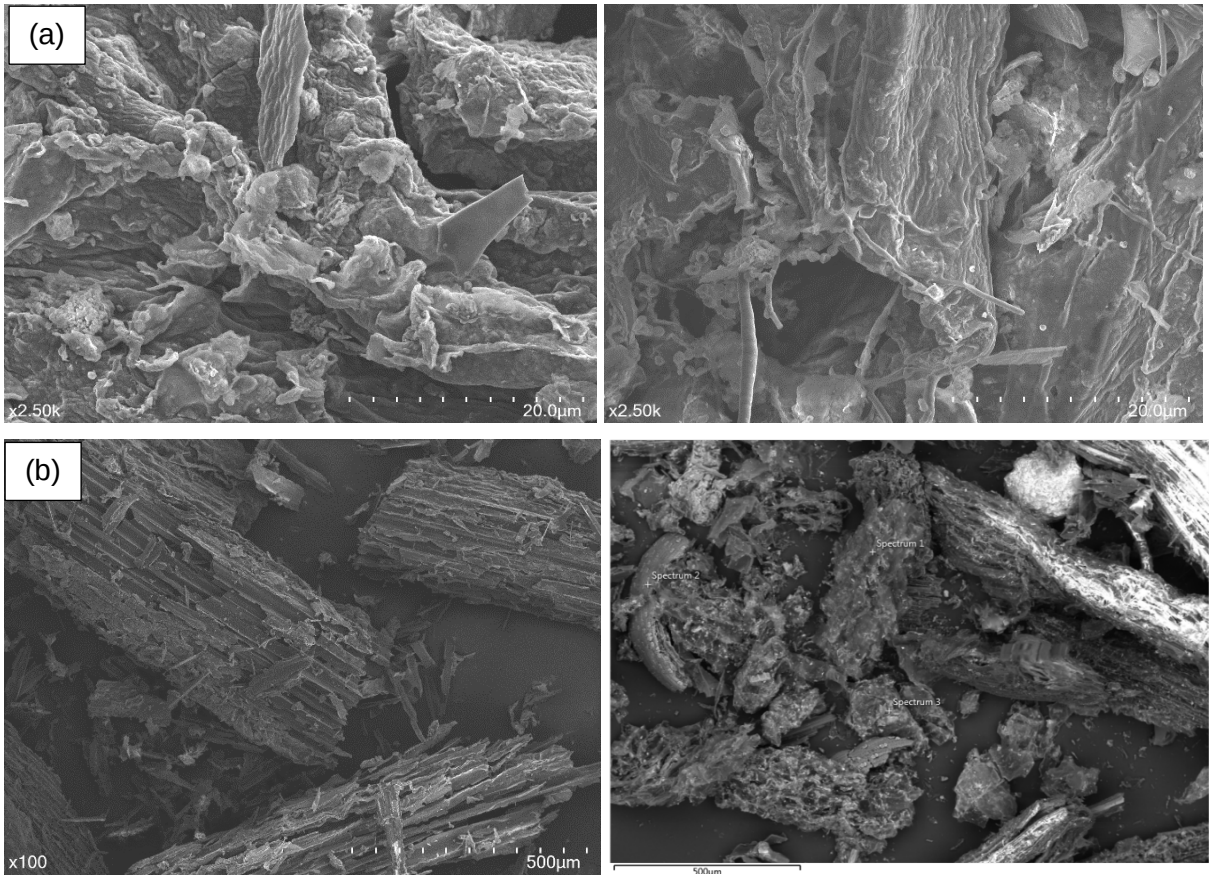

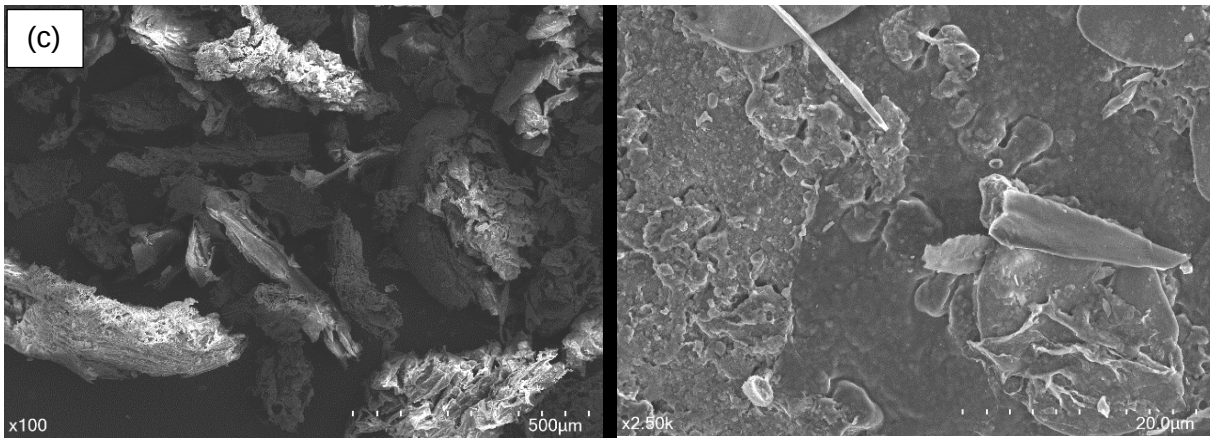

Figure 3.16. Scanning Electron Microscope (SEM) images of sugarcane bagasse biochar, generated at (a) 1.5 kW for 30 minutes and 10% microwave susceptor; (b) 1 kW for 40 minutes and 10% microwave susceptor; (c) 2 kW for 30 minutes and 10% microwave susceptor.

Diverse studies have reported that biochar, generated from microwave pyrolysis, presents a higher BET surface area and pore volume than conventional pyrolysis (Selvam S and Paramasivan, 2022; Suriapparao et al., 2022b). Those properties determine the biochar quality for a combustion process (Halim and Swithenbank, 2016; Li et al., 2016; Sieng-Huat Kong; Su Shiung Lam; Peter Nai Yuh Yek; Rock Keey Liew; Nyuk Ling Ma; Mohammad Shahril Osman; Chee Chung Wong, 2018; Wallace et al., 2019b). Table 3.18 indicates the surface area properties of the biochar optimisation. Results show that high microwave power and longer treatment time are the optimal conditions for obtaining a higher BET surface area, adsorption efficiency and micropore volume. For example, the surface area improved by 74% (cases BCa and BCc) when the microwave power and the microwave susceptor increased from 1.5 kW to 2 kW and 10% to 15%, respectively.

Higher power leads to a structural modification of the biochar pores due to the high volatilization of larger molecules and the rapid release of small molecules (volatile matter) generated by the increased pyrolysis temperature (Halim and Swithenbank, 2016; Li et al., 2016). For instance, high lignin decomposition promotes the quick release of H_2 and CH_4 and aromatic condensation. These conditions result in better surface pore formation during

microwave pyrolysis (Mierzwa-Hersztek et al., 2019; Tomczyk et al., 2020a). On the other hand, the increment of microwave susceptor and treatment time promote higher heat energy, releasing more volatiles from the surface of the sugarcane bagasse, and increasing the area and volume of the biochar. This characteristic is related to the fragmentation, depolymerization and cracking of lignocellulosic compounds (Shin Ying Foong, 2020; Zhang et al., 2017a). Higher pyrolysis heat energy leads to higher carbon stability (M.Waqasa et al., 2018). The surface area increased by 3 % when the treatment time was incremented by 10 min (cases BCe and BCd). Then, the BET surface area improved by 62 % when the microwave susceptor increased from 10 % to 20 % (cases BCa and BCd).

A low BET surface area is produced when biomass presents a high content of inorganic compounds, which can block the micropores in the biochar surface (Tomczyk et al., 2020a). Another factor in the surface area reduction is elevated power, which can lead to excessive pyrolysis temperature, generating destruction in the biochar structure. In terms of morphologies, the biochar has agglomerates of hexagonal prism-shaped (rough surface) (Halim and Swithenbank, 2016; Shin Ying Foong, 2020). The work reported by (Leng et al., 2021) affirmed that if the temperature is not high enough (above 400 °C), the pyrolysis process won't be completed, reducing the volatile generation and pore formation. For example, sample BCb obtained the lowest surface area (11.23 m^2/g) due to short pyrolysis time and low microwave susceptor were insufficient to cause the release of volatiles.

3.3.3.2 Bio-oil analysis.

Table 3.19 shows the elemental components of bio-oil produced at different microwave power, reaction time and microwave susceptor (M.S) combinations. The results show a variation in carbon, oxygen and hydrogen content based on the increment of the microwave operational

conditions. For instance, the lowest oxygen content (34.41 %) was obtained at 2 kW, 40 min of pyrolysis and 20 % microwave susceptor. However, the highest oxygen content (42.59 %) was produced at 1 kW, 30 min of pyrolysis and 20 % susceptor. The main reason for this phenomenon is the deoxygenation reaction of the raw biomass generated at high microwave power, which reduces the number of functional groups during pyrolysis (Ferrera-Lorenzo et al., 2014). At the same time, a higher H/C value was achieved with lower microwave power and reaction time, involving an increase in the aliphatic group due to the decrease in microwave heating. In contrast, a lower H/C ratio was obtained with higher microwave power, higher reaction time and microwave susceptor, whose effects in bio-oil resulted in higher aromatic content (Halim and Swithenbank, 2016).

Table 3.19. Ultimate analysis of bio-oil obtained at different operational conditions.

Microwave pyrolysis sample condition	**N%**	**C%**	**H%**	**O*%**	**H/C**	**O/C**	**LHV (MJ/kg)**
1.5kW/30min/10%M.S	0.33	55.25	5.88	38.54	9.40	0.70	29.89
2kW/30min/10%M.S	0.44	55.46	6.11	37.99	9.08	0.68	30.20
2kW/30min/15%M.S	0.56	53.48	5.92	40.04	9.03	0.75	29.50
1kW/30min/20%M.S	0.42	51.39	5.60	42.59	9.18	0.83	28.63
1kW/40min/10%M.S	0.35	55.03	6.10	38.52	9.02	0.70	30.09
2kW/40min/20%M.S	0.45	57.73	7.41	34.41	7.79	0.60	32.24

O*, oxygen was calculated employing the difference between the total percentage and all the remaining elements.

The heating value of bio-oil is directly associated with the elemental composition of bio-oil. Decreasing the oxygen concentration cause increases its heating value due to the chemical reaction related to ketones and aldehyde concentrations. 32.24 MJ/kg was the highest heating value achieved at the lowest oxygen content. High oxygen concentration is associated with

chemical instability, storage permanence, acidity, and immiscibility properties of the bio-oil (Panwar and Paul, 2021; Si et al., 2017).

The elemental analysis can be contrasted by the bio-oil functional groups shown in Table 3.20 and Table 3.21. The bio-oil composition involves carboxylic acid, ketones, aromatic, sugar, phenols, guaiacol, alkanes, alkynes, and alcohol. Microwave pyrolysis produces more phenol compounds due to higher condensation temperature at the early stage (Zhao et al., 2021). Results show that the concentration of phenol groups is 33 % higher in bio-oil samples produced at 1 kW than at 2 kW. The combination of lower power and higher addition of susceptor allowed reaching a higher pyrolysis temperature, leading to the cracking of lignin compounds to the conversion into phenol groups. Hence, higher microwave power leads to the breakdown of phenols, reducing their concentration (Mohammed et al., 2015; Zhao et al., 2021). High phenol content is associated with a higher H/C ratio (Halim and Swithenbank, 2016).

Table 3.20. Distribution of chemical compounds of bio-oil generated at 1 kW during 30 minutes of microwave pyrolysis and 20% M.S.

Classification	Compound	Concentration (microgram/gram)	Concentration (%)
Carboxylic acid	Acetic acid, methyl ester	673	1.54
	Acetic acid	1641	3.76
			5.30
Ketone	2-Butanone	149	0.34
	Benzaldehyde, 4-hydroxy-	380	0.87
			1.21
	Phenol	552	1.26
	Phenol, 3-methyl-	931	2.13
	Phenol, 2,6-dimethyl-	216	0.49
	Creosol	752	1.72

Phenols	Phenol, 4-ethyl-	1623	3.72
	2-Allylphenol	349	0.80
	3,5-Dimethoxy-4-hydroxytoluene	1517	3.47
	Benzaldehyde, 3-hydroxy-4-methoxy-	1406	3.22
	5-tert-Butylpyrogallol	380	0.87
			17.69
Guaiacol	2-Methoxy-4-vinylphenol	126	0.29
	Phenol, 2-methoxy-4-(1-propenyl)-	522	1.20
	Phenol, 2,6-dimethoxy-	2083	4.77
	Phenol, 2,6-dimethoxy-4-(2-propenyl)-	420	0.96
	Phenol, 2,6-dimethoxy-4-(2-propenyl)-	321	0.73
			7.95
Alkanes	Undecane	370	0.85
	Heptane, 2,2,4,6,6-pentamethyl-	1909	4.37
	Cyclotrisiloxane, hexamethyl-	106	0.24
			5.46
Alkynes	Methylcodeine	728	1.67
			1.67
Alcohols	Silane, trimethoxymethyl-	89	0.20
	1-(2-Acetoxyethyl)-3,6-diazahomoadamantan-9-one oxime	322	0.74
	Cyclopropyl carbinol	300	0.69
			1.63
Aromatic	Toluene	274	0.63
	Benzofuran, 2,3-dihydro-	2330	5.33
			5.96
Sugars	2,3-Anhydro-d-galactosan	1670	3.82
	Aminocarb	664	1.52
	Apocynin	401	0.92
	Triacetyl-d-mannosan	2791	6.39

	1,3-Di-O-acetyl-à-á-d-ribopyranose	1027	2.35
	Alpha-D-Glucopyranose, 1,6-anhydro-	16659	38.14
			53.14

Table 3.21. Distribution of chemical compounds of bio-oil generated at 2 kW during 30 minutes of microwave pyrolysis and 10% M.S.

Classification	Compound	Concentration (microgram/gram)	Concentration (%)
Carboxylic acid	Acetic acid, methyl ester	832	0.83
	Acetic acid	2130	2.13
	Hexanoic acid, 2-ethyl-	673	0.67
	3-Isoxazolecarboperoxoic acid, 4,5-dihydro-5-phenyl-, 1,1-	751	0.75
	o-Ethylhydroxylamine	3971	3.98
			8.37
Ketone	2-Butanone	156	0.16
	2-Methyliminoperhydro-1,3-oxazine	1057	1.06
	4-Methyl-2-oxopentanenitrile	1277	1.28
			2.49
Phenols	Phenol	1169	1.17
	Creosol	1488	1.49
	Phenol, 3-methyl-	681	0.68
	Phenol, 2,6-dimethyl-	463	0.46
	Phenol, 4-ethyl-	2648	2.65
	Phenol, 4-ethyl-3-methyl-	618	0.62
	1,2-Benzenediol, 3-methoxy-	743	0.74
	3,5-Dimethoxy-4-hydroxytoluene	2153	2.16

	Benzaldehyde, 3-hydroxy-4-methoxy-	1819	1.82
	5-tert-Butylpyrogallol	623	0.62
	Benzaldehyde, 4-hydroxy-	896	0.90
			13.32
Guaiacol	Phenol, 2,6-dimethoxy-4-(2-propenyl)-	1376	1.38
	Phenol, 2-methoxy-	544	0.54
	2-Methoxy-4-vinylphenol	561	0.56
	Phenol, 2,6-dimethoxy-	3281	3.29
			5.77
Aromatic	Benzofuran, 2,3-dihydro-	5370	5.38
			5.38
Alkanes	Heptane, 2,2,4,6,6-pentamethyl-	660	0.66
	Alpha-Hydroxyquebrachamine	607	0.61
			1.27
Alcohols	1-Decanol, 2-hexyl-	715	0.72
	Silane, trimethoxymethyl-	318	0.32
	Cyclopropyl carbinol	1126	1.13
			2.16
Sugars	1,3-Di-O-acetyl-à-á-d-ribopyranose	1434	1.44
	Aminocarb	876	0.88
	Triacetyl-d-mannosan	5715	5.72
	Apocynin	587	0.59
	Alpha-D-Glucopyranose, 1,6-anhydro-	49663	49.75
	2,3-Anhydro-d-galactosan	2849	2.85
			61.23

Lower microwave power produces slightly higher aromatic content (10 %) due to the higher pyrolysis temperature leading to the breakdown of aromatics, generating more phenol groups (Lyu et al., 2015). The concentration of aromatic groups is related to a high heating value and bio-oil quality because of the low concentration of oxygenated compounds (Khuenkaeo et al., 2021) On the other hand, 2 kW achieved more concentration of sugars (61.23 %), ketones (2.49 %), and carboxyl acid (8.37 %). The higher sugar content is due to the breakdown of cellulose compounds generated with higher microwave power. For example, alpha-d-Glucopyranose, 1,6-anhydro- (49.75 %) is associated with the feedstock type (Lyu et al., 2015; Zhang and Xiong, 2016). Since the pyrolytic sugar has water-solubility properties, it can be removed from the bio-oil by applying some liquid-liquid extraction method. Furthermore, pyrolytic sugar is extracted from bio-oil to convert it into fuels, and by using phenols, it is possible to obtain chemical products, like green diesel and adhesives (Rover, 2013; Yu et al., 2016).

Ketone groups are generated by the decomposition of hemicellulose (from hexoses) and cellulose compounds. The study reported by (Lyu et al., 2015) established that a high concentration of metal ions can produce a secondary reaction of sugar compounds like levoglucosan and generate ketones. The ketone concentrations increased by 2.5 % when the microwave power increased to 2 kW. This phenomenon is explained by the ketonization reaction, which means that two carboxylic acids are converted into a ketone, carbon dioxide and water by applying higher heat (higher power) (Pham et al., 2013; Wang et al., 2018). At the same time, increased microwave power produced slightly higher carboxylic acid content (37 %) which can represent higher oxygen content, a reduction of storage stability, and increased corrosiveness (Ferrera-Lorenzo et al., 2014; Panwar and Paul, 2021; Si et al., 2017; Wang et al., 2012). Higher carboxylic acid concentration can increase the polarity of bio-oil, involving higher solubility in other polar solvents (Rover, 2013).

Figure 3.17 and Figure 3.18 show the thermogravimetric analysis (TGA) and derivative thermogravimetry analysis (DTG). The results did not show much variation in the thermal deformation between the different bio-oil samples. The initial thermal decomposition happens between 250 °C and 350 °C, which involves moisture evaporation and highly volatile compounds. Also, at that temperature range, hemicellulose degradation occurs (Armando T. Quitain, 2015). The bio-oil generated at 2 kW for 30 min and 10 % microwave susceptor resulted in around 39 % weight loss. Differently, the weight reduction of the bio-oil produced at 1 kW for 30 min and 20 % microwave susceptor was 24 %. The rapid thermal degradation is generated by the volatilization of residual solvent (alcohols), water and light components (Sainab Omar, 2019; Suzanne Anouti, 2016). The last thermal decomposition is between 400 °C and 600 °C conducted by the breakdown of heavy compounds, stability, and lignin degradation (Armando T. Quitain, 2015).

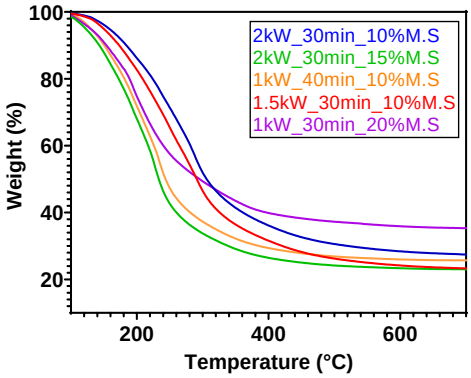

Figure 3.17. TGA curve of bio-oil generated at different microwave power, reaction time and microwave susceptor.

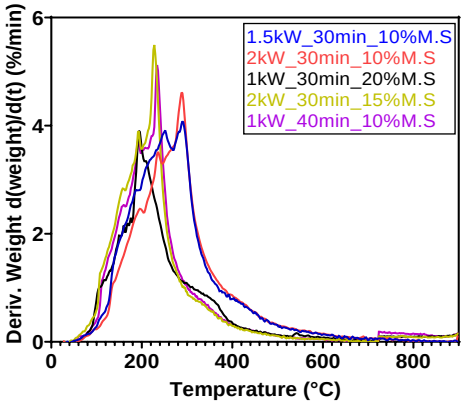

Figure 3.18. DTG curve of bio-oil generated at different microwave power, reaction time and microwave susceptor.

3.3.3.3 Biogas analysis.

Through Gas Chromatograph (Shimadzu GC 2030), it was possible to determine biogas compounds obtained under various operational conditions. Table 3.22 shows the energy values of sugarcane bagasse gas obtained in the pyrolysis process. The biogas yield is directly relative to its heating value due to a higher yield achieved when the secondary breakdown of non-condensable volatiles occurs, increasing the formation of H_2, CO and CH_4. This phenomenon is relative to the self-gasification of the biochar during the high pyrolysis power (Lin and W.Chen, 2015; Shi et al., 2020a; Zhang et al., 2017a).

Table 3.22. Composition and low heating value of six biogas samples at different pyrolysis conditions.

Operational conditions	**CO_2 (% Mol)**	**CH_4 (% Mol)**	**H_2S (%Mol)**	**O_2 (%Mol)**	**N_2 (%Mol)**	**LHV (MJ/kg)**
1.5kW/30min/10%M.S	2.81	0.70	0.08	17.32	78.59	0.251
1kW/40min/10%M.S	2.12	0.57	0.05	17.37	79.39	0.206
2kW/30min/10%M.S	3.86	1.24	0.19	7.54	86.65	0.445
2kW/30min/15%M.S	2.07	0.84	0.07	18.10	78.22	0.302
1kW/30min/20%M.S	2.19	0.66	0.09	17.81	79.24	0.237
2kW/40min/20%M.S	6.89	1.47	0.28	12.78	78.04	0.528

The heating value was calculated considering the H_2, CO and CH_4 formation. Higher methane formation and energy value are obtained using higher microwave power, longer pyrolysis time and higher microwave susceptor. For instance, the biogas heating value generated at 1 kW for 30 minutes was 55% lower than the biogas produced at 2 kW for 40 minutes. Increased microwave power leads to a quicker microwave absorbance capacity of the biochar and

thermochemical reaction. The high presence of a carbon microwave susceptor could produce elevated CO_2 due to the thermal decomposition of methane gas and light hydrocarbons (Shi et al., 2020b). The biogas impurities comprise the H_2S gas associated with the sulphuric and nitrogen content in the formation of pyrolysis gas and its presence in the lignocellulosic biomass (Juan Camilo Solarte-Toro, 2018).

3.3.4 Energy balance of microwave pyrolysis process.

Table 3.23. Recovered energy of sugarcane bagasse by-products using microwave pyrolysis for 65 g of SCB.

By-product optimised	Operational conditions	By-product energy (kWh)			Total output energy (kWh)
		Char	Oil	Gas	
Biochar	1.5kW/30min/10%M.S	0.111	0.119	0.002	0.23
	1kW/40min/10%M.S	0.058	0.068	0.002	0.13
Bio-oil	2kW/30min/10%M.S	0.096	0.138	0.004	0.24
	2kW/30min/15%M.S	0.012	0.129	0.003	0.14
Biogas	1kW/30min/20%M.S	0.014	0.033	0.003	0.05
	2kW/40min/20%M.S	0.007	0.083	0.006	0.1

The output energy of the by-products was calculated considering their heating value, yield, and biomass weight. Table 3.23 shows that the highest total output energy (0.24 kWh) was obtained at 2 kW, 30 minutes of pyrolysis and 10% of microwave susceptor. Mainly, this performance was obtained by the high yield and heating value of bio-oil (0.498 MJ/kg). In contrast, the output energy in by-products generated at 1 kW and 10 % M.S. was 95 % lower than samples produced at 2 kW and 20 % M.S. Low pyrolysis power, short treatment time and high microwave susceptor are not the optimal combinations to achieve the energy by-products.

These operating conditions were insufficient to reach the pyrolysis temperature and complete the thermochemical conversion of lignocellulosic compounds into biochar, bio-oil, and biogas.

Table 3.24. Energy recovery efficiency of microwave pyrolysis system.

B.O*	Microwave power kW	Time, min	E.E** kWh/kg	Electrical consump. kWh	Biomass energy kWh	Total input energy kWh	Energy conversion effic %
	1.5	30	0.8	0.9		1.8	12.6
Biochar	1	40	0.7	0.8		1.7	7.4
	2	30	1.0	1.3	0.9	2.2	11.1
Bio-oil	2	30	1.0	1.3		2.2	6.7
	1	30	0.5	0.6		1.5	3.3
Biogas	2	40	1.3	1.7		2.6	3.8

*B.O: By-product optimised, ** E. E: Energy expended during the microwave pyrolysis of SCB, considering microwave power and treatment time.

The electrical consumption of the microwave pyrolysis system was calculated considering the input power, treatment time, and 80% electrical efficiency conversion of the microwave pyrolysis process. On the other hand, the biomass energy was obtained by the heating value of the SCB and the sample weight (65 grams). The total input energy was calculated assuming the energy supplied by the microwave system and the biomass. Table 3.24 shows the different energy recovery values obtained from the optimisation process. The results showed a significant energy difference between the operating combinations of the microwave system. The energy conversion efficiency for the samples generated at 1 kW/30 min/20%M.S. and 2 kW/40 min/20%M.S. were 74 % and 70 % lower than the setting scenario of 1.5 kW for 30 min and 10 % M.S., respectively. In this way, a longer treatment time or low input power is not necessarily convenient for reaching higher energy efficiency. It is important to note that this

optimal operational energy condition is relative to the required quality of each by-product. For example, a higher biochar quality is achieved using low power and longer treatment time, but better bio-oil properties (HHV, oxygen content, and aromatic functional groups) are developed at higher power and longer pyrolysis time.

The output energy of the by-products showed that biomass exposed at 2 kW for 30 min and 10 % microwave susceptor obtained the highest output energy (0.24 kWh), with bio-oil representing 68 % of the total energy value. The bio-oil quality analysis showed that increasing pyrolysis temperature increased ketones functional groups concentration by up to 2.5 %, improving its quality. The highest biochar output energy was obtained at 1.5 kW/30 min/10%M.S., considering 37.16 % yield, 0.21 MJ/kg LHV, 55.33 % carbon and 41.72 % oxygen content. The same setting operating parameters achieved optimal energy recovery (12.6 %).

3.3.5 Economic analysis.

The economic analysis is based on the lab-scale microwave pyrolysis system. Table 3.25 shows the economic analysis of the microwave pyrolysis system. Some operating costs are feedstock, electricity purchased, microwave susceptor and maintenance (0.23 AUD/day) (Lam et al., 2019b). The incurred cost of feedstock and microwave susceptor (M.S) was free because agricultural waste was used as biomass, and biochar produced in the pyrolysis process was utilised as M.S. The average electricity usage rate in Queensland is 20.19 c/kWh (Mullane, 2022). The unit values generated from the by-products are 0.55 AUD/kg biochar (Wang et al., 2015), 1.45 AUD/L bio-oil (Inayat et al., 2022; Wang et al., 2015), and 0.099 AUD/kWh biogas (Wattanasilp et al., 2021). The economic analysis was estimated considering 975 g of biomass and the highest and lowest energy recovery obtained from the pyrolysis

process. The economic balance shows that the income generated at 1 kW was 88 % lower than 1.5 kW pyrolysis power. High-income capacity is associated with the high energy generation of bio-oil (1.8 kWh) and biochar (1.67 kWh). Then, an acceptable utility cost is reached at 1.5 kW, with a total income was $1.28. The microwave pyrolysis system has economic viability and the potential to scale up the energy generation of by-products at low-cost production. Microwave pyrolysis optimisation leads the sustainable development due to its energy efficiency and economic balance (Inayat et al., 2022).

Table 3.25. Techno-economic analysis of the microwave pyrolysis system for 975 grams of biomass.

	1.5kW/30min/10%M.S			**1 kW/30min/20%M.S**		
Item	**Energy (kWh)**	**Value/unit**	**Amount (AUD)**	**Energy (kWh)**	**Value/unit**	**Amount (AUD)**
Feedstock	-	-	-	-	-	-
Microwave susceptor	-	-	-	-	-	-
Electricity consumed	0.9	20.19, (c/kWh)	0.18	0.6	20.19, (c/kWh)	0.12
Maintenance			0.03			0.02
Total operating cost			**0.21**[c]			**0.14**[d]
Item	**Energy (kWh)**	**Value/unit**	**Amount (AUD)**	**Energy (kWh)**	**Value/unit, $/kWh**	**Amount (AUD)**
Biochar, AUD/kg	1.67	0.55	0.89	0.21	0.55	0.11
Bio-oil, AUD/L	1.8	1.45	0.39	0.495	1.45	0.04
Biogas, AUD/kWh	0.03	0.099	0.03	0.045	0.099	0.004

Total income $		**1.28**[e]		**0.15**[f]
Total energy gained kWh	**2.58**		**0.15**	
Total $ gained		**1.07**		**-0.01**

[c] Total operating cost ($) at 1.5 kW/30 min/10%M.S; [d] Total operating cost ($) at 1 kW/30 min/20%M.S; [e] Total income ($) from by-products generated 1.5 kW/30 min/10%M.S; [f] Total income ($) from by-products generated 1 kW/30 min/20%M.S.

The economic analysis indicated that the total income decreased by 88 % when operating conditions changed from 1.5 kW/30 min/10%MS to 1 kW/30 min/20%MS. Therefore, the microwave pyrolysis system has the potential to scale up the energy generation of by-products at low-cost production.

3.3.6 Carbon footprint analysis.

GHG emissions depend on biomass management and energy generation methods. Table 3.26 shows a CO_2 emissions estimation for two different biomass management scenarios and a commonly used method for electricity generation. The evaluation was calculated considering the total biomass used during the experimental phase (65 g) and the highest energy output provided by the by-products at 1.5 kW/30 min/10%M.S. Production of 0.23 kWh, using a coal-based thermal power plant produces 0.314 kg CO_2, considering a factor of 1.57 kg CO_2/kWh (Fodah and Abdelwahab, 2022). Biomass management as stored waste (landfilling) causes the release of 0.004 kgCO_2, as the emission factor of raw feedstock is 57 kg CO_2/t (Cheng et al., 2020). The emission factor for burning 1 kg of biomass is 1.5 kg CO_2 (Fodah et al., 2021), releasing 0.1 kg CO_2 for the indicated sample.

Table 3.26. Life cycle impact of biomass management and energy generation methods.

The energy supplied (kWh)	Biomass (kg)	Biomass as residues kg_CO_2	Incineration kg_CO_2	Power plant kg_CO_2
0.23	0.065	0.004	0.1	0.314

The environmental impact can be prevented by converting biomass into valuable products using microwave pyrolysis. Unlike bio-oil and biogas, biochar has the potential for carbon capture (Mong et al., 2022). Liquid and gaseous by-products are used as biofuels for heat and electricity production. These approaches are not carbon capture (Huang et al., 2015; Mong et al., 2022). However, biochar works as an absorbent for carbon dioxide sequestration due to its affinity to CO_2 (Huang et al., 2015). Figure 3.19 shows the balance of CO_2 adsorption capacity of by-products obtained at 1.5 kW for 30 minutes and 10% M.S. The CO_2 adsorption capacity of biochar was 47.9 CO_2 eq kg^{-1}, whose value was calculated by Equation (1) (Venkatesh et al., 2022). The evaluation of the carbon sequestration of the microwave pyrolysis conversion consists of 37.9% biochar yield ($B.Y$) and 43.1% fixed carbon content (FC).

$$CO_2\ reduction\ potential = B.Y * FC * (\frac{80}{100}) * (\frac{44}{12}) \quad (32)$$

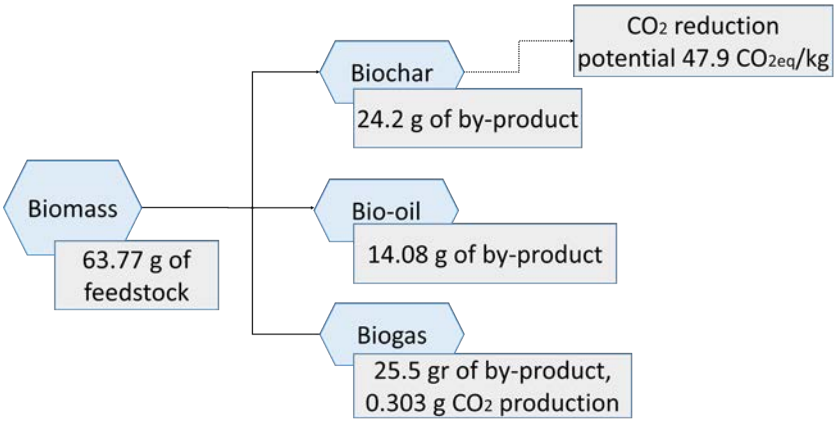

Figure 3.19. Bioenergy yield balance of SCB using microwave pyrolysis and its CO_2 sequestration potential.

The life cycle impact assessment of the microwave pyrolysis by-products indicated a carbon dioxide reduction potential of 47.9 CO_2eq kg^{-1}. Carbon sequestration capacity is related to biochar application, whose purpose is carbon storage.

3.4 Conclusions.

This work substantiated that the breakdown of sugarcane bagasse and the energy recovery under microwave pyrolysis are influenced by the input microwave power, susceptor and treatment time. Higher microwave power and susceptor reduce the biochar yield. These operating conditions contribute to increased heating rates and facilitate the formation of volatiles from the bagasse and the thermal breakdown of heavy hydrocarbon, generating more liquid and gas compounds, which can lead to the critical secondary breakdown of oil components into non-condensable volatiles, and hence could conclude that maximum operational conditions were not always the desirable parameters to obtain the optimal bio-oil yield.

CHAPTER 4

4 PARACETAMOL SENSORS USING ACTIVATED BIOCHAR

Chapter 3 demonstrated that biochar produced from sugarcane bagasse has a good potential to produce activated biochar by its processing with low microwave power and long treatment time. The activation process is complemented by chemical treatment to improve the biochar properties, e.g., carbon content, porosity, morphology, etc. These characteristics make the carbon material suitable for electrochemistry applications by the sensing of molecules. The following chapter presents the synthesis of activated biochar from sugarcane bagasse for the fabrication of an electrochemical sensor using a drop casting technique on the surface of a glassy carbon electrode for paracetamol detection.

Abstract

Agro-industrial waste is an abundant bio-resource which can be used as a feedstock to develop carbon nanomaterials. This research identifies the specific microwave pyrolysis operating conditions to generate activated biochar from sugarcane bagasse (SCB) biomass. The synthesis of activated biochar from SCB involves a chemical activation followed by a thermochemical conversion using microwave-assisted pyrolysis. The resulting carbon material attained a 278 m2/g BET surface area and a relatively pure carbon structure with a minor concentration of oxygen and silicon. The activated biochar was used to develop an electrochemical sensor using the drop-casting method. The SCB-activated biochar electrochemical sensor achieved significant electrocatalytic properties to detect paracetamol,

showing 71% less charge transfer resistance and 96% higher electrocatalytic properties than the bare glassy carbon electrode (GCE). The linear range of paracetamol current responses demonstrated a considerable sensitivity with a 2.5 µM limit of detection. The modified GCE indicates a promising performance in paracetamol detection in a real sample.

Keywords: Biochar; Microwave-assisted pyrolysis; Paracetamol; Sugarcane bagasse.

This chapter is under review for being published as S. Allende, Y. Liu, and M. V. Jacob, 'Electrochemical sensing of paracetamol based on sugarcane bagasse-activated biochar', in the journal Industrial Crops and Products, special issue: Lignocellulosic Biomass-derived Functional Materials.

4.1 Introduction

The solid residues from agricultural production represent around 2 billion tons globally (Millati et al., 2019). Some agricultural wastes are rice straw, rice husk, coffee pulp, sugarcane bagasse, seeds, crop/tree, wheat straw, and coconut husk (Dhanya et al., 2020a; Zhao et al., 2022). Annually the global waste of wheat straw, hardwoods and rice straw are 709.2, 58 and 673.3 million tons, respectively (Millati et al., 2019; Sadh et al., 2018). High demand for agricultural resources increases the waste material and subsequently increases the greenhouse gas emissions associated with the disposal and storage of wastes (Millati et al., 2019; Sadh et al., 2018). The abundance of feedstock and the lack of energy sources are crucial factors for developing efficient bioenergy technologies to produce clean energy and carbon material, solve waste management issues and reduce environmental hazards (Belyakov, 2019; Guan et al., 2019; Li et al., 2022b). Microwave pyrolysis converts biomass into char, oil, and gas by a thermochemical process, in which microwave heating implies volumetric absorption of electromagnetic energy (Ethaib et al., 2020; Hadiya et al., 2022). Microwave pyrolysis heating comprises energy transfer, quick start-up, feedstock versatility application, and rapid and efficient heating (Hadiya et al., 2022; Li et al., 2022e).

The activation methods of biochar have gained considerable interest due to their potential as an electrocatalytic material for sensing applications (Godwin et al., 2019; Spanu et al., 2020; Sudha et al., 2019). The microwave pyrolysis treatment of feedstock generates a carbon-rich material with a microporous structure, a high BET surface area, and pore volume (Allende et al., 2023b). Activated biochar development considers physicochemical properties, environmental benefits, and low-cost production (Luo et al., 2022). Biochar modification consists of two stages: biomass chemical activation and thermal treatment. To improve the porosity and optimise functional groups of the biochar, is the biomass chemically activated before the thermal treatment by using acid (H_3PO_4, HNO_3, HCl, H_2O_2, $ZnCl_2$), alkaline (KOH,

NaOH) or sulfonation additives (H_2SO_4) (Baharak Sajjadi, 2019; Cheng et al., 2017; Spanu et al., 2020). After the chemical impregnation, the biomass is exposed to a thermochemical conversion such as pyrolysis. The pyrolysis process accelerates chemical reactions and thermal breakdown of lignocellulosic biomass components (Cheng et al., 2017; Godwin et al., 2019). The operating conditions of the pyrolysis process have a relevant influence on the surface area and functional groups on the biochar surface (Allende et al., 2022; Allende et al., 2023a). High pyrolysis temperature and prolonged treatment time induce a decreased particle size, increase surface area, enhance pore volume, and enriched concentration of carboxylic and hydroxyl functional groups on the biochar surface (Godwin et al., 2019; Monticelli, 2020; Tang et al., 2020).

The global consumption of pharmaceutical products has increased rapidly through the years (Alfhaid, 2022; Benyekkou et al., 2020). During these products' fabrication, diverse pharmaceutical substances are released into natural water, causing a significant environmental hazard due to toxic elements that can contaminate natural sources, e.g., water, underground water, food and soil, etc. (Benyekkou et al., 2020; Escapa et al., 2017). Paracetamol (acetaminophen) is a common drug used for its antipyretic and analgesic properties, which chemical product has been detected in recycled water (Benyekkou et al., 2020; Villota et al., 2019). Accurate and rapid detection of paracetamol is crucial for conserving environmental sources (natural water and sewage treatment plants), avoiding improper disposal, and active pharmaceutical ingredients removal in recycled water. Current detection methods are capillary electrophoresis, mass spectroscopy, fluorescence spectrum and gas chromatography (Boumya et al., 2021; Wang et al., 2020a). The applications of those methods represent extended procedure time, complex equipment, and expensive technologies (Zafar et al., 2022). Nevertheless, activated biochar is an emerging alternative with promising properties of electrochemical sensing, e.g., high sensitivity, simplicity, reliability, inexpensive, and low time-consuming for detecting paracetamol (Boumya et al., 2021; Wang et al., 2020a).

Various studies report synthesising carbon materials to modify electrodes in detecting diverse species (Bhujel et al., 2019; Martínez-Sánchez et al., 2019; Wang et al., 2020b). Nonetheless, the most common activation process required the addition of metal/metal oxide, complex and less sustainable procedures (Li et al., 2022f). This research studies the synthesis of activated biomass-derived material as a metal-free sensor for paracetamol detection. Sugarcane bagasse (SCB) was the biomass used as feedstock, sulphuric acid (H_2SO_4) as an acidic chemical activation method and microwave pyrolysis as a heating conversion method. The analytical performance of SCB-activated biochar was explored as an electrode material applied on a glassy carbon electrode (GCE) for the detection of paracetamol. The electrochemical performance was evaluated based on the sensitivity, selectivity, stability, and reproducibility properties of modified GCE.

4.2 Material and methods

4.2.1 Synthesis of activated biochar.

The preparation of H_2SO_4-activated biochar consists of the chemical activation and microwave pyrolysis of the raw biomass and thermochemical post-treatment of the biochar. The feedstock used in biochar production was sugarcane bagasse (Wilmar Sugar Australia, Queensland). To remove the impurities the raw SCB was washed first with ethanol and then multiple times with distilled water. The SCB was soaked in a 1:1 ratio of sulphuric acid (H_2SO_4) for 24 hours. After the acid treatment, the feedstock was dried at 110 ºC overnight. The criteria selection of H_2SO_4 as an activating agent was based on its intrinsic ability to generate carbon material with catalyst properties. A low concentration of sulfuric acid (1:1 ratio) was used due to the high addition of H_2SO_4 in the microwave heating process can induce over-gasification of biochar by the dehydration of surplus water, contributing to the destruction of biochar pore structure (Baharak Sajjadi, 2019).

Unlike other studies related to the biochar-modified electrode (Madhu et al., 2014; Wang et al., 2020b), this work used larger pre-treated biomass (75 gr) for pyrolysis, then higher power and longer treatment time was required to fully process the feedstock (complete thermal decomposition of lignocellulosic fibre compounds). After being activated chemically, the biomass is pyrolysed at 1.5 kW for 2 hours in an oxygen-free environment (N_2 flow of 5 $Lmin^{-1}$) and under negative pressure of 25 kPa. The modified biochar was washed with hydrochloric acid (1 M) and successive rinsing with distilled water. The activated biochar is then heated at 110 ºC in the oven for 24 hours to remove the moisture. Figure 4.20 shows the scheme of the synthesis process of SCB-activated biochar and the microwave pyrolysis components. The microwave-assisted pyrolysis system used in the activated biochar synthesis involves the following sections: (i) a nitrogen cylinder that maintains an oxygen-free environment; (ii) a chamber where the biomass was placed during the pyrolysis process; (iii) a tuner applied to control the reflected power; (iv) 3 kW microwave generator (brand Sairem); (v) condenser system and (vi) vacuum pump.

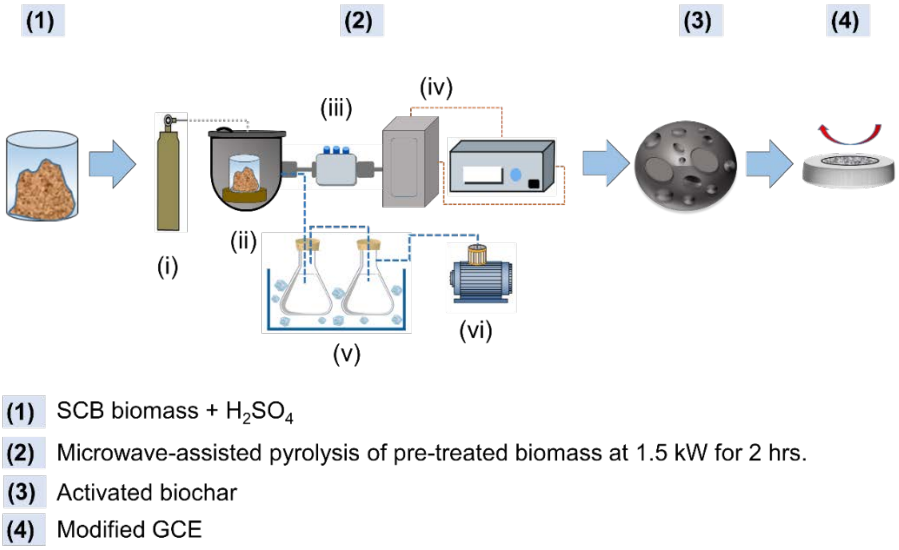

Figure 4.20. Synthesis process of SCB-activated biochar using microwave pyrolysis.

4.2.2 Preparation of SCB-activated biochar/GCE

The carbon nanocomposites were prepared by grounding SCB-activated biochar into a fine powder using a mortar. The resulting material was dispersed in ethanol and then exposed to ultrasonication for 40 minutes until it reached fine and uniform particles. Before applying the coating, the surface of the GCE was carefully polished using 0.3 µm and 0.5 µm alumina slurry. The bare glassy carbon electrode was cleaned under sonication treatment with ethanol and deionised water for 15 minutes, and then 2 µL of 1.5 mg m/L dispersable activated SCB-biochar was added dropwise to the surface of the bare GCE. The modified working electrode was dried at ambient temperature before testing.

4.2.3 Reagents and apparatus.

98 % sulphuric acid purchased from AJAX-Finechem (Univar) and 1 M hydrochloric acid from Sigma were used as reagents. The dibasic-Na2HPO4 and monobasic-NaH2PO4 were considered for the preparation of buffer solution (PBS, pH 7.0). Electrochemical work was developed using a three-electrode scheme comprising a glassy carbon electrode (GCE) working electrode (3.0 mm diameter), a platinum wire counter electrode, and an Ag/AgCl reference electrode. The electrochemical study was achieved utilizing PalmSens4 potentiostat (PalmSens, Netherlands). BET surface area data of SCB-activated biochar were measured using a micromeritics 3-flex surface. Scanning electron microscopy (SEM) and transmission electron microscopy (TEM) imaging were obtained using JEOL 7001F SEM and JEOL 2100 TEM, respectively. The thermogravimetric analysis (TGA) was performed on Netzsch STA 449F3 Jupiter Simultaneous Thermal Analyser. The Raman spectroscopy curve was conducted by a Renishaw In-Via Micro-Raman spectrometer.

4.3 Result and discussion

4.3.1 Characterisation of H_2SO_4 activated SCB-biochar.

The elemental composition is vital to understanding the behaviour of the activated biochar. Table 4.27 shows FlashSMART CHNSO elemental analysis of the raw biomass treated with sulphuric acid before the pyrolysis process and the activated SCB-biochar. After H_2SO_4 impregnation and microwave pyrolysis, the carbon content of the activated biochar is increased by 24%, and the oxygen concentration is decreased by 45%. The chemical activation before microwave pyrolysis can reduce the carboxylic group and increase lactonic compounds (Baharak Sajjadi, 2019). On the other hand, the activation can produce high oxidation of H_2SO_4, generating a high C=O form and reducing oxygen-containing functional groups (Liu et al., 2020). SCB-activated biochar shows lower H/C and O/C molar ratios than nonactivated biochar. A Low H/C ratio involves higher biochar carbonization, low cellulose and hemicellulose content compounds and a high aromatic structure (Hassan et al., 2020; Peiris et al., 2019). Furthermore, a low O/C value comprises a decrease in the hydrophilic and polarity properties of the biochar, which is associated with the volatilization of polar functional groups (Godwin et al., 2019; Hassan et al., 2020; Liu et al., 2020; Peiris et al., 2019).

Table 4.27. CHNSO elemental analysis of raw biomass and SCB-activated biochar.

Element	N%	C%	H%	O%	H/C	O/C
Raw biomass	0.15	43.37	5.83	40.7	0.13	0.94
SCB-activated biochar	0.43	53.95	1.92	22.53	0.036	0.42

Table 4.28 shows the BET analysis of SCB-activated biochar. The chemical activation by H_2SO_4 impregnation and microwave pyrolysis led to an increased surface area of up to 278 m^2/g and 0.075 cm^3/g pore volume. The acid impregnation in the raw biomass increases the

formation of oxygen-containing functional groups on the modified biochar surface. The chemical activation generates sulphuric oxidation and carbon gasification, increasing the specific surface area and pore volume (Baharak Sajjadi, 2019; Spanu et al., 2020). The biomass nature and the pyrolysis parameters are crucial to developing biochar surface area properties, e.g., the morphology structure of lignocellulosic biomass (tubular) promotes microporosity formation. The greater surface area and porosity are related to the raw sugarcane bagasse's high lignin content and the prolonged pyrolysis time (Cheng et al., 2017; Leng et al., 2021; M.Waqasa et al., 2018).

Table 4.28. Surface area data of raw biomass with H_2SO_4 before pyrolysis and SCB-activated biochar.

Analysis	**Raw biomass+H_2SO_4**	**H_2SO_4 activated SCB-biochar**
Surface area (m^2/g)		
BET Surface Area	3.47	277.7
t-Plot Micropore Area		188.2
t-Plot external surface area	5.44	188.26
BJH Adsorption cumulative surface area of pores (1.7-300 nm diameter)	2.57	13.47
Pore volume (cm^3/g)		
t-Plot micropore volume	0.0013	0.075
Total pore volume calculated <1.0228 nm diameter at p/p°	0.000129	0.089

Figure 4.21 (b1) and (b2) show the TEM of SCB-activated biochar. The thermochemical activation of biochar produced crystalline rods of approximately 5-10 nm wide. There are some layered semi-organised carbon clusters, and no single sheets of carbon are observed. The impregnation of SCB with sulphuric acid promoted the formation of pores due to carbon gasification (Baharak Sajjadi, 2019; Monticelli, 2020). At the same time, the use of high

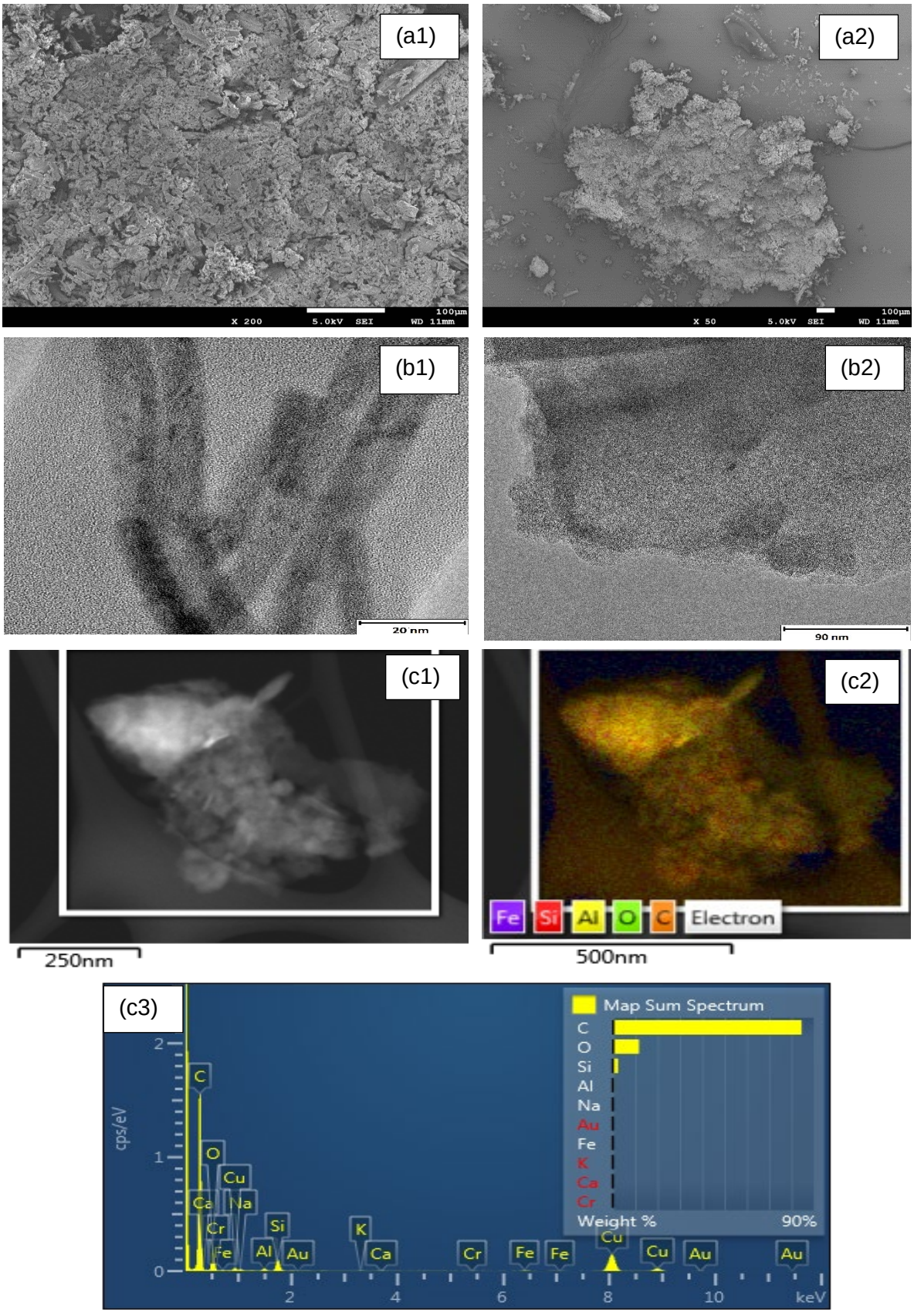

Figure 4.21. (a1) (a2) Scanning Electron Microscope (SEM), (b1) (b2) Transmission Electron Microscopy (TEM), and (c1) (c2) (c3) EDS of SCB-activated biochar generated by the H_2SO_4 chemical activation and microwave pyrolysis process at 1.5 kW for 2 hours.

microwave power evidences high biochar quality in terms of carbon elemental content, and uniform and larger pores formation. These properties are caused by the increased heating rates, which produce a large release of volatile in a short time throughout the biochar surface-rapid thermal decomposition of the lignocellulosic biomass compounds (Wallace et al., 2019a; Zhang et al., 2022c). Figure 4.21 (c1), (c2) and (c3) show the EDS of activated biochar. The results indicate a relatively pure carbon structure with a minor concentration of O and Si.

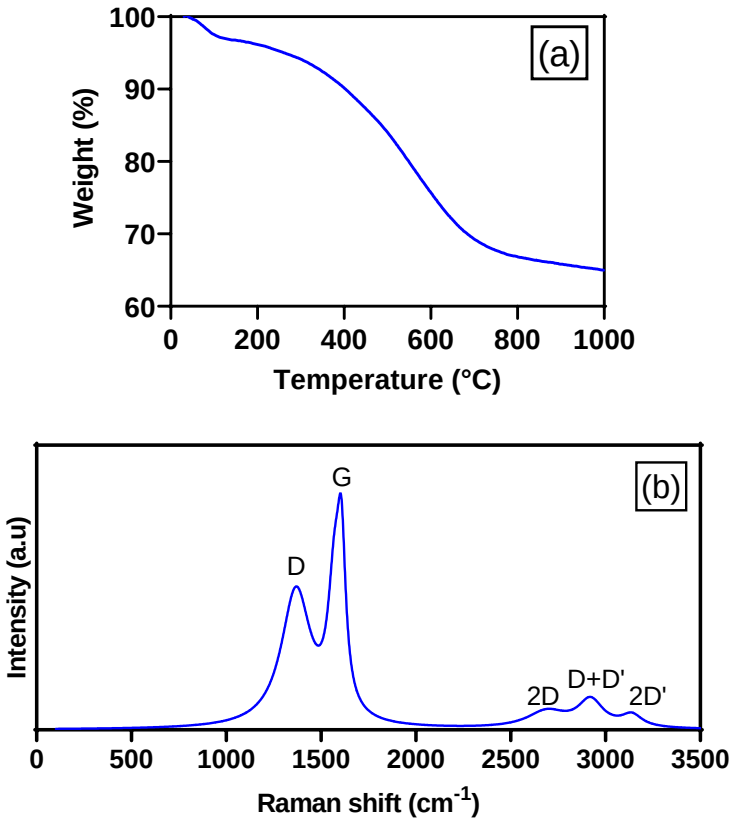

Figure 4.22. (a) Thermogravimetric analysis and (b) Raman spectra curves of SCB-activated biochar.

Thermogravimetric analysis (TGA) of activated biochar is shown in Figure 4.22 (a). The curve reveals that biomass weight loss started between 150 ºC to 350 ºC. The principal thermochemical decomposition was between 350 ºC and 450 ºC. The final mass loss was associated with the breakdown of lignin compound over 450 ºC to 800 ºC (Elkhalifa et al., 2022). Figure 22 (b) shows the Raman spectroscopy curve of activated SCB-biochar. The D and G peaks were observed at 1350 cm^{-1} and 1550 cm^{-1}, respectively. The D band intensity is

related to existing defects in the structure (Muzyka et al., 2018a), and the G peak is associated with graphitization grade (Khan et al., 2017). A small 2D peak was observed at 2700 cm^{-1}, involving the existence of graphite and some layers of graphene (Merlen et al., 2017). 2D and D+D' are linked to sp2 graphitic presence (Muhammad Hafiz et al., 2014). The 2D' band specifies two or more graphene layers in the material composition (Muzyka et al., 2018a).

4.3.2 Electrochemical characterisation of the modified electrode

The interfacial behaviour of the modified glassy carbon electrode (GCE) was assessed by the electrochemical impedance spectra (EIS). Figure 4.23 shows the electron transfer kinetic properties at the surface of the bare and modified GCE. EIS diagram consists of a semi-circular and linear part. The semicircle diameter represents the charge-transfer resistance (R_{ct}), which describes the conductivity property (resistance of electron movement). The linear section at low frequency symbolizes the diffusion process (Foroughi, 2021; Randviir and Banks, 2013; Zamfir et al., 2020). A decreased charge transfer resistance (R_{ct}) was observed in modified GCE (0.35 kΩ to 0.1 kΩ), representing lower mass transport resistance and improving the electron transfer kinetics.

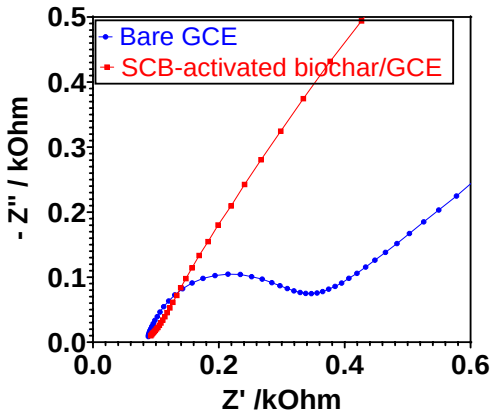

Figure 4.23. Electrochemical impedance spectra (EIS) of bare GCE and SCB-activated biochar/ GCE in 0.1 M KCl containing 5 mM $K_3[(Fe(CN)_6)]$ at 5 mV potential amplitude.

The Cyclic voltammetry (CV) curves of the bare and modified electrode in 0.1 M PBS with and without the presence of paracetamol are shown in Figure 4.24. In a blank solution, oxidation responses were not observed for non-modified and modified electrodes. There is a considerable difference between the capacitance of bare GCE and SCB-activated biochar/GCE, whose property is related to a higher surface area of the SCB-activated biochar compared to the specific surface of the bare GCE. CV curve of the bare electrode showed a pair of oxidation peaks. The first peak could indicate acetaminophen oxidation to semiquinone radical formation. Then, the second peak could be assigned to the complete oxidation of a quinone (Chikere et al., 2019; Luk et al., 2021). The evidence of only one oxidation peak on modified GCE can be attributed to the large surface area of SCB-activated biochar provides a well-defined oxidation peak at the lower potential in an irreversible reaction (El-Azazy et al., 2022; Fu et al., 2018; Shanbhag et al., 2022). In this study analysis, only the predominant oxidation current peak is considered on bare GCE. Bare glassy carbon showed a current oxidation peak of ~ 6.2 µA for 0.5 mM paracetamol was recorded at 0.55 V. An increased oxidation peak in SCB-activated biochar/GCE (17 µA) was detected at 0.49 V. The CVs response in modified GCE showed a beneficial effect on paracetamol oxidation, demonstrating that the existence of SCB-activated biochar improved the catalytic activity of the electrode.

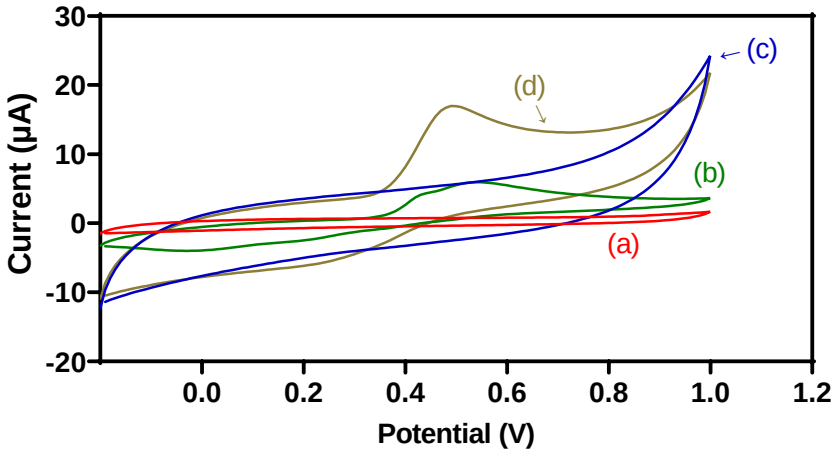

Figure 4.24. Cyclic voltammetry (CV) response of bare GCE and SCB-activated biochar/ GCE in the absence (a and c) and presence of 0.5 mM paracetamol (b and d) in 0.1 M phosphate buffer solution (pH 7.0) at 0.05 V/s scan rate.

4.3.3 Electrochemical detection of paracetamol at H_2SO_4 activated SCB-biochar/GCE

The chronoamperometry technique was used to analyse the sensitivity of activated SCB-activated biochar/GCE at different paracetamol concentrations. The current-time response investigated was set at the optimal of 0.8 V. Consecutive addition of paracetamol in 0.1 M PBS was evaluated in the experimental part. Figure 4.25 indicates a correlation curve between the paracetamol concentration and its current response. The linear regression is given by the equation $I(\mu A) = 0.0743(\mu M) - 4.400,\ R^2 = 0.982$ for the range of concentration from 5 µM to 950 µM. Table 4.29 shows the performance comparison of SCB-activated biochar/GCE with other published electrodes for paracetamol detection. This work achieved a limit of detection (LOD) of 2.5 µM. The analytical performance of SCB-activated biochar/GCE was competitive compared to sensors found in the literature due to low LOD value and wide linear range, which indicates that the modified electrode has promising electrochemical characteristics to be applied in real samples.

Table 4.29. Performance comparison of various modified electrodes for paracetamol detection.

Electrode	Linear range concentration (µM)	LOD (µM)	Reference
NiCu-CAT/GCE	5-190	5	(Wang et al., 2020a)
DMBQ-MCNTPE	5-500	1	(Karimi-Maleh et al., 2014)
GCE-M221-Fe_3O_4	50-2000	16	(Mulyasuryani et al., 2019)
AGCE	0.1-100	0.72	(Câmpean et al., 2011)
GO/GCE	0.1-430	0.021	(Alagarsamy, 2018)
SCB-activated biochar/GCE	5-950	2.5	This work

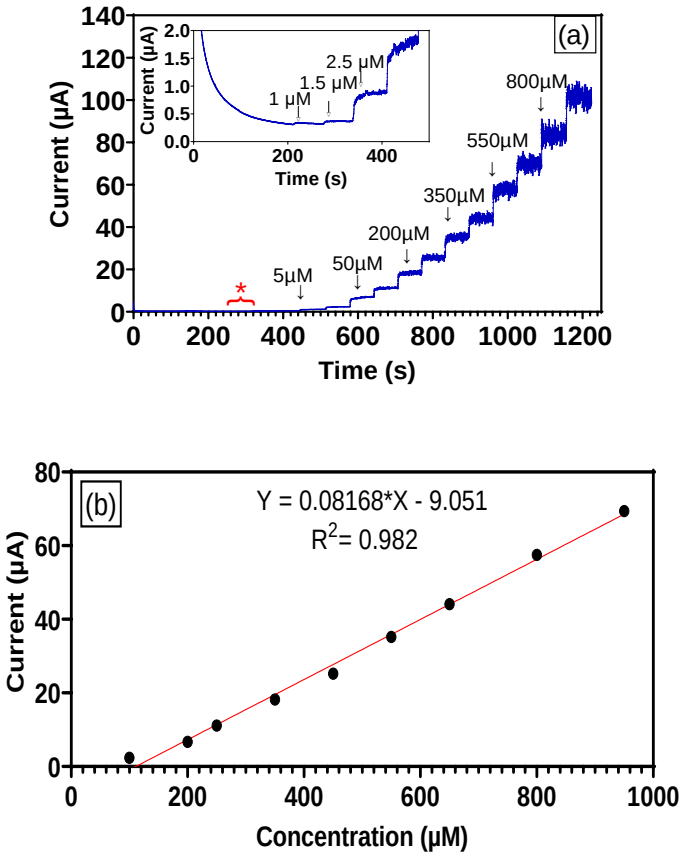

Figure 4.25. (a) Chronoamperometry current response of modified GCE with activated SCB-biochar at different concentrations of paracetamol in 0.1 M PBS (pH 7.0); (b) linear calibration plot of peak current vs. paracetamol concentration.

4.3.2 Selectivity, stability, and reproducibility of the modified electrode

Selectivity of modified GCE for paracetamol detection was studied by the chronoamperometric response in the presence of common interference substances, e.g., uric acid (UA), urea, calcium chloride ($CaCl_2$), potassium chloride (KCl), glucose and potassium nitrate (KNO_3). Figure 4.26 shows the current-time response for the 0.5 mM paracetamol injections and various interfering species. The results demonstrated that adding 0.5 mM of interfering substances had not affected the current peak oxidation of paracetamol. Hence, SCB-activated biochar/GCE has promising anti-interference properties and selectively detects paracetamol.

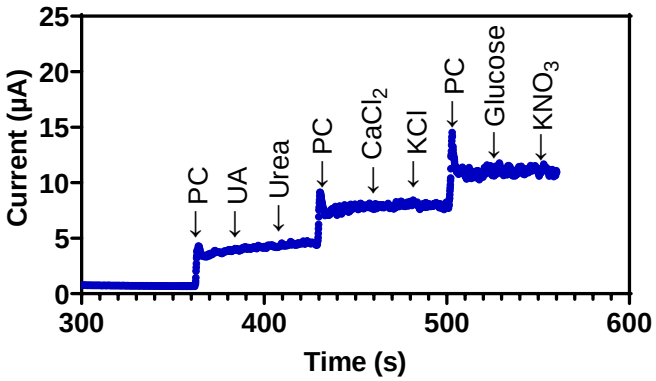

Figure 4.26. Interference studies of activated SCB-activated biochar/ GCE for paracetamol detection in the presence of various interfering components in 0.1 M PBS (pH 7.0) at 0.8 V potential.

Reproducibility and stability of SCB-activated biochar/GCE were assessed by the differential pulse voltammetry (DPV) method at 6 mV step potential. The DPV technique provides better clarity than chronoamperometry to observe oxidation current peaks using low paracetamol concentrations. The reproducibility was evaluated by the successive detections of five modified GCE in response to 0.5 Mm paracetamol concentration. The relative standard deviation (RSD) from the oxidation current response of five modified GCE was 2.5%, confirming an acceptable reproducibility. The stability was studied considering the oxidation current of one modified GCE after 2, 3, 4, 6 and 8 days of its fabrication and storage at room temperature. The RSD obtained in the stability test was 2.32%. Electrochemical results of SCB-activated biochar showed a stable current response through the storage time.

4.4 Conclusion

The large generation of agricultural waste and the lack of carbon sources make sugarcane bagasse biomass an excellent candidate for resource recovery, particularly from biochar. The synthesis of the SCB-activated biochar using chemical pre-treatment and microwave pyrolysis developed clustered semi-organised carbon layers with improved surface area up to 278 m^2/g

and increased carbon concertation by 24%. The electrochemical analysis of the modified GCE showed high electron transfer, electric conductivity, and potential redox behaviour. Fabrication of biosensors using biochar has received significant attention due to its practical electrode synthesis method, eco-friendly advantages and potential electrochemical activity. Current detection methods represent extended procedure time, complex equipment, and expensive technologies. The modified biochar with electrocatalytic properties is suitable for paracetamol detection and will be ideal for traces of pharmaceutical material in wastewater. The application of modified GCE for paracetamol detection has demonstrated an acceptable sensitivity, considering 2.5 µM LOD, substantiating that H_2SO_4-activated biochar/GCE is promising for real applications. Thus, developing carbon material from agricultural waste using microwave-assisted pyrolysis allowed electrochemical feasibility and an environmentally friendly alternative for paracetamol sensing in media such as wastewater.

CHAPTER 5

5 FOOD WASTE BIOCHAR FOR ELECTROCHEMICAL SENSING OF NITRITE

The application of various agro wastes is unlimited in activated biochar production. Food waste is an excellent candidate for the fabrication of eco-friendly carbon sensors due to its abundance, natural properties, and rapid and simple synthesis without the addition of metals. This chapter explores the use of pineapple peel as feedstock for the fabrication of activated biochar and its application on nitrite detection by the modification of a glassy carbon electrode.

Abstract

Developing applications for the by-products obtained from waste processing is vital for resource recovery. The synthesis of $ZnCl_2$-activated biochar with high electrocatalytic activity was carried out by the microwave-assisted pyrolysis of pineapple peel and the subsequent chemical activation process. Activated biochar is employed in the electrochemical sensing of nitrite by drop casting in a glassy carbon electrode (GCE). The activated biochar exhibited a stacked carbon sheet, 254 m^2/g Brunauer, Emmett and Teller (BET) surface area, 0.076 $cm^3 g^{-1}$ pore volume, 189.53 m^2/g micropore area and oxygen-containing functional groups. The electrochemical impedance spectroscopy of the modified GCE showed a reduced charge transfer resistance of 61%. This is crucial to determine the electrochemical properties of biochar. The sensor showed a significant current response and an excellent limit of detection

of 0.97 µmol L^{-1}. The modified-activated biochar electrochemical sensor demonstrated high selectivity, reproducibility (RSD=2.4%), and stability (RSD=2.6%).

Keywords: Microwave-assisted Pyrolysis; Biochar; Nitrite; Electrochemical **S**ensor.

This chapter was published as S. Allende, Y. Liu, M. A. Zafar, and M. V. Jacob, "Nitrite sensor using activated biochar synthesised by microwave-assisted pyrolysis," Waste Disposal & Sustainable Energy, 2023/01/17 2023, doi: 10.1007/s42768-022-00120-4.

5.1 Introduction.

The agricultural industry generates around 23.7 million tonnes of food per day globally (Duque-Acevedo et al., 2020), but one-third of the solid food produced annually is wasted (Adejumo; and Adebiyi, 2020). Food waste causes 8% of global greenhouse gas emissions (Energy, 2017). Apart from food, agricultural waste residues also have negative impacts on the environment and economy (Awasthi et al., 2022; Wainaina et al., 2020; Wu et al., 2020a). The agricultural residues are classified into two types: agricultural wastes (husk, seed, bagasse, leaves) and industrial residues (orange peel, coconut oil cake, cassava peel, soybean oil cake, etc.) (Sadh et al., 2018). The depletion and excessive use of natural sources have caused a greater interest in renewable materials generated from waste in the agricultural sector (Cai et al., 2021b; Kalinke et al., 2021; Liu et al., 2022). The efficient and rapid conversion of agro-industrial waste into valuable products is highly desirable for reducing greenhouse gases related to waste accumulation (Kalinke et al., 2021; Wu et al., 2020b).

The conversion of solid agri-food waste into value-added products, i.e., biochar, bio-oil and biogas, can transform an unvalued material into versatile opportunities and applications (Dhanya et al., 2020b; Duque-Acevedo et al., 2020; Sarangi et al., 2022). Microwave-assisted pyrolysis of agri-food waste could efficiently convert by-products into a valued carbon material due to its electromagnetic heating allowing instantaneous volumetric heating and uniform distribution in the energetic coupling (Ethaib et al., 2020; Ge et al., 2021; Hadiya et al., 2022). The synthesis of modified biochar from natural waste using microwave pyrolysis is an attractive alternative to producing ecological sensing materials (Cao et al., 2020b; Spanu et al., 2020; Zhang et al., 2019a). The fabrication of biochar-modified electrodes can be done in two ways, i.e., drop casting on glassy carbon electrodes (GCE) or by making the carbon paste of the biochar (Spanu et al., 2020). The application of biochar-modified electrodes allows the determination of different analytes associated with the food, agriculture, and medical industries

(Cao et al., 2020a; Spanu et al., 2020). The satisfactory detection capacity depends on the electrochemical and morphological properties of the biochar achieved during its activation process (Cheng et al., 2017; Spanu et al., 2020; Sudha et al., 2019).

The activation of biochar can be attained by two main mechanisms: physical and chemical activation methods. The physical modification consists of thermal treatment that produces more pore volume and a larger surface area (Wu et al., 2020b; Zhang et al., 2022a). For example, biomass activated by microwave pyrolysis can improve the surface area and surface functional groups. The improved composition of biochar can promote electron transfer and ion insertion rates (Cheng et al., 2017; Kalinke et al., 2021; Spanu et al., 2020). The chemical activation implicates exposing the biomass or biochar (before or after pyrolysis) to chemical agents, such as nitric, sulfonic, phosphoric, and sulphuric acids. The activation through metal salt agents, i.e., $ZnCl_2$ produces dehydration of the carbon during the pyrolysis process, generating carbonyl and carboxylate functional groups (Cheng et al., 2017; Kalinke et al., 2021).

For the biochar activation, the literature shows different biomass feedstock and thermal and chemical methods. However, the relationship between the intrinsic properties of activated biochar and electrochemical sensor performance has not been completely studied. The purpose of this paper is to synthesise electrocatalytic biochar using pineapple peel as a biomass feedstock and microwave-assisted pyrolysis as a thermochemical treatment. The experimental parameters of the microwave-assisted pyrolysis process were essential for developing a biochar material with sensing properties and analytical performance. The physicochemical and electrochemical characterisation of activated biochar indicated high biochar Brunauer, Emmett and Teller (BET) surface area, micropore structure, increased pore volume, notable charge transferability, good selectivity, and high carbon stability.

5.2 Experimental.

5.2.1 Biochar synthesis using microwave-assisted pyrolysis.

The breakdown of biomass using microwave pyrolysis involves electromagnetic volumetric heating in the absence of air to produce biochar, bio-oil, and biogas (Hadiya et al., 2022; Li et al., 2022e; Wang et al., 2020d). The microwave heating method transfers the energy through the interaction of the molecules inside the biomass rather than by heat transfer from external sources (dielectric heating) (Ethaib et al., 2020; Yu et al., 2022a). The advantages of microwave-assisted pyrolysis are high heating efficiency, rapid reaction time, and control over heating (Li et al., 2022e; Toscano Miranda et al., 2021; Zhang et al., 2022d). Unlike conventional pyrolysis, microwave irradiation generates biochar with a higher fixed carbon content, significant thermal decomposition of the lignin network, better carbon stability and higher surface area and pore volume (Hidalgo et al., 2019; Selvam S and Paramasivan, 2022; Tang et al., 2020). The heating rate (~ 132 °C/min) of microwave pyrolysis is beneficial for the activation of biochar because it promotes the formation of microporous structures, develops oxygen functional groups on the surface, and gives rise to catalytic properties (Lam et al., 2020; Selvam S and Paramasivan, 2022; Sun et al., 2022b; Yek et al., 2020). Therefore, the thermochemical treatment of pineapple peel biomass and modified biochar was carried out using microwave-assisted pyrolysis.

Figure 5.27 shows the microwave pyrolysis scheme used, which comprises N_2 flow (5 $Lmin^{-1}$) that maintains an inert atmosphere during the experiments; a custom-made chamber where the biomass is placed; a reflected power controller; a 3 kW microwave generator; power controller; various condensers, whose functionality is collect liquid and gas by-products; and a vacuum pump. The synthesis process of $ZnCl_2$-activated biochar comprises three stages. The first phase is biochar production using microwave-assisted pyrolysis. For this, pineapple peel

was first washed with ethanol and distilled water. The cleaned biomass was dried in an oven at 110 °C for 24 h to reduce its moisture content to 10%. Then, the biomass was pyrolysed at 3 kW for 30 min. The produced biochar was soaked in $ZnCl_2$ for 24 h for chemical activation. Afterwards, the biochar was dried overnight in an oven at 110 °C. The third phase comprised the second pyrolysis (calcination process) of activated biochar at 1.5 kW for 20 min. After the activated biochar was cooled to room temperature, it was washed with 1 mol/L HCl and distilled water. Finally, the modified biochar was dried at 110 °C overnight.

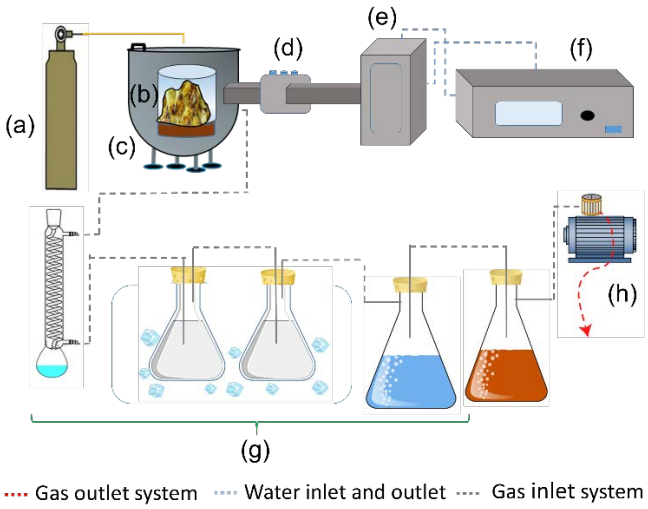

Figure 5.27: Microwave pyrolysis system used in the $ZnCl_2$- activated biochar synthesis. The system components are (a) nitrogen gas supply system; (b) pineapple peel biomass contained in quartz beaker; (c) custom-made chamber; (d) tuner; (e) 3 kW microwave generator; (f) microwave power controller; (g) various condensers; (h) vacuum pump.

5.2.2 Electrode preparation for electrochemical study.

The powder-activated biochar was dispersed in ethanol and subjected to ultrasonic cleaning for 30 min. The electrochemical study was carried out by a three-electrode system. A GCE, Ag/AgCl electrode and platinum wire were used as working, reference, and counter electrodes, respectively. The GCE surface was polished with 0.3 µmol/L and 0.5 µmol/L alumina slurry to remove impurities before coating. Subsequently, it was cleaned with ultra-sonification for

10 min in ethanol and deionised water. The GCE was dried at room temperature. Last, the GCE was coated with 2 µL of 1.5 mg/mL $ZnCl_2$-activated biochar using the drop-casting technique.

5.2.3 Reagents and instruments.

Sodium nitrite ($NaNO_2$), zinc chloride ($ZnCl_2$, 1 mol/L), and hydrochloric acid (1 mol/L) were purchased from Sigma Aldrich. The phosphate-buffered saline (PBS, pH 7.0) solution was prepared using dibasic-Na_2HPO_4 and monobasic-NaH_2PO_4. Biomass feedstock applied in the production of modified biochar was pineapple peel which was obtained as food waste. The electrochemical experiments were carried out on PalmSens4 potentiostat (PalmSens, Houten, Netherlands). The characterisation techniques of the material involve the following: surface area obtained from micromeritics 3-flex surface and porosity analyser; transmission electron microscopy (TEM) imaging acquired from JEOL 2100 200 kV Transmission Electron Microscope (Joel, Peabody, MA, USA); X-ray photoelectron spectroscopy (XPS) using a Kratos Axis Supra (AXIS Supra$^+$, Manchester, UK); Raman spectrum was collected using a Renishaw In-Via Micro-Raman spectrometer (inVia Qontor, Keyborough, Australia); thermogravimetric analysis (TGA) was achieved using Netzsch STA 449F3 Jupiter Simultaneous Thermal Analyser (Netzsch, Wittelsbacherstrasse, Germany).

5.3 Result and discussion.

5.3.1 Characterisation of $ZnCl_2$- activated biochar.

Table 5.30 shows the FlashSMART CHNSO elemental analysis of non-activated and activated biochar. The ultimate analysis of raw biomass showed oxygen as the main component (50%). The progressive thermochemical treatment causes partial chemical oxygen removal and

increased carbon content (Hidalgo et al., 2019; Selvam S and Paramasivan, 2022). The reduced O/C and H/C ratios indicate that during microwave pyrolysis decarboxylation reaction ensued, leading to a strong bond formation (carbon bonding) and decreased oxygen concentration (Lam et al., 2020; Selvam S and Paramasivan, 2022; Yek et al., 2020). Unlike raw biomass, the carbon content increased in $ZnCl_2$-activated biochar by 18%, and the oxygen concentration decreased by 75%. However, after the chemical activation, the H/C ratio in $ZnCl_2$-activated biochar was slightly higher (32%) than that in non-activated biochar, and the O/C value increased up to 0.24. According to the literature, the reduction of carbon content is related to the formation of amorphous microporous structures of aromatic sheets, which occurs after the chemical activation and second pyrolysis process (Lay et al., 2020). The increased O/C ratio indicates the formation of oxygen functional groups during the thermochemical modification process of biochar (Godwin et al., 2019; Hassan et al., 2020; Yang et al., 2021). Specifically, the biochar activation process with $ZnCl_2$ promotes the formation of carbonyl and hydroxyl groups (XPS data, Figure 5.28 (c1)) (Godwin et al., 2019; Sajjadi et al., 2019). The presence of oxygen-containing functional groups in biochar improves the physical adsorption and total capacitance of modified electrodes (Dehkhoda et al., 2014; Liu et al., 2021b).

Table 5.30. Elemental analysis of raw biomass, non-activated and activated biochar.

Sample	**N%**	**C%**	**H%**	**O%**	**H/C**	**O/C**
Pineapple peel	1.4	43.37	5.83	49.4	0.13	1.13
Non-activated biochar	1.02	69.25	1.37	7.27	0.02	0.11
$ZnCl_2$- activated biochar	1.52	51.39	1.32	12.31	0.026	0.24

The microwave-assisted biomass activation (thermal pre-treatment) is attached to operational conditions, i.e., microwave power and reaction time. High input power leads to micropore formation, and extended exposure to microwave irradiation involves a higher surface area and pore volume (Godwin et al., 2019; Selvam S and Paramasivan, 2022; Tomczyk et al., 2020b).

Between 400 °C and 900 °C was reached at a 1.5–3 kW power range for 20–30 min. The high heating rate made microwave pyrolysis an appropriate thermal decomposition method for quick biomass breakdown (cracking of organic matter) (Godwin et al., 2019; Tomczyk et al., 2020b). During the microwave pyrolysis process at 3 kW, biochar rapidly releases H_2 and CH_4 and produces carbonyl and carboxylate groups, which develop a higher surface area and micropores (Cheng et al., 2017; Sajjadi et al., 2019; Spanu et al., 2020). These physicochemical characteristics are essential for catalytic activity (Cheng et al., 2017; Tamizhdurai et al., 2017; Yan et al., 2020).

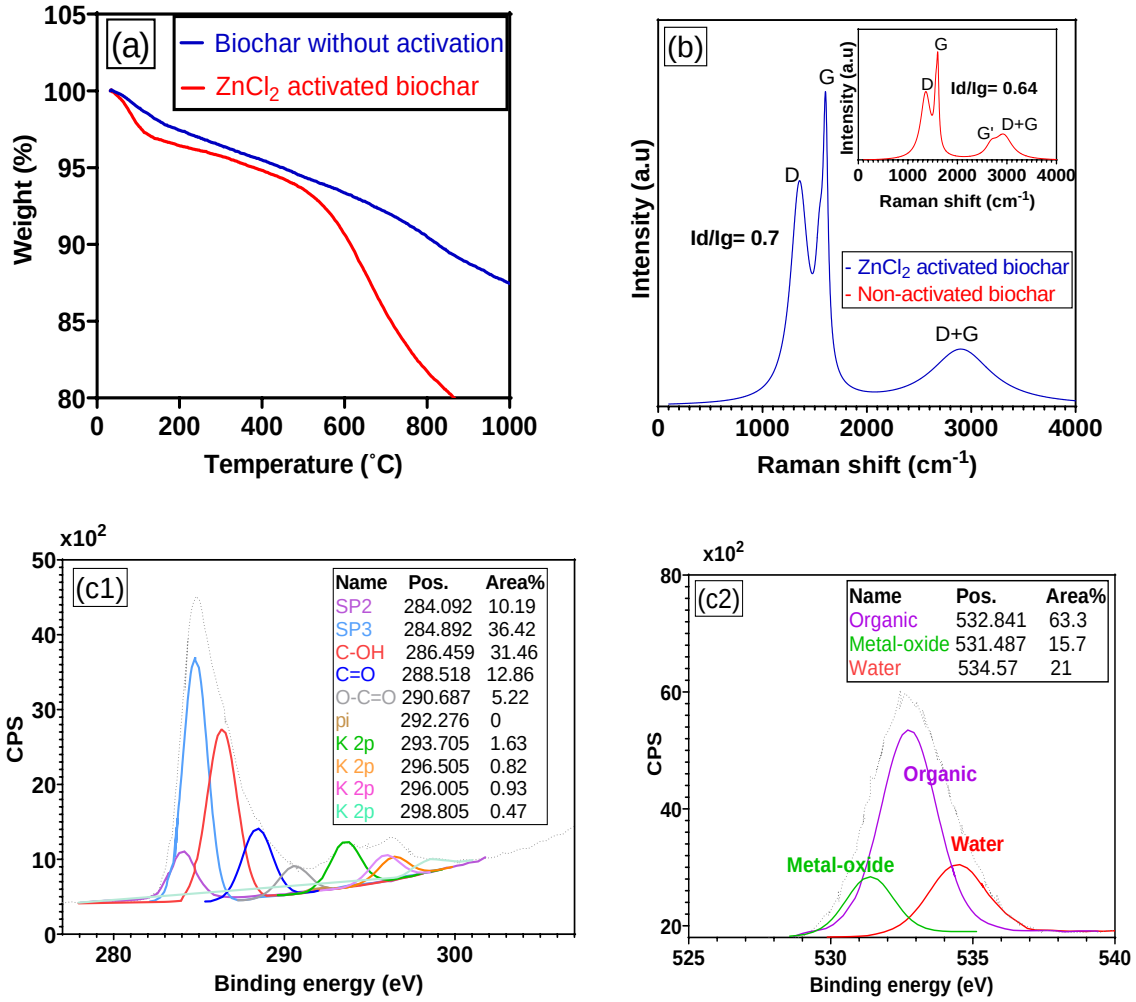

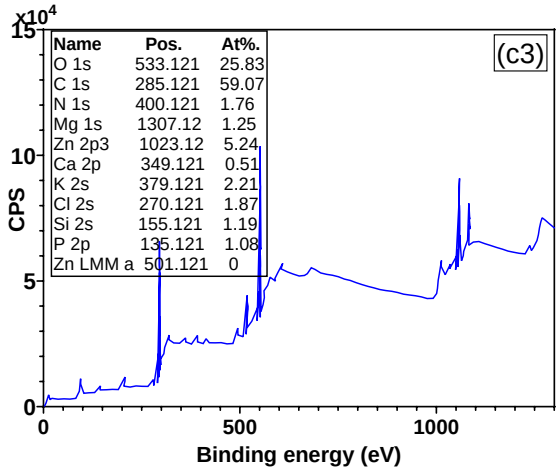

Figure 5.28. (a) TGA curves of non-activated biochar generated at 3 kW for 30 minutes and activated biochar produced after chemical activation and second pyrolysis process at 1.5 kW for 20 minutes, (b) Raman spectra, and (c1) (c2) (c3) XPS of $ZnCl_2$- activated biochar.

$ZnCl_2$ impregnation acts as an activating agent, causing the generation of deep cavities in the biochar. The BET surface area and pore volume of the activated biochar increased to 254.91 m^2/ g and 0.076 cm^3/ g, respectively. After the activation, the micropores also increased up to 189.53 m^2/ g. Micropore formation contributes to the electrocatalytic performance of modified electrodes by improving the adsorption of the analyte, facilitating the electrical conductivity and enhancing the sensor response (Casanova et al., 2022; Cheng et al., 2017). Table 5.31 shows the specific surface area comparison between unmodified and modified biochar.

Table 5.31. BET data of activated and non-activated biochar.

Analysis	**Non-activated biochar**	**$ZnCl_2$-activated biochar**
Surface area (m^2/g)		
BET surface Area	88.51	254.91
t-Plot micropore Area	39.50	189.53
t-Plot external surface area	49.01	65.38
BJH Adsorption cumulative surface area of pores (1.7-300 nm diameter)	25.45	27.10
Pore volume (cm^3/g)		

t-Plot micropore volume	0.02	0.076
Total pore volume calculated < 1.0228nm	0.03	0.09

Figure 5.29 (a) and (b) show Scanning Electron Microscope (SEM) images of the biochar produced from the impregnation of $ZnCl_2$ and the calcination process. The activation process had a notable impact on the surface structure of the biochar, causing a high concentration of pore formation with uniform distribution. Specifically, the penetration of $ZnCl_2$ into the biochar pores generates an expansion of pores through all the biochar surfaces, explaining the increased pore volume (Sun et al., 2018). Also, instead of a solid structure, the formation of thin sheets was observed in $ZnCl_2$-activated biochar. Figure 5.29 (c1) and (c2) show high sheet carbon structure, semi-organised carbon layers, and stacked sheets. No crystalline rods or crystalline patches were observed.

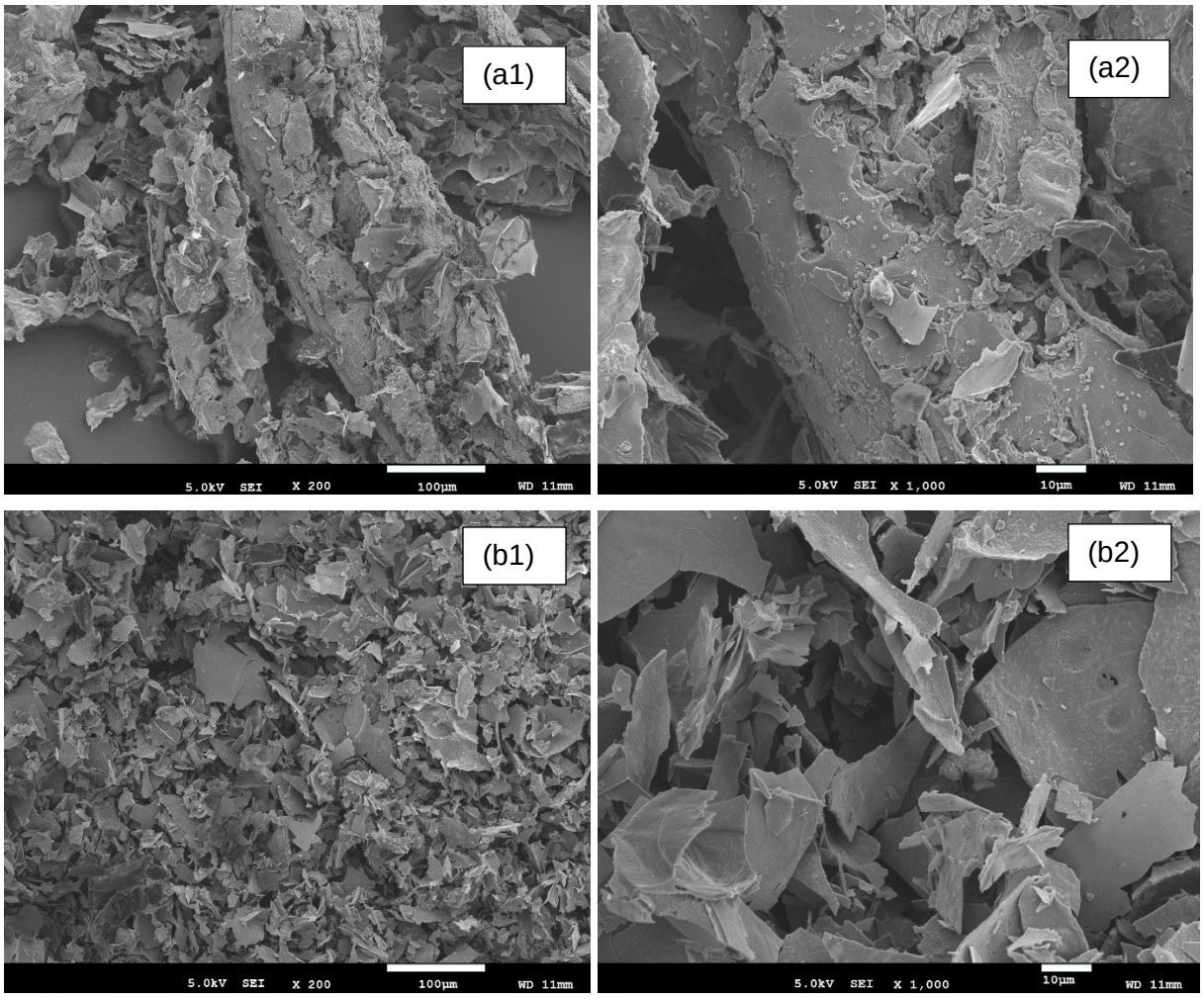

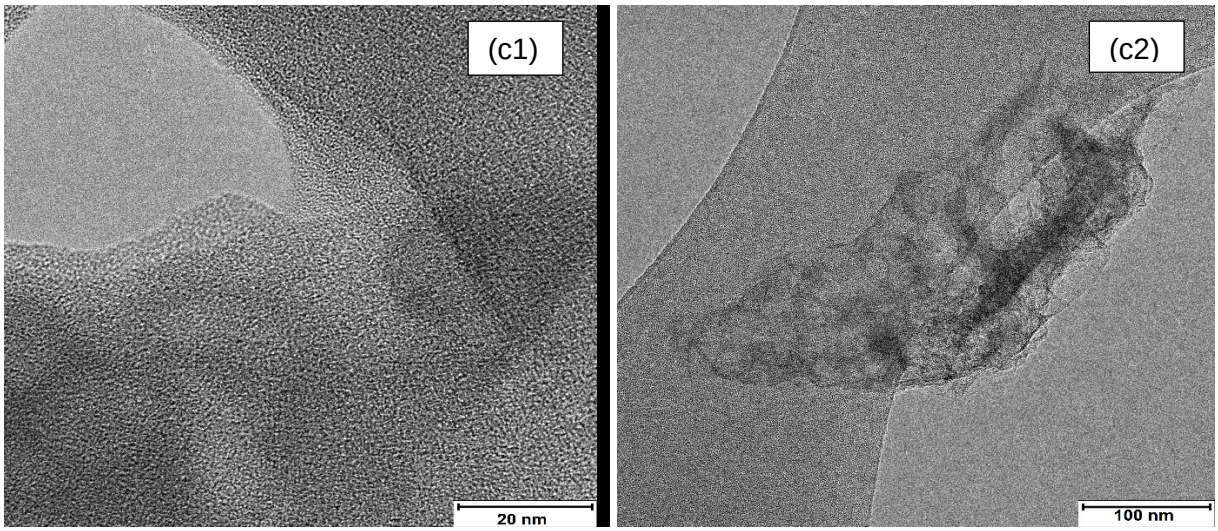

Figure 5.29. Scanning Electron Microscope (SEM) images of (a1) (a2) non-activated biochar obtained at 3kW for 30 minutes; (b1) (b2) SEM of $ZnCl_2$-activated biochar after chemical activation and calcination process at 1.5 kW for 20 minutes; (c1) (c2) High-resolution transmission electron microscopy (HRTEM) of $ZnCl_2$- activated biochar.

TGA of activated and non-activated biochar is shown in Figure 5.28 (a). The results show that between 32 °C and 150 °C, there is slightly more weight loss in $ZnCl_2$-activated biochar (5%) than in the non-activated biochar (3%). The main reason is the moisture loss and adsorption of organic components at an early stage. Between 500 °C and 650 °C, the activated biochar suffered a higher weight loss (10%), which can be attributed to the thermal decomposition of pineapple peel compounds (holocellulose and lignin structures) and inorganic impurities (Ani, 2018; Raji and Pakizeh, 2013; Sukruansuwan and Napathorn, 2018). At temperatures of 700 °C and 850 °C, the activated biochar was less affected by the volatilisation of the agent ($ZnCl_2$) inside pores, increasing the thermal decomposition resistance (Chatterjee et al., 2020; Nikkhah et al., 2020). Thus, the TGA curve indicates that non-activated biochar is more thermally stable than $ZnCl_2$-activated biochar.

Figure 5.28 (b) shows the Raman spectrum of the biochar, showing the D-band at 1355 cm^{-1} and G-band at 1620 cm^{-1} (Alagarsamy, 2018; Cao et al., 2020b). Specifically, the D-band is due to the condensed existence of benzene rings in an amorphous carbon structure, and the

G-band comprises the aromatic ring in biochar (Eshun et al., 2019). Moreover, the D+G peak (observed at 2899 cm^{-1}) describes the sp2 graphitic structure (Khan et al., 2017). The results were like the Raman spectra of graphite oxide reported by (Muzyka et al., 2018b). An increase in the I_D/I_G factor was observed after the biochar activation, whose I_D/I_G value in $ZnCl_2$-activated biochar was 9.4% higher than in non-activated biochar. A higher peak intensity ratio represents a large disordered (amorphous carbon atoms) and reduced graphite structure of biochar (Lay et al., 2020; Li et al., 2019; Yu et al., 2020). The high pyrolysis temperature reached 3-1.5 kW could cause a change in biochar structure. Figure 5.28 (c1), (c2), and (c3) show the XPS of activated biochar. Along with carbon, nitrogen, and oxygen as the principal components. Some metals were detected, i.e., Zn, Fe and Mg. High oxidation of carbon in the form of C—OH, O—C=O and C=O was observed. The C=O, O-C=O and C—OH structures are associated with the carbonyl, ester and hydroxyl groups, respectively (Liu et al., 2020). The formation of carbonyl functional groups is related to the extraction of the H group from aromatic rings, whose reactions occur during the microwave pyrolysis and activation process (Sajjadi et al., 2019). XPS results revealed that using microwave pyrolysis as thermal treatment (high temperature) and $ZnCl_2$ as a chemical activator generates biochar with high carbon content with oxygen functionalities (Dehkhoda et al., 2014; Fan et al., 2011; Liu et al., 2021b). These characteristics are relevant to determining the electrochemical performance of activated biochar. The discussion is developed in section 5.3.2.

5.3.2 Electrochemical characterisation.

The electrochemical behaviour of bare GCE and $ZnCl_2$-activated biochar/GCE was investigated by electrochemical impedance spectroscopy (EIS) and cyclic voltammetry (CV) techniques. The EIS method evaluates the charge transfer resistance (kinetics) at the surface of the $ZnCl_2$-activated biochar/GCE. The impendence curve comprises a semi-circular area at higher frequencies and a linear portion, which is related to the electron transfer limited process

and the diffusion process at lower frequencies, respectively (Cao et al., 2020b; Haldorai et al., 2017; Lei et al., 2020; Tamizhdurai et al., 2017). The diameter symbolises the electron transfer resistance (R_{ct}), whose value depends on the dielectric properties of the modified electrode interface (Cao et al., 2020b; Tamizhdurai et al., 2017).

Figure 5.30 shows the Nyquist plots obtained through EIS. The measurement parameters in the experimental procedure consist of a 10^5 to 0.1 Hz frequency range and 5 mV potential amplitude in 0.1 M KCl containing 5.0 mM $K_3[(Fe(CN)_6)]$. The EIS curves show that the diameter of bare GCE (R_{ct} = 280 Ω) is higher than that of the $ZnCl_2$-activated biochar/GCE (R_{ct} = 110 Ω). Increased miporous structure (189.53 m^2/g) and surface area (254.91 m^2/g) of activated biochar promoted the adsorption properties, contributing to the accessibility and diffusion of the electrolyte along the porous structure. These can improve the charge electron transfer and sensor response. Moreover, higher conductivity is achieved due to the binding affinity between oxygen-containing functional groups on the surface of activated biochar and the analyte (Casanova et al., 2022; Dehkhoda et al., 2014). These results confirm that $ZnCl_2$-activated biochar enhanced the electron transfer kinetic properties of the modified electrode.

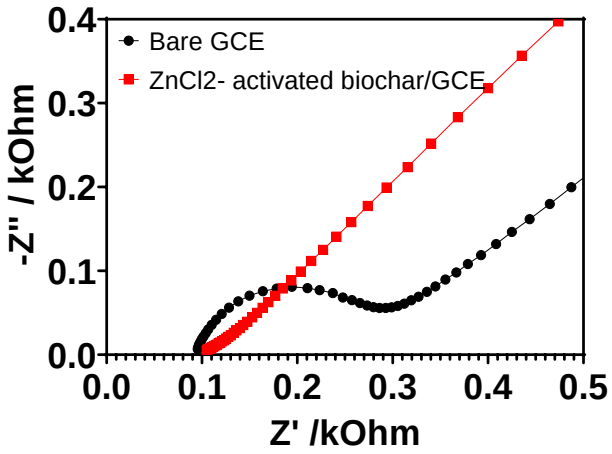

Figure 5.30. Electrochemical impedance spectra of bare GCE and $ZnCl_2$-activated biochar/GCE in 0.1 M KCl containing 5 mM $K_3[(Fe(CN)_6)]$ at 5 mVs^{-1}

The electrocatalytic property of the modified electrode towards nitrite oxidation was studied in 0.1 M PBS containing 0.7 mM nitrite, as represented in Figure 5.31. There was no oxidation response in the blank solution in either of the two electrodes (curves a and b). Bare GCE showed a minor oxidation peak with a peak current of 8 µA in nitrite solution at 1 V (curve c). By comparison, $ZnCl_2$-activated biochar/GCE presented a higher peak current of 19 µA (curve d) than non-modified GCE. A high surface area and increased micropore volume of $ZnCl_2$-activated biochar on the GCE improved the contact area between the biochar and the analyte, contributing to the charge propagation along the porous structure. Thus, using $ZnCl_2$-activated biochar as a modification material for the GCE enhanced the oxidation peak current and electrocatalytic activity.

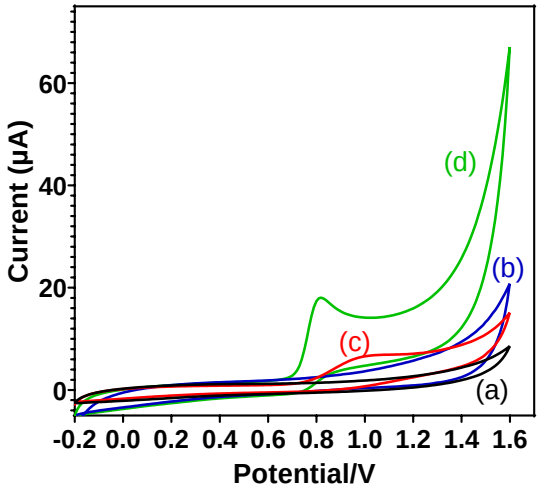

Figure 5.31. Cyclic voltammetry response of bare GCE and $ZnCl_2$-activated biochar/GCE in the absence (a and b) and presence of 0.7 mM nitrite (c and d) in 0.1 M phosphate buffer solution (pH 7.0) at 50 mV/s scan rate.

5.3.3 Electrochemical detection of nitrite on $ZnCl_2$ activated biochar/GCE.

The current responses of $ZnCl_2$-activated biochar/GCE in chronoamperometry for nitrite detection are shown in Figure 5.32. The technical setting used was 0.8 V potential, whose value was optimal for response to noise ratio. The concentration range applied was from 10 µM to 2850 µM, 250 µM per interval. The current response of modified GCE was increased

proportionally to the nitrite addition range. The calibration curve between concentration and the current signal shows a direct relationship. The linear regression function is represented as $I(\mu A) = 0.0627(\mu M) - 1.392,\ R^2 = 0.9939$. The limit of detection (LOD) achieved was 0.97 µM. Table 5.32 shows a comparison of linear ranges and LOD in previous studies. The performance exhibited by $ZnCl_2$-activated biochar/GCE was better or comparable to the electrochemical sensors reported in the literature.

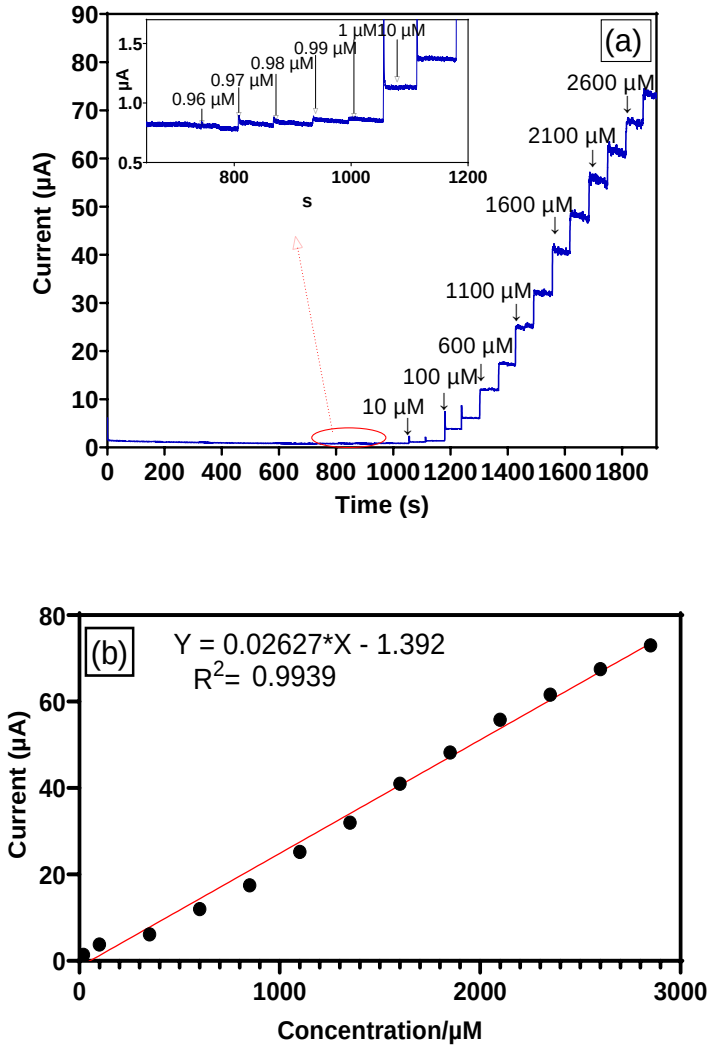

Figure 5.32. (a) Chronoamperometry response of $ZnCl_2$-activated biochar/GCE at successive addition of $NaNO_2$ in 0.1 M PBS (pH 7.0); (b) Calibration curve for nitrite concentration against peak currents.

Several studies indicate the addition of metal (copper, silver and gold) as the principal source for synthesising electrocatalytic active materials (Cao et al., 2020a; Mani et al., 2014; Manoj

et al., 2018; Sudha et al., 2019; Tamizhdurai et al., 2017). Some papers reported the use of conventional pyrolysis heating, and hydrothermal and exfoliation procedures. Due to the sophisticated synthesis methods, the $ZnCl_2$-activated biochar/GCE showed lower charge transfer resistance (less than 150 Ω) compared to that of some materials registered in (Cao et al., 2020a; Lei et al., 2020; Manoj et al., 2018). The CV response of the modified GCEs was similar to that of our activated biochar, showing a significant oxidation current peak. These electrocatalytic properties make $ZnCl_2$-activated biochar an excellent material for nitrite detection.

Table 5.32. Comparison of the analytical performance of nitrite sensor with various modified electrodes.

Electrode	**Linear range (µM)**	**LOD (µM)**	**Reference**
ABC-800/GCE	4.9-1184	2.7	(Sudha et al., 2019)
GCE/CeO2NPs	0.02-1200	0.21	(Tamizhdurai et al., 2017)
Cu^{2+}-Cu/Biochar	1-300	0.63	(Cao et al., 2020b)
Au/CNHN	0.05-1150	0.017	(Lei et al., 2020)
Cu/MWCNTs/GCE	5-1260	1.8	(Manoj et al., 2018)
RGO-MWCNT-Pt/Mb/GCE	1-1200	0.93	(Mani et al., 2014)
$ZnCl_2$-activated biochar/GCE	100-1400	0.97	This work

5.3.4 Selectivity, stability, reproducibility of $ZnCl_2$- activated biochar/GCE.

The chronoamperometry response of $ZnCl_2$-activated biochar/GCE and the effect of interfering substances on the peak current response of $NaNO_2$ is shown in Figure 5.33. The anti-interference property of the modified GCE was studied considering 1 mM nitrite, followed by the separate addition of 1 mM of six potential interfering components into the stirred PBS at 0.8 V working potential. The results revealed that the presence of KCl, KNO_3, $CaCl_2$, glucose, KBr and urea did not influence the determination of $NaNO_2$. A notable response was observed

for nitrite injections, but a weak current signal was observed for electroactive species additions. Therefore, it can be rightly said that $ZnCl_2$-activated biochar/GCE demonstrates excellent selectivity.

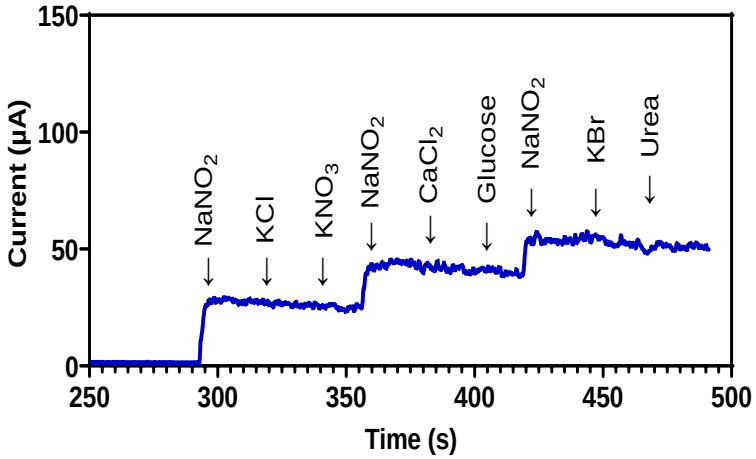

Figure 5.33. Anti-interference property of $ZnCl_2$-activated biochar/GCE towards detection of nitrite in the presence of electroactive species KCl, KNO_3, $CaCl_2$, glucose, KBr and urea.

The reproducibility and stability of the modified glassy carbon were studied by differential pulse voltammetry (DPV). This technique was appropriate to determine the nitrate response, unlike chronoamperometry, DPV provided clarity to observe oxidation current peaks using low nitrate concentrations. The reproducibility and stability of the $ZnCl_2$-activated biochar/GCE electrode are shown in Figure 5.34 (a) and (b), respectively. Five GCEs were modified using $ZnCl_2$-activated biochar to evaluate their reproducibility for 0.3 mM nitrite in 0.1 M PBS (pH 7.0) solution. The results show that the modified GCEs have significant reproducibility behaviour, whose relative standard deviation (RSD) value was 2.4%. Then, the stability was evaluated for the electrochemical nitrite sensor every two days until the completion of ten days of storage at room temperature. The test was achieved in a 0.1 M PBS (pH 7.0) solution containing 0.25 mM nitrite. The DPV measurements for stability analysis demonstrate consistency in oxidation current response of up to 10 days, observing an excellent RSD of 2.6%.

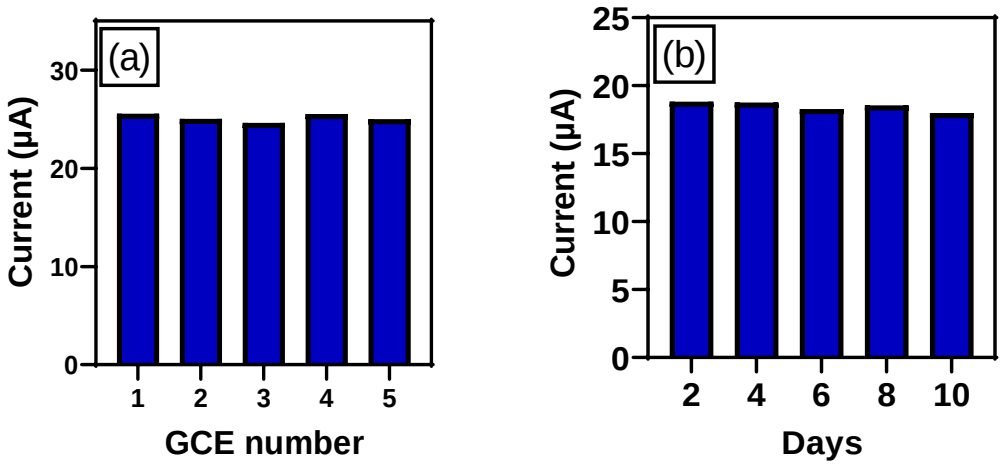

Figure 5.34. (a) reproducibility analysis of five $ZnCl_2$-activated biochar/GCE in the presence of 0.3 mM nitrite in 0.1 M PBS; (b) stability results of modified GCE in 0.25 mM of nitrite in 0.1 M PBS (pH 7.0).

5.4 Conclusion.

This work synthesised the biochar through microwave pyrolysis and studied its electrochemical performance. Microwave-assisted pyrolysis had a significant role in the development of higher fixed carbon content, improved thermal decomposition of the lignin network, better carbon stability, and higher surface area and pore volume. The biochar was activated by soaking in $ZnCl_2$. The activated biochar showed amorphous microporous structures of aromatic sheets, oxygen-containing functional groups on the biochar surface, strong carbon bonding, and a relatively higher I_D/I_G peak intensity ratio (owing to the amorphous form of carbon). These properties facilitated the adsorption of the analyte and enhanced the electrocatalytic activity and hence the sensor response. Modified GCE presented a higher peak current (19 µA) compared to that of bare GCE (9 µA) and reduced the charge transfer resistance value (110 Ω). The electrochemical behaviour of $ZnCl_2$-activated biochar/GCE for nitrite detection revealed comparable LOD (0.97 µmol/L), and high selectivity, leading to the promising potential for real applications.

CHAPTER 6

6 BIOCHAR-BASED GRAPHENE OXIDE FOR HIGH SELECTIVE ELECTROCHEMICAL DETECTION OF DOPAMINE.

Food waste can also be converted into graphene oxide by the thermochemical processing of biochar. The synthesis of this carbon material with negative charge properties is essential to achieve high selectivity on the sensing of positive charge molecules. The present chapter investigates the electrostatic interaction between the surface of the biochar-based graphene oxide material and dopamine in the presence of interfering species by the modification of a screen-printed carbon electrode. Banana peel is used as feedstock.

Abstract

Bio-based graphene derived from food waste is an attractive emerging research field, considering its eco-friendly and valuable applications. This work reports the synthesis of graphene oxide from biochar, which is initially produced using the microwave pyrolysis of banana peel waste. The performance of carbon-based material is evaluated in the fabrication of a modified screen-printed carbon electrode (SPCE) for selective dopamine (DA) detection in the coexistence of ascorbic acid (AA) and uric acid (UA). The material achieved 64.53% carbon elemental content, 345.79 m^2/g surface area, 0.074 cm^3/g micropore volume, large reactive surface area, and ribbon/banded organisation. The electrostatic interactions between the negatively charged biochar-based graphene oxide (BBGO) on the surface SPCE and opposite-charged dopamine assisted the oxidation potential with interfering species by

electrostatic repulsion of AA and UA. The modified electrode exhibited superior electrochemical results and stronger surface attraction of DA over bare SPCE. The BBGO/SPCE showed a high electroactive surface area, low charge-transfer resistance (~ 0.3 kΩ), superior conductivity (shift oxidation potential from 0.2 V to 0.1 V), higher DA oxidation peak (12.12 μA), notable selectivity and sensitivity. The synthesised biochar has a promising analytical performance and hence will be useful for many other positively charged species.

Keywords: Biochar; Microwave-assisted pyrolysis; Graphene oxide; Dopamine.

This chapter is under review for being published by S. Allende, Y. Liu., M. A. Zafar, and M. V. Jacob, ‘Sustainable Utilization of Food Waste: Microwave-Assisted Conversion into Graphene Oxide for Sustainable Sensor Applications’ in the journal Materials Today Sustainability.

6.1 Introduction

Food waste has become a serious issue due to environmental, economic and health effects. The excess of waste generation from agricultural industries and households is attributed to the increased population and high food loss (non-consumed). The level of waste estimated for the year 2025 is around 416 million tonnes, whose 23-65% corresponds to vegetables and fruits (Mohanty et al., 2022; Su et al., 2022b). Food waste dumping is responsible for releasing greenhouse gases (GHG), e.g., methane, carbon dioxide and carbon monoxide during its decomposition, contributing to global warming (Mohanty et al., 2022). This type of biomass management involves composting, landfill, incineration, and animal feed (Capanoglu et al., 2022; Sadh et al., 2018). However, none of these alternatives is viable in terms of sustainability, pollution mitigation, scale-up, efficiency and circular economy. The selection of biomass treatment is based on waste conversion efficiency, limited resource consumption (energy, chemical, space, etc.), processing time, and target by-products (Allende et al., 2023a). Microwave-assisted is an efficient biomass conversion method that offers a short treatment time, generation of three by-products (biochar, bio-oil, biogas), uniform heating distribution, reduced environmental footprint and potential CO_2 sequestration (Allende et al., 2022; Su et al., 2022b). Microwave pyrolysis results in the final by-product namely biochar, which has superior properties than other conversion mechanisms, e.g., higher carbon concentration, large reactive surface area, higher microporosity volume, rich carboxylic and hydroxyl surface group, etc. (Allende et al., 2023b; Sridhar et al., 2021; Su et al., 2022b).

The activation of biochar has gained immense interest in the fabrication of bio-based graphene derived from agricultural waste due to sustainable process methods and diversity of functions. This carbon material is highly valued in electrochemical applications, like the detection of numerous molecules by using biochar-modified sensors (Li et al., 2022f; Spanu et al., 2020). Some examples of sensing organic species are ascorbic acid (AA), dopamine (DA), and uric

acid (UA). AA, DA, and UA are electrochemically active biomolecules that coexist in biological fluids (Cho et al., 2020; Mohan et al., 2020). Ascorbic acid is a vital vitamin found in different life processes (human metabolism); dopamine is a neurotransmitter molecule that exists in the central nervous system; and uric acid is the main final compound of purine catabolism in humans (Patella et al., 2021; Zhang et al., 2018). Several studies report the simultaneous detection of AA, UA, and DA (Wei et al., 2020; Zhang et al., 2018). However, the selectivity property of bare electrodes is limited for dopamine detection in the presence of other species. The electrochemical oxidation of AA, DA, and UA occurs at similar potential, which means poor selective electrochemical response for the single detection of molecules (Li et al., 2013; Patella et al., 2021). The electrostatic interactions between the electrode and the analyte have a relevant role in the detection of dopamine, e.g., dopamine (pKa = 8.87) and ascorbic acid (pKa = 4.10)/ uric acid (pKa = 5.40) are oppositely charged species at physical pH 7.0 (Li et al., 2013). Therefore, the fabrication of a modified electrode with electrostatic attraction to positively charged molecules is essential to resolve the overlap oxidation response between the species. This research evaluates the synthesis of a negatively charged carbon-based material obtained from the microwave pyrolysis of banana peel (BP) waste into biochar and then conversion into BBGO. The properties of banana peel biochar-based graphene oxide (BBGO) are studied in the fabrication of an environment-friendly modified screen-printed carbon electrode (SPCE) for selective detection of DA in ascorbic acid and uric acid coexistence.

6.2 Experimental methods

6.2.1 Synthesis of activated biochar

The biomass treatment was developed mainly by a thermochemical conversion process achieved by microwave-assisted pyrolysis. Figure 6.35 describes the pyrolysis system used for the synthesis of BBGO; the system is comprised of the following units: (i) a chamber where

pyrolysis occurs under an oxygen-free environment applying 5 L/min nitrogen as a carrier gas, (ii) a manual tuner for controlling reflected power; (iii) a 3 kW microwave generator; (iv) flask condensers system, and (vi) a vacuum pump (-50 kPa). The synthesis of BBGO involves four stages. First, the selected biomass was pyrolyzed at 1.5 kW for 1.5 hours, considering the 10% microwave susceptor of biomass weight. Banana peel (BP) was used as feedstock. The resulting banana biochar was immersed in NaOH with distilled water in a 1:1 ratio for 2 days at room temperature. After this period the treated biochar was washed successive times with distilled water and then cured with $ZnCl_2$ in a 1:1 ratio for three days. The next activation procedure of BP biochar requires successive rinsing with distilled water and drying at 80 °C for five hours. Then treated biochar was subjected to a second pyrolysis at 1 kW for 40 minutes, resulting in BBGO from the banana peel (BP BBGO).

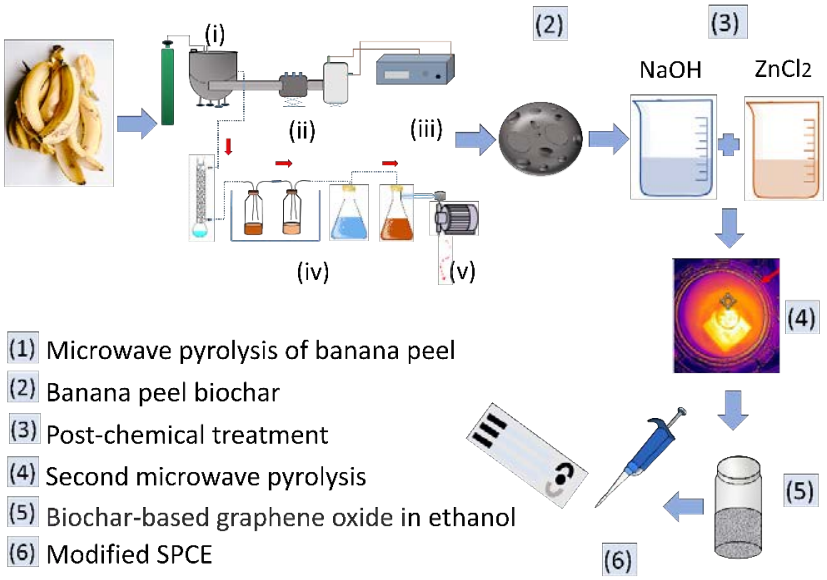

Figure 6.35. A scheme on the BBGO synthesis process using microwave pyrolysis.

6.2.2 Electrode preparation for electrochemical study

The biochar obtained from the chemical and pyrolysis treatments was ground in a mortar until it reached a uniform particle size. The BP BBGO was dispersed in ethanol and then exposed to ultrasonication until achieved fine biochar particles (~ 30 minutes). Then 1 µL of 1 mg mL^{-1} dispersed material was used as a coating on the surface of the screen-printed carbon electrode (SPCE). Before using the electrode, the modified SPCE was dried at room temperature.

6.2.3 Reagents and apparatus

The chemical treatment of biochar was developed using sodium hydroxide pellets from Univar and Zinc Chloride Solution (1 M) from Sigma. The reagents used in the electrochemical analysis were ascorbic acid, dopamine, and uric acid purchased from Sigma. The buffer solution (PBS, pH 7.0) was produced using dibasic-Na_2HPO_4 and monobasic-NaH_2PO_4. ItalSens screen-printed carbon electrodes (SPCE) were used in the electrochemical study purchased from PalmSens. The SPCE characteristics are global dimensions of 0.8 x 4.5 cm, working electrode dimensions of 7.06 mm^2, substrate of polyester, 200 µm thickness, 2.54 mm contact pad pitch, and 2% coefficient of variation (CV). The electrochemical measurements were achieved using PalmSens4 potentiostat (PalmSens, Netherlands). The surface area of SCB-activated biochar was measured using a micromeritics 3-flex surface and porosity analyser; FlashSMART CHNSO elemental analysis, scanning electron microscopy (JEOL 7001F SEM); transmission electron microscopy (JEOL 2100 TEM), thermogravimetric analysis (TGA) achieved on Netzsch STA 449F3 Jupiter Simultaneous Thermal Analyser; X-ray photoelectron spectroscopy was performed using a Kratos Axis Supra, Raman spectroscopy completed by Renishaw In-Via Micro-Raman spectrometer.

6.3 Result and discussion

6.3.1 Characterisation of Graphene Oxide

BP BBGO's quality and electrochemical analytical performance mainly depend on the CHNSO elemental analysis and high specific surface area. The pre/post-pyrolysis and chemical treatment favoured the BET surface area formation and micropore volume. After the impregnation with NaOH, the carbon structure of biochar changed (Na_2CO_3 breakdown) by the microwave heating method, releasing CO, CO_2 and H_2 ($2Na + 2Na_2CO_3 + 3H_2$) and causing higher porous generation (Liu et al., 2021a). The addition of $ZnCl_2$ contributes to the physically enhanced porosity and surface functionalization (Liu et al., 2021a; Yi et al., 2020). Table 6.33 shows the non-activated and activated biochar's surface area and elemental analysis. A significant increase in surface area was observed after the thermochemical treatment of BP biochar, achieving 345.7911 m^2/g BET surface area, 173.999 m^2/g micropore area and 0.074 cm^3/g micropore volume. The carbon content of BP BBGO is 2% higher than non-activated biochar. After activation, the H/C and O/C ratios were reduced by 60% and 10%. Reduced H/C value indicates high biochar carbonization, large aromaticity degree, and high aromatic structure (Meng et al., 2018). A low O/C ratio of activated biochar denotes a reduction of hydrophilic and polarity properties (Allende et al., 2023b; Meng et al., 2018).

Table 6.33*:* Surface area and CHNSO elemental analysis of banana peel biochar and BP BBGO.

Analysis	**Banana peel biochar**	**BP BBGO**
Surface area (m^2/g)		
BET Surface Area	27.65	345.7911
t-Plot micropore Area		173.999
t-Plot external surface area	40.83	171.79

BJH Adsorption cumulative surface area of pores (1.7-300 nm diameter)	22.07	91.96
Pore volume (cm^3/g)		
t-Plot micropore volume	-0.011	0.074
Total pore volume calculated <1.0228 nm diameter at p/p°		0.106
Elemental analysis		
N (%)	4.2	0.7
C (%)	63.18	64.53
H (%)	3.13	1.36
O (%)	29.49	33.41
H/C	0.05	0.02
O/C	0.47	0.52

Figure 6.36 (a1) and (a2) show the SEM images of raw banana peel biochar and BP BBGO, respectively. These figures demonstrate a notable difference in the biochar structure. Non-activated biochar has a solid and uniform surface, but after the chemical and thermochemical process biochar experienced the breakdown of fibre compounds, forming pores and some carbon layers. Figure 6.36 (b1) and (b2) correspond to the TEM images of BP BBGO. The particles observed are more clusters of mixed material than layered, with areas of ribbon/banded organisation, where the lattice spacing is ~ 3.4 A- shown in Figure 6.36 (c1) and (c2). The TEM-EDS data reveals that carbon and oxygen are primary elements in the base matrix with a minor presence of heavier metal and organic-based particles (Ca, Fe, P, Si and Ti). Some carbon areas exhibit semi-organisation in crumpled packed particles, not layers.

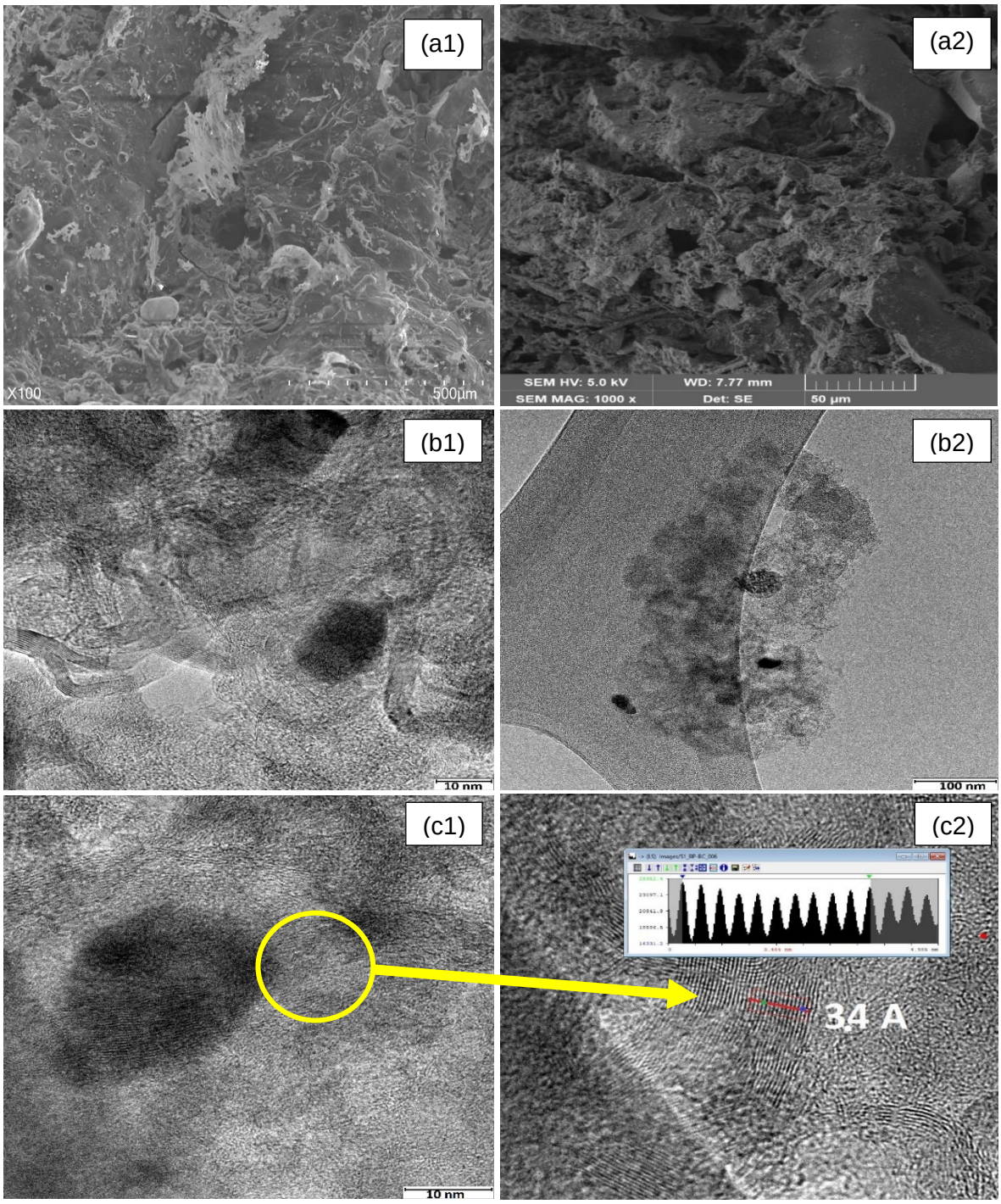
(a1)
X100
500µm
(a2)
SEM HV: 5.0 kV
WD: 7.77 mm
SEM MAG: 1000 x
Det: SE
50 µm
(b1)
10 nm
(b2)
100 nm
(c1)
10 nm
(c2)
3,4 A

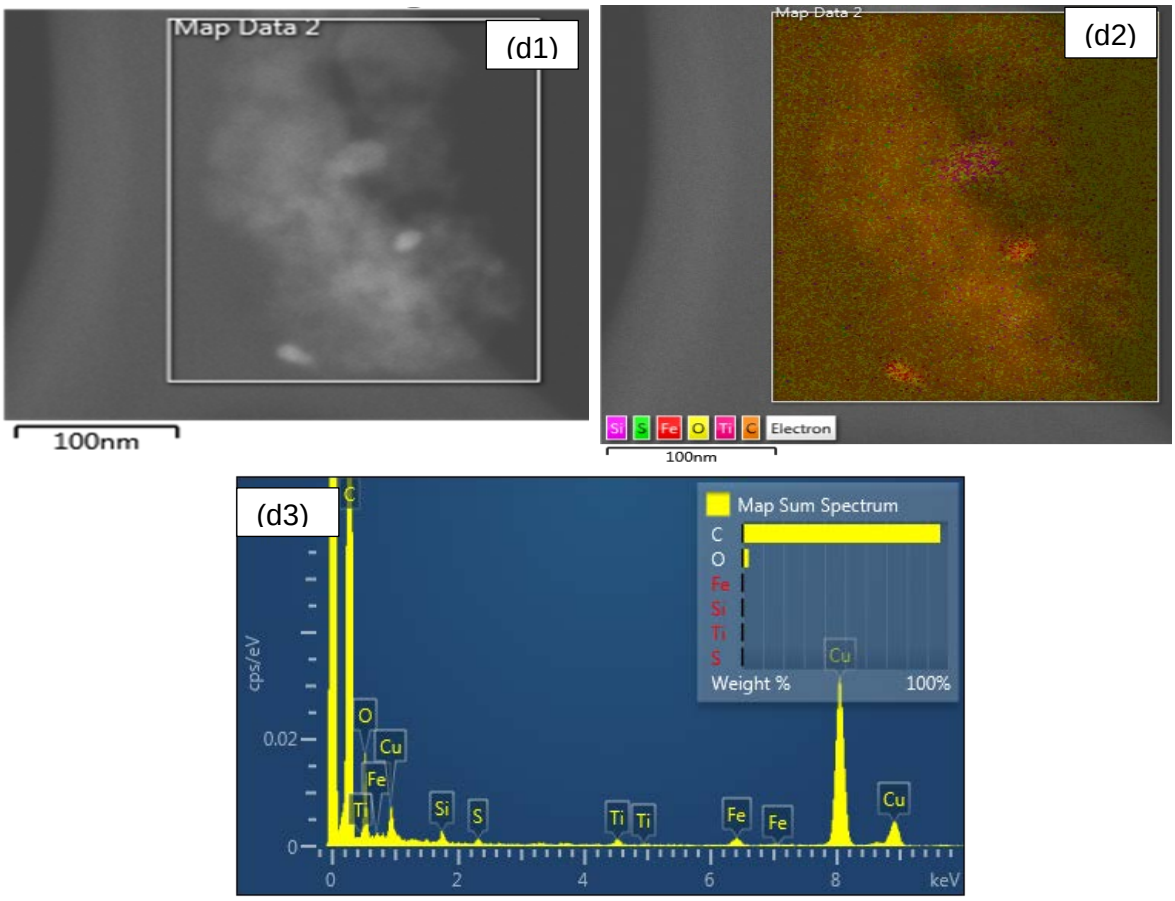

Figure 6.36. Scanning Electron Microscope (SEM) of non-activated (a1) and activated biochar (a2) and, (b1) (b2) Transmission Electron Microscopy (TEM), (c1) (c2) lattice spacing, and (d1) (d2) (d3) TEM- EDS images of BP BBGO.

The thermogravimetric analysis (TGA) curve of BP BBGO is shown in Figure 6.37 (a). The result reveals an initial weight loss between 100 ºC and 200 ºC. This decreased mass weight is associated with moisture content. A constant mass loss was observed between 200 ºC and 800 ºC, decreasing by 9.55%. The residual mass was around 90.45% at 849.8 ºC. The Raman spectroscopy curve indicates a high G peak at 1600 cm^{-1}, which denotes a high graphitization grade (Allende et al., 2023b). Lower intensity is detected in the D band, this value involves the existing defects in the structure (Muzyka et al., 2018a). The Raman curve of BP BBGO was comparable to the GO material reported by (Muhammad Hafiz et al., 2014; Yan et al., 2021). Figure 6.37 (c1) and (c2) of XPS results indicate an atomic concentration of 59.5% carbon and 30.7% oxygen. A minor presence of calcium, potassium, nitrogen, sodium, silicon, and zinc

was detected. Nitrogen and other heteroatoms are favourable for electron transfer and ion insertion (Spanu et al., 2020). The zeta potential of BP BBGO is a negative charge (-9.34 mV) shown in Table 6.34. This value indicates the electrostatic behaviour on the carbon material surface and gives an idea about the electrostatic interaction with different charge species.

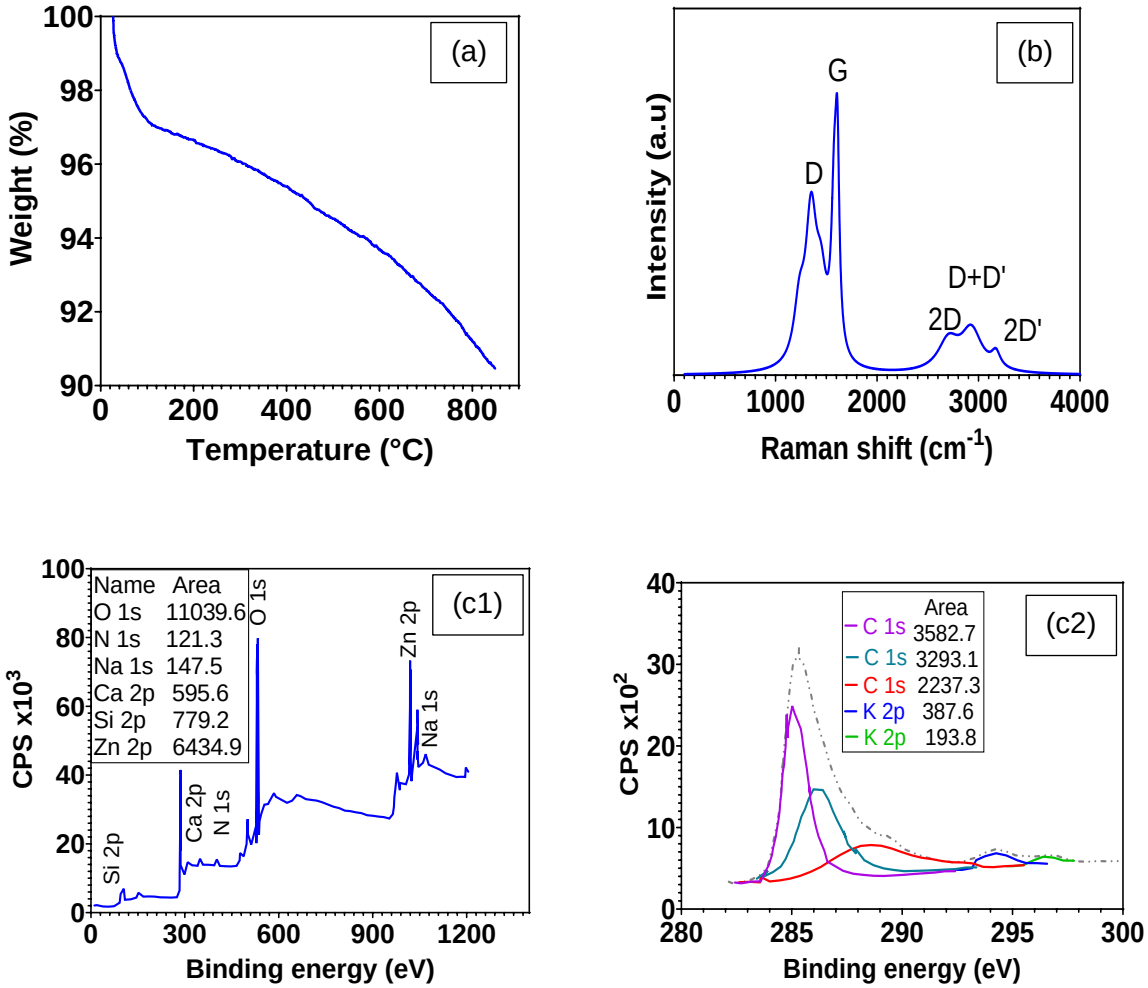

Figure 6.37. (a) Thermogravimetric analysis, (b) Raman spectra curves and (c1) (c2) XPS of BP BBGO.

Table 6.34: Zeta potential data of BP BBGO.

	Value
Zeta Potential (mV)	-9.34
Conductivity (mS/cm)	0.0134
Measured Current (mA)	0.00358
Measured Voltage (V)	149

6.3.2 Electrochemical characterisation of the modified electrode

The electrochemical properties of BP BBGO/SPCE are determined by the material sensor properties on the electrode surface, evaluating its active surface area and the electron transfer behaviour of the carbon material (Kokab et al., 2021). The electron transfer resistance of BP BBGO/SPCE was studied from EIS measurement. The EIS spectra are based on two main parts: (i) a semicircle that indicates electron transfer resistance (R_{ct}), and (ii) a linear section that represents solution diffusion resistance (Allende et al., 2023b). Figure 6.38 (a) shows the Nyquist plot of bare SPCE and modified electrode. The surface property of BP BBGO/SPCE from EIS denotes a smaller semicircle diameter (0.3 kΩ) than the bare electrode (~ 7.5 kΩ). This result implies that the modified electrode has lower charge-transfer resistance than bare SPCE. The cyclic voltammetry (CV) response of modified SPCE at 5 mV and 5 mM potassium ferricyanide was also analysed in Figure 6.38 (b). The current density of BP BBGO/SPCE was significantly higher than that of the bare SPCE, confirming the superior electrochemical active surface area of the modified SPCE. The potential peak-to-peak separation of bare SPCE and the modified electrode was 0.2 V and 0.1 V, respectively. This small peak-to-peak difference and potential shift (~ 1 V) indicate a greater electron transfer reaction (Wang et al., 2021a).

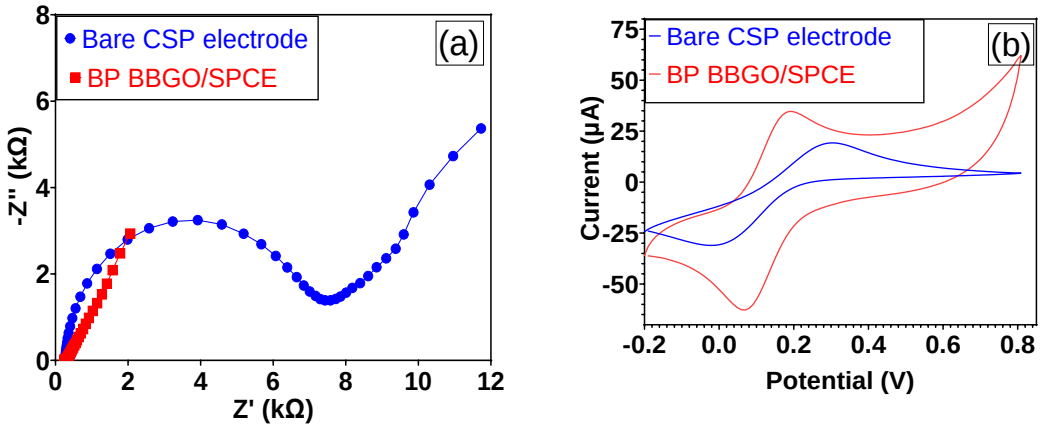

Figure 6.38. (a) Electrochemical impedance spectra (EIS) and (b) cyclic voltammetry (CV) response of bare SPCE and BPBBGO/SPCE in 0.1 M KCl containing 5 mM K_3 [(Fe $(CN)_6$)] at 5 mV potential amplitude.

6.3.3 Electrochemical detection of dopamine in the presence of ascorbic acid and uric acid

Ascorbic acid (AA), dopamine (DA) and uric acid (UA) are usually found simultaneous in biological human fluids. However, it was reported that AA, DA and UA have similar redox potentials (Patella et al., 2021; Wang et al., 2020c), which makes it challenging for selective dopamine detection. Herein, the selectivity of BP BBGO/SPC electrode towards determination of dopamine in the coexistence with these interferents was tested by voltammetry. Figures 6.39 (b) and (c) show the oxidation current response of non-modified and modified electrodes in the presence of individual AA and UA. The electrochemical results of modified SPCE do not exhibit a current response to AA and UA. These CV curves were analogous to the modified electrode in the blank solution. Nonetheless, a distinctive oxidation peak was observed in the presence of 0.5 mM DA (12.12 µA peak), whose current intensity was around three times higher than the bare electrode, shown in Figure 6.39 (a). A potential shift (reduction) of 0.09 V was also noticed, the oxidation peak of bare SPCE was achieved at 0.15 V, while the BP BBGO/SPC electrode was at 0.06 V.

In terms of selectivity, the bare electrode shows a similar oxidation potential for single detection of the species, e.g., the current response of ascorbic acid was 6.47 µA at 0.21 V, dopamine was 5.72 µA at 0.18 V, uric acid was 0.8 µA at 0.2 V, AA+UA+DA was 7.29 µA at 0.135 V. The non-modified electrode evidences a notable limitation for dopamine detection due to the bare SPCE showing only one oxidation peak in the co-existence of molecules, and it was not able to sense the analytes separately in the presence of 0.5 mM AA+UA+DA. This indicates that the oxidation peaks for all the species overlapped. In contrast, as shown in Figure 6.39 (a) and (d) BP BBGO/SPCE only shows an oxidation peak in the presence of DA, with no electro-activity for interfering species. This finding reveals that the carbon material on the electrode surface has improved the electrochemically active area for dopamine oxidation.

The electrostatic interactions between the carbon material on the surface of the SPCE and the interfering species were analysed to resolve the oxidation peaks of DA. This phenomenon can be explained by the intrinsic properties of BP BBGO, e.g., the carbon material is negatively charged (shown in zeta potential data), the same as ascorbic acid (pKa = 4.10) and uric acid (pKa = 5.40), but dopamine is oppositely charged (pKa = 8.87) at physical pH 7.0 (Li et al., 2013). Therefore, the electrostatic interactions on the surface of the modified electrode repel the negatively charged species of AA and UA, however, high attraction to positive change DA molecules. These properties are the main principles for achieving selective DA detection and resolving the oxidation response in co-existence with interference species. The electrostatic reaction between the carbon material and molecules is illustrated in Figure 6.39 (e).

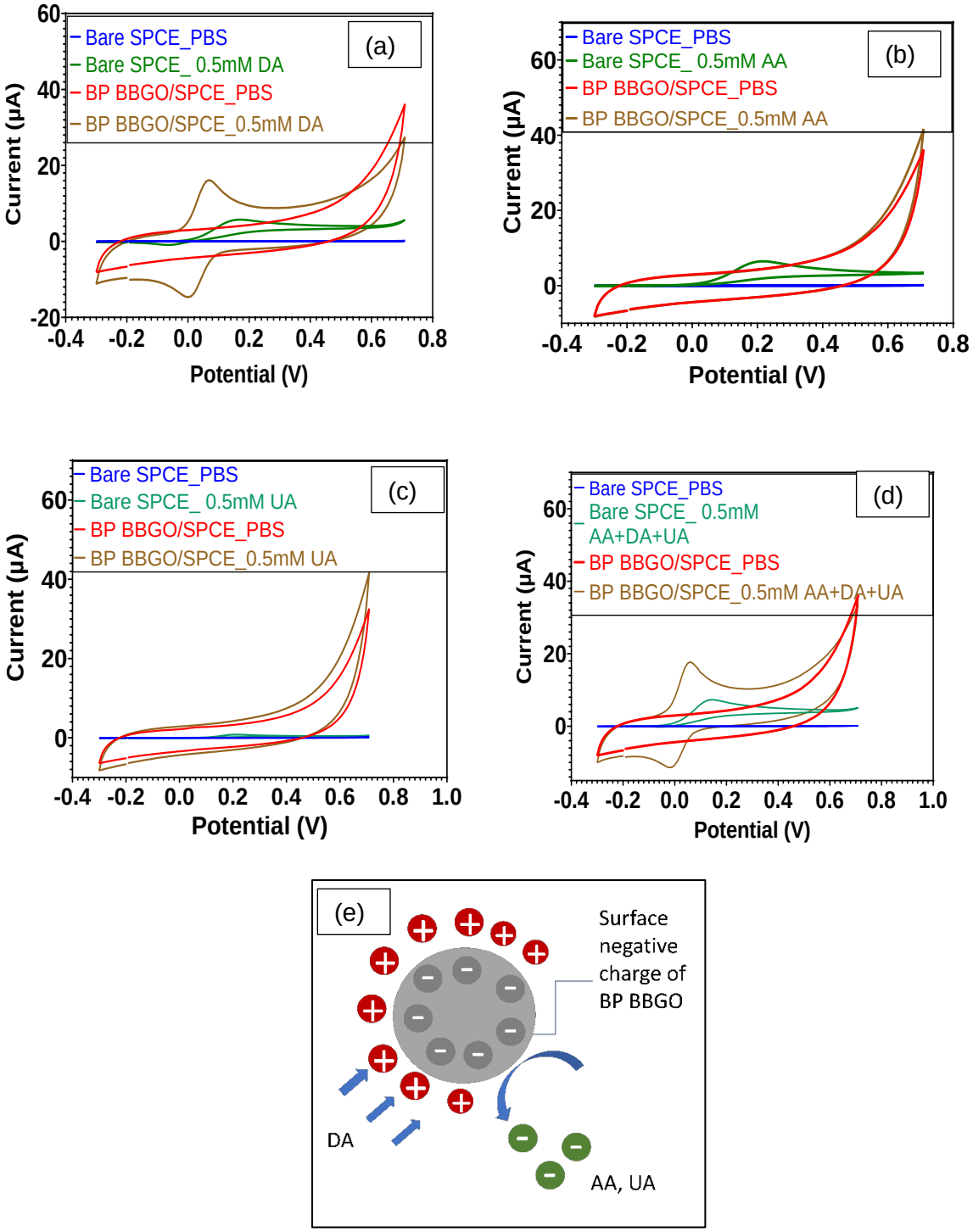

Figure 6.39. Cyclic voltammetry (CV) curves of bare SPC electrode and BP BBGO/SPCE in 0.5 mM ascorbic acid (a), 0.5 mM dopamine (b), 0.5 mM uric acid (c), and a combination of 0.5 mM AA+ 0.5 mM DA+ 0.5 mM UA (d) in 0.1 M phosphate buffer solution (pH 7.0) at 0.05 V/s scan rate, (e) surface potential reaction between the surface negative charge material and the charged molecules.

The sensitivity of the BP BBGO/SPC electrode was studied in Figure 6.40 (a) and (b). The DPV curves show that the oxidation current response of DA was not affected by the presence of AA and UA. The linear range region of the modified SPC electrode was between 0.02 mM and 1.5 mM DA. The linear regression equation is represented by I_{DA}= 12.268X_{DA}+ 36.315 with a correlation coefficient of 0.9866 and a limit of detection (LOD) of 0.02 mM. Table 6.35 reports the sensing characteristics of different DA sensors. The modified electrode demonstrates promising electrochemical performance for dopamine detection.

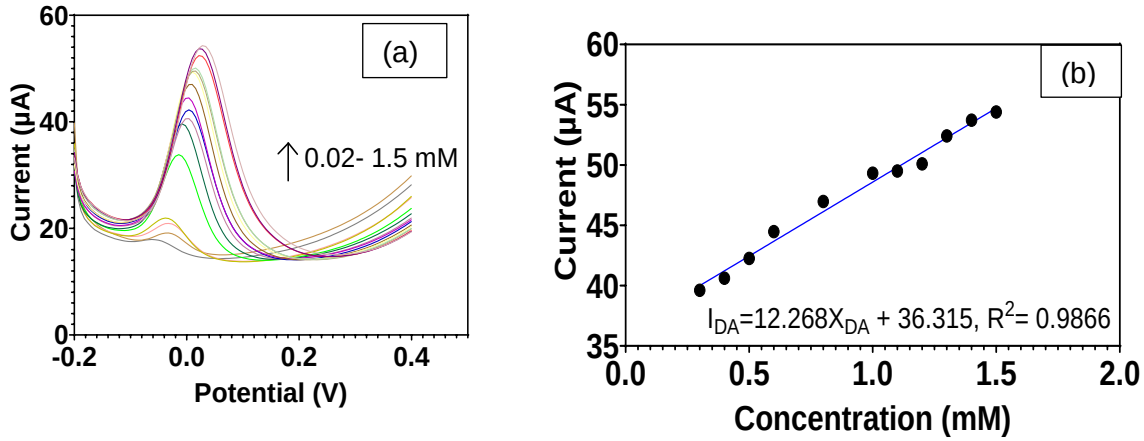

Figure 6.40. Differential pulse voltammetry (DPV) of dopamine (0.02 to 1.5 mM) at the (a) BP BBGO/SPCE in the presence of 0.5 mM AA and 0.5 mM UA (b) and the corresponding calibration curve.

Table 6.35. Comparison of the analytical performance of various modified electrodes for dopamine detection.

Electrode	**Linear range (µM)**	**LOD (µM)**	**Reference**
Sulfonated graphene	0.2-20	0.02	(Li et al., 2013)
PtNPs-rGO-ITO	0.1-20	0.075	(Patella et al., 2021)
PtAu/GCE	24–384	24	(Thiagarajan and Chen, 2007)
S-MC-1/GCE	0.01–5	3	(Emran et al., 2018)

PG/GCE	5–710	2	(Qi et al., 2015)
BP BBGO/SPCE	20-1500	20	This work

6.4 Conclusion

This manuscript reports the use of food waste as feedstock for the synthesis of graphene oxide for application in the electrochemical selectivity of dopamine detection. The resulting banana peel-derived biochar-based graphene oxide (BBGO) has carbon and oxygen as primary elements in the base matrix with a minor presence of heavier metal and organic-based particles, ~ 3.4 A lattice spacing, 345.79 m^2/g BET surface area, 173.99 m^2/g micropore area, and 0.074 cm^3/g micropore volume. The fabrication of the modified SPC electrode using BP BBGO showed higher selectivity and sensitivity of dopamine detection compared to the bare electrode. The improvements are related to the intrinsic properties of the modified electrode, such as high electrical conductivity, lower charge-transfer resistance, a higher electroactive area that increases the charge propagation of analytes and surface negative charge that attracts positively charged dopamine and repelling the negatively charged species like ascorbic acid and uric acid. The electrochemical detection of dopamine in the modified electrode demonstrated better selectivity in co-existence with interference species than the bare SPC electrode. This green carbon material has the potential to be applied in the sensing of other positively charged molecules. Overall, the developed technique is a highly efficient method for adding value to agricultural waste and converting the biochar into much more valuable graphene oxide, thereby developing various sensors.

CHAPTER 7

7 CONCLUSION AND RECOMMENDATION

This thesis investigated the feasibility of resource recovery from agricultural waste feedstock using microwave-assisted pyrolysis and identified various potential applications. The following points describe the conclusion ideas of the sub-topic considered in this work. The implications associated with the research project and recommendations for future works are also discussed.

7.1 Energy recovery under varying microwave pyrolysis conditions.

Sugarcane bagasse (SCB) is a valuable feedstock for clean energy generation. Microwave pyrolysis provides an efficient conversion method because of its short treatment time and heating mechanism. The optimisation of the microwave operating conditions is vital to reach the optimal energy and quality of biochar, bio-oil and biogas. Low microwave power and longer treatment time (over 30 min) produce biochar with a high heating value, carbon content, and uniform pore formation. The excess of pyrolysis power and microwave susceptor is unfavourable for bio-oil production due to the secondary reaction of non-condensable gases causing permanent gaseous. In contrast, high microwave heating, longer pyrolysis time and high addition of microwave susceptor are beneficial for syngas generation. The energy recovery demonstrated considerable efficiency (3-13%).

7.2 Paracetamol sensor using activated biochar.

Water contamination with pharmaceutical chemicals is a serious environmental issue. The detection methods of these molecules have attracted the attention of the electrochemical field. The synthesis of a sustainable sensor for the detection of paracetamol was studied. Microwave pyrolysis offers the generation of high-quality carbon materials for sensing applications without needing to add metals. The modified working electrode (SCB-activated biochar/GCE) was fabricated by the generation of activated biochar, which was synthesised by the chemical (sulphuric acid) and thermochemical (microwave pyrolysis) treatment of sugarcane bagasse. The resulting electrode revealed superior electron transfer kinetics properties and a higher current oxidation response of paracetamol. The limit of detection of SCB-activated biochar/GCE was comparable (2.5 µM) with previous work reporting metal-added material.

7.3 Food waste biochar for electrochemical sensing of nitrite.

The conversion of agro-waste into appreciated carbon material has attracted attention in the electrochemistry sector due to its multiple sensing applications. Pineapple peel is an excellent feedstock for the generation of activated biochar. The activated material was obtained by exposing the biochar to chemical treatment ($ZnCl_2$) and the carbonization process (second pyrolysis). The carbon was used in an ethanol solution for coating the surface of a glassy carbon electrode (GCE) for nitrite detection. The modified electrode exhibited a dielectric response, whose quality was mainly achieved by the intrinsic properties of the activated biochar (oxygen-containing functional groups, porosity, etc.). The $ZnCl_2$-activated biochar/GCE reached acceptable selectivity, sensibility, stability and reproducibility.

7.4 Graphene oxide-like biochar with high selective for dopamine detection.

A notable interest has been the development of eco-friendly carbon material for the highly selective detection of positive charge molecules. Biochar-based graphene oxide (BBGO) was synthesised using banana peel as feedstock, NaOH and $ZnCl_2$ as post-chemical treatment and microwave pyrolysis as the carbonization method. The BBGO showed a negative charge surface, which was suitable for the detection of positive charge analyte, e.g., dopamine. The selectivity of the material was tested using the carbon material in a screen-printed carbon electrode (SPCE) in the coexistence of negative charge species (ascorbic and uric acid). The modified SPC electrode proved highly selective for dopamine detection by the high electrical conductivity, lower charge-transfer resistance, and a higher electroactive area of the BBGO.

7.5 Overall conclusion.

The development of renewable energies from waste biomass is gaining notable interest due to the significant concern existing for waste management, excess consumption of agricultural resources, depletion of fossil fuel, and rapid population growth. This work demonstrated an efficient and environmentally friendly method of processing agricultural waste by using microwave-assisted pyrolysis. This thermochemical conversion process offers desirable quality on the by-products, e.g., high energy value, great carbon-rich content, high energy recovery, CO_2 sequestration potential, etc. These properties propose a clean alternative for energy generation and varied sustainable applications.

7.6 Implications of this research.

This work has a significant contribution to the sustainable development of various industrial sectors that covers the following aspects:

- The valorisation and quantification of agricultural waste provide an idea about the serious environmental and economic issues of the storage and disposal of waste- proving an eco-friendly alternative to waste processing by microwave-assisted pyrolysis.
- The lack of energy sources and depletion of fossil fuels carries the need to rely on emerging energy technologies- The conversion of agricultural waste into biochar, bio-oil, and biogas products by using microwave-assisted pyrolysis provides an energy recovery efficiency between 3 % and 13 %.
- The synthesis of carbon material has gained great interest in water treatment, water metal recovery and the fabrication of electrodes. However, the synthesis of this carbon material is complex, costly and involves no eco-friendly methods (addition of metals)—the proposed synthesis of carbon material is a favourable alternative to producing large quantities of activated biochar and graphene oxide-like biochar with excellent electrochemical properties.
- Water contamination by pharmaceutical and agricultural sectors has caused an alarming necessity for molecule detection. Nevertheless, the sensors available are highly costly and not accurate for all the analytes existing in these industries- This research applied the properties of biochar to fabricate a modified electrode for sensing nitrite, paracetamol, and dopamine.

7.7 Recommendations.

This research addressed diverse aspects of the conversion of agricultural waste into valuable products, e.g., energy recovery and biochar applications. The first part of the study showed promising performance in the bio-oil fuel application due to its high yield and phenol functional groups. The purification of bio-oil is suggested to remove the impurities and improve its quality. Depending on the purification process, the bio-oil can be used as biodiesel. In terms, of energy generation from biogas is recommended the integration of other technologies in the microwave system, like a solid oxide fuel cell, which advantage is the direct use of methane and hydrogen as a fuel for electricity production- implementing a cogeneration system.

Biochar has the potential for multiple applications in the energy sector, agricultural soil conditioners and the development of high-quality carbon material. The synthesis and activation method of biochar is relevant to determine its properties and uses. The electrochemical results (cyclic voltammetry) of the three agricultural carbon materials revealed a high capacitance performance. This property makes the synthesised biochar a good candidate for the fabrication of electrochemical supercapacitors.

REFERENCES

Abanades, S. A., H., et al., 2022. A critical review of biogas production and usage with legislations framework across the globe. Int J Environ Sci Technol (Tehran). 19**,** 3377-3400.

Abdelsayed, V., et al., 2019. Effect of Microwave and Thermal Co-pyrolysis of Low-Rank Coal and Pine Wood on Product Distributions and Char Structure. Energy & Fuels. 33**,** 7069-7082.

Abdurrahman, G., Biomass Conversion Technologies for Bioenergy Generation: An Introduction. In: B. Thalita Peixoto, et al., Eds.), Biotechnological Applications of Biomass. IntechOpen, Rijeka, 2020, pp. Ch. 1.

Abhijeet, P., et al., 2020. Prediction of pyrolytic product composition and yield for various grass biomass feedstocks. Biomass Conversion and Biorefinery. 10**,** 663-674.

Adejumo;, I. O., Adebiyi, O. A., 2020. Agricultural Solid Wastes: Causes, Effects, and Effective Management. Strategies of Sustainable Solid Waste Management.

Agu, O. S., et al., 2022. Impact of Biochar Addition in Microwave Torrefaction of Camelina Straw and Switchgrass for Biofuel Production. Fuels. 3**,** 588-606.

Alagarsamy, P., 2018. Amperometric Determination of Acetaminophen (paracetamol) Using Graphene Oxide Modified Glassy Carbon Electrode. International Journal of Electrochemical Science. 13**,** 7930-7938.

Alfhaid, L. H. K., 2022. Adsorption of paracetamol in contaminated water through pH-responsive polymer-brush-grafted mesoporous silica nanoparticles. International Journal of Environmental Analytical Chemistry. 1-17.

Allen, J. A., Downie, A. E., 2020. Predicting Slow Pyrolysis Process Outcomes with Simplified Empirical Correlations for a Consistent Higher Heating Temperature: Biochar Yield and Ash Content. Energy & Fuels. 34**,** 14223-14231.

Allende, S., et al., 2022. Energy recovery from sugarcane bagasse under varying microwave-assisted pyrolysis conditions. Bioresource Technology Reports. 20**,** 101283.

Allende, S., et al., 2023a. Breakdown of biomass for energy applications using microwave pyrolysis: A technological review. Environmental Research. 226**,** 115619.

Allende, S., et al., 2023b. Nitrite sensor using activated biochar synthesised by microwave-assisted pyrolysis. Waste Disposal & Sustainable Energy.

Aller, D., et al., 2017. Modified method for proximate analysis of biochars. Journal of Analytical and Applied Pyrolysis. 124**,** 335-342.

Amalina, F., et al., 2022. Advanced techniques in the production of biochar from lignocellulosic biomass and environmental applications. Cleaner Materials. 6**,** 100137.

Anca-Couce, A., et al., 2021. Bioenergy technologies, uses, market and future trends with Austria as a case study. Renewable and Sustainable Energy Reviews. 135**,** 110237.

Ani, M. d. F. S. A. M. A. M. M. J. J. A. P. S. a. F. N., Preparation of activated carbon from babassu endocarpunder microwave radiation by physical activation. In: I. C. S. E. a. E. Scienc, (Ed.), 2nd international Tropical Renewable Energy Conference Vol. 105, 2018.

Ansari, K. B., et al., 2019. Fast Pyrolysis of Cellulose, Hemicellulose, and Lignin: Effect of Operating Temperature on Bio-oil Yield and Composition and Insights into the Intrinsic Pyrolysis Chemistry. Industrial & Engineering Chemistry Research. 58**,** 15838-15852.

Armando T. Quitain, C. Y. H., Susana Yusup, Mitsuru Sasaki and Yoshimitsu Uemura 2015. Conversion of Biomass to Bio-Oil in Sub- and Supercritical Water. Biofuels - Status and Perspective.

Arpia, A. A., et al., 2021. Sustainable biofuel and bioenergy production from biomass waste residues using microwave-assisted heating: A comprehensive review. Chemical Engineering Journal. 403**,** 126233.

Awasthi, M. K., et al., 2022. Bacterial dynamics during the anaerobic digestion of toxic citrus fruit waste and semi-continues volatile fatty acids production in membrane bioreactors. Fuel. 319**,** 123812.
Babu, S., et al., 2022. Exploring agricultural waste biomass for energy, food and feed production and pollution mitigation: A review. Bioresource Technology. 360**,** 127566.
Badger, P., et al., 2011. Techno-Economic Analysis: Preliminary Assessment of Pyrolysis Oil Production Costs and Material Energy Balance Associated with a Transportable Fast Pyrolysis System. Bioresources. 6**,** 34-47.
Baharak Sajjadi, T. Z., Danuta Leszczynska, Jerzy Leszczynski and Wei Yin Chen, 2019. Chemical activation of biochar for energy and environmental applications: a comprehensive review. Reviews in Chemical Engineering. 35**,** 777-815.
Bartoli, M., et al., 2019. An Overview of Temperature Issues in Microwave-Assisted Pyrolysis. Processes. 7**,** 658.
Basu, P., Chapter 2 - Biomass Characteristics. In: P. Basu, (Ed.), Biomass Gasification and Pyrolysis. Academic Press, Boston, 2010, pp. 27-63.
Belyakov, N., Chapter Nineteen - Bioenergy. In: N. Belyakov, (Ed.), Sustainable Power Generation. Academic Press, 2019, pp. 461-474.
Beneroso, D., et al., 2017. Microwave pyrolysis of biomass for bio-oil production: Scalable processing concepts. Chemical Engineering Journal. 316**,** 481-498.
Benyekkou, N., et al., 2020. Elimination of paracetamol from water by a spent coffee grounds biomaterial. Environmental Nanotechnology, Monitoring & Management. 14**,** 100396.
Bhujel, R., et al., 2019. Capacitive and Sensing Responses of Biomass Derived Silver Decorated Graphene. Scientific Reports. 9**,** 19725.
Boumya, W., et al., 2021. Chemically modified carbon-based electrodes for the determination of paracetamol in drugs and biological samples. J Pharm Anal. 11**,** 138-154.
Brickler, C. A., et al., 2021a. Comparing Physicochemical Properties and Sorption Behaviors of Pyrolysis-Derived and Microwave-Mediated Biochar. Sustainability. 13**,** 2359.
Brickler, C. A., et al., 2021b. Comparing Physicochemical Properties and Sorption Behaviors of Pyrolysis-Derived and Microwave-Mediated Biochar. Sustainability. 13.
Brodie, G., 2008. The Influence of Load Geometry on Temperature Distribution During Microwave Heating. Transactions of the ASABE. 51**,** 1401-1413.
Bu, Q., et al., Catalytic Microwave Pyrolysis of Lignocellulosic Biomass for Fuels and Chemicals. Advances in bioenergy. Advances in bioenergy, Amsterdam, 2016, pp. 69-123.
Budarin, V. L., et al., 2015. The potential of microwave technology for the recovery, synthesis and manufacturing of chemicals from bio-wastes. Catalysis Today. 239**,** 80-89.
Burhenne, L., et al., 2013. The effect of the biomass components lignin, cellulose and hemicellulose on TGA and fixed bed pyrolysis. Journal of Analytical and Applied Pyrolysis. 101**,** 177-184.
Cai, J. M., et al., 2021a. Review on Aging of Bio-Oil from Biomass Pyrolysis and Strategy to Slowing Aging. Energy & Fuels. 35**,** 11665-11692.
Cai, Z., et al., 2021b. The choice of cooperation mode in the bioenergy supply chain with random biomass feedstock yield. Journal of Cleaner Production. 311**,** 127587.
Câmpean, A., et al., 2011. Voltammetric determination of some alkaloids and other compounds in pharmaceuticals and urine using an electrochemically activated glassy carbon electrode. Open Chemistry. 9**,** 688-700.
Cao, L., et al., 2020a. Rapid pyrolysis of Cu2+-polluted eggshell membrane into a functional Cu2+-Cu+/biochar for ultrasensitive electrochemical detection of nitrite in water. Science of The Total Environment. 723**,** 138008.
Cao, L., et al., 2020b. Rapid pyrolysis of Cu(2+)-polluted eggshell membrane into a functional Cu(2+)-Cu(+)/biochar for ultrasensitive electrochemical detection of nitrite in water. Sci Total Environ. 723**,** 138008.
Capanoglu, E., et al., 2022. Novel Approaches in the Valorization of Agricultural Wastes and Their Applications. Journal of Agricultural and Food Chemistry. 70**,** 6787-6804.

Casanova, A., et al., 2022. Recent progress in the development of porous carbon-based electrodes for sensing applications. Analyst. 147**,** 767-783.
Chatterjee, R., et al., 2020. Effect of Pyrolysis Temperature on PhysicoChemical Properties and Acoustic-Based Amination of Biochar for Efficient CO2 Adsorption. Frontiers in Energy Research. 8.
Chen, D. Y., et al., 2015. Bamboo pyrolysis using TG-FTIR and a lab-scale reactor: Analysis of pyrolysis behavior, product properties, and carbon and energy yields. Fuel. 148**,** 79-86.
Chen, M., et al., 2008. Catalytic effects of eight inorganic additives on pyrolysis of pine wood sawdust by microwave heating. Journal of Analytical and Applied Pyrolysis. 82**,** 145-150.
Chen, W. H., et al., 2021. Progress in biomass torrefaction: Principles, applications and challenges. Progress in Energy and Combustion Science. 82.
Cheng, B. H., et al., 2017. Recent developments of post-modification of biochar for electrochemical energy storage. Bioresour Technol. 246**,** 224-233.
Cheng, F., et al., 2020. Slow pyrolysis as a platform for negative emissions technology: An integration of machine learning models, life cycle assessment, and economic analysis. Energy Conversion and Management. 223**,** 113258.
Chikere, C. O., et al., 2019. The synergistic effect between graphene oxide nanocolloids and silicon dioxide nanoparticles for gallic acid sensing. Journal of Solid State Electrochemistry. 23**,** 1795-1809.
Cho, Y.-W., et al., 2020. Recent advances in nanomaterial-modified electrical platforms for the detection of dopamine in living cells. Nano Convergence. 7**,** 40.
Cong, H. B., et al., 2018. Slow Pyrolysis Performance and Energy Balance of Corn Stover in Continuous Pyrolysis-Based Poly-Generation Systems. Energy & Fuels. 32**,** 3743-3750.
Czajczyńska, D., et al., 2017. Potential of pyrolysis processes in the waste management sector. Thermal Science and Engineering Progress. 3**,** 171-197.
Dai, L., et al., 2020. A review on selective production of value-added chemicals via catalytic pyrolysis of lignocellulosic biomass. Science of The Total Environment. 749**,** 142386.
Dai, L., et al., 2019. Comparative study on characteristics of the bio-oil from microwave-assisted pyrolysis of lignocellulose and triacylglycerol. Science of The Total Environment. 659**,** 95-100.
Daneshmandi, M., et al., 2022. The incorporated environmental policies and regulations into bioenergy supply chain management: A literature review. Science of The Total Environment. 820**,** 153202.
Dehkhoda, A. M., et al., 2014. Electrosorption on activated biochar: effect of thermo-chemical activation treatment on the electric double layer capacitance. Journal of Applied Electrochemistry. 44**,** 141-157.
Dhanya, B. S., et al., 2020a. Development of sustainable approaches for converting the organic waste to bioenergy. Science of The Total Environment. 723**,** 138109.
Dhanya, B. S., et al., 2020b. Development of sustainable approaches for converting the organic waste to bioenergy. Sci Total Environ. 723**,** 138109.
Domingues, R. R., et al., 2017. Properties of biochar derived from wood and high-nutrient biomasses with the aim of agronomic and environmental benefits. PloS one. 12**,** e0176884-e0176884.
Domínguez, A., et al., 2007. Conventional and microwave induced pyrolysis of coffee hulls for the production of a hydrogen rich fuel gas. Journal of Analytical and Applied Pyrolysis. 79**,** 128-135.
Du, Z., et al., 2011. Microwave-assisted pyrolysis of microalgae for biofuel production. Bioresour Technol. 102**,** 4890-6.
Duarah, P., et al., 2022. A review on global perspectives of sustainable development in bioenergy generation. Bioresource Technology. 348**,** 126791.
Dungani, R., et al., 2015. Agricultural Waste Fibers Towards Sustainability and Advanced Utilization: A Review. Asian Journal of Plant Sciences. 15**,** 42-55.

Duque-Acevedo, M., et al., 2020. Agricultural waste: Review of the evolution, approaches and perspectives on alternative uses. Global Ecology and Conservation. 22**,** e00902.
El-Azazy, M., et al., 2022. Electrochemical Analysis of Sulfisoxazole Using Glassy Carbon Electrode (GCE) and MWCNTs/Rare Earth Oxide (CeO2 and Yb2O3) Modified-GCE Sensors. Molecules. 27.
Elkhalifa, S., et al., 2022. Biochar development from thermal TGA studies of individual food waste vegetables and their blended systems. Biomass Conversion and Biorefinery.
Ellison, C., et al., 2017. Dielectric Properties of Biomass/Biochar Mixtures at Microwave Frequencies. Energies. 10**,** 502.
Emran, M. Y., et al., 2018. One-step selective screening of bioactive molecules in living cells using sulfur-doped microporous carbon. Biosensors and Bioelectronics. 109**,** 237-245.
Energy, D. o. t. E. a., National food waste strategy: Halving Australia's food waste by 2030. In: C. o. Australia, (Ed.). The Australian Government, National Food Waste Strategy, 2017.
Escapa, C., et al., 2017. Paracetamol and salicylic acid removal from contaminated water by microalgae. Journal of Environmental Management. 203**,** 799-806.
Eshun, J., et al., 2019. Characterization of the physicochemical and structural evolution of biomass particles during combined pyrolysis and CO2 gasification. Journal of the Energy Institute. 92**,** 82-93.
Ethaib, S., et al., 2020. Microwave-Assisted Pyrolysis of Biomass Waste: A Mini Review. Processes. 8**,** 1190.
Fan, X., et al., 2011. Reversible redox reaction on the oxygen-containing functional groups of an electrochemically modified graphite electrode for the pseudo-capacitance. Journal of Materials Chemistry. 21**,** 18753-18760.
Fang, Z., et al., 2021. Influence of microwave-assisted pyrolysis parameters and additives on phosphorus speciation and transformation in phosphorus-enriched biochar derived from municipal sewage sludge. Journal of Cleaner Production. 287**,** 125550.
Fermanelli, C. S., et al., 2020. Pyrolysis and copyrolysis of three lignocellulosic biomass residues from the agro-food industry: A comparative study. Waste Management. 102**,** 362-370.
Fernandez, Y., et al., Microwave Heating Applied to Pyrolysis. Advances in Induction and Microwave Heating of Mineral and Organic Material. Intech, Spain, 2011, pp. 723-752.
Ferrari, G., et al., 2022. Where and how? A comprehensive review of multicriteria approaches for bioenergy plant siting. Journal of Cleaner Production. 346**,** 131238.
Ferrera-Lorenzo, N., et al., 2014. Conventional and microwave pyrolysis of a macroalgae waste from the Agar-Agar industry. Prospects for bio-fuel production. Bioresour Technol. 151**,** 199-206.
Fodah, A. E. M., Abdelwahab, T. A. M., 2022. Process optimization and technoeconomic environmental assessment of biofuel produced by solar powered microwave pyrolysis. Scientific Reports. 12**,** 12572.
Fodah, A. E. M., et al., 2021. Studies on Microwave-Assisted Pyrolysis of Rice Straw Using Solar Photovoltaic Power. BioEnergy Research. 14**,** 190-208.
Fodah, A. E. M., et al., 2022. Microwave-assisted pyrolysis of agricultural residues: current scenario, challenges, and future direction. International Journal of Environmental Science and Technology. 19**,** 2195-2220.
Foong, S. Y., et al., 2020. Valorization of biomass waste to engineered activated biochar by microwave pyrolysis: Progress, challenges, and future directions. Chemical Engineering Journal. 389**,** 124401.
Foroughi, S. H. D. S. J. D. M. M., 2021. Simultaneous voltammetric determination of tramadol and paracetamol exploiting glassy carbon electrode modified with FeNi3 nanoalloy in biological and pharmaceutical media. Analytical Chemistry. 6**,** 8797-8808.

Fu, L., et al., 2018. Graphene Ink Film Based Electrochemical Detector for Paracetamol Analysis. Electronics. 7**,** 15.
Gabhane, J. W., et al., 2020. Recent trends in biochar production methods and its application as a soil health conditioner: a review. SN Applied Sciences. 2**,** 1307.
García-Depraect, O., et al., 2022. Two-stage anaerobic digestion of food waste: Enhanced bioenergy production rate by steering lactate-type fermentation during hydrolysis-acidogenesis. Bioresource Technology. 127358.
Gautam, P., et al., Energy-Aware Intelligence in Megacities. In: S. K. R. K. A. Pandey, (Ed.), Current Developments in Biotechnology and Bioengineering. Current Developments in Biotechnology and Bioengineering, 2019, pp. 211-238.
Ge, S., et al., 2021. Progress in microwave pyrolysis conversion of agricultural waste to value-added biofuels: A batch to continuous approach. Renewable and Sustainable Energy Reviews. 135**,** 110148.
Ghesti, G. F., et al., 2022. Towards a sustainable waste-to-energy pathway to pequi biomass residues: Biochar, syngas, and biodiesel analysis. Waste Management. 143**,** 144-156.
Ghosh, P., et al., Life cycle assessment of waste-to-bioenergy processes: a review. In: A. Y. Lakhveer Singh, Durga Madhab Mahapatra, (Ed.), Bioreactors. Sustainable Design and Industrial Applications in Mitigation of GHG Emissions, 2020, pp. 105-122.
Giorcelli, M., et al., 2021. A Review of Bio-Oil Production through Microwave-Assisted Pyrolysis. Processes. 9**,** 561.
Godwin, P. M., et al., 2019. Progress in Preparation and Application of Modified Biochar for Improving Heavy Metal Ion Removal From Wastewater. Journal of Bioresources and Bioproducts. 4**,** 31-42.
Gomes, G. M. F. S. D. F. T. N. d. Q. F. Z. J. H. d. Q. F., 2018. Characterization and Potential Evaluation of Residues from the Sugarcane Industry of Rio Grande do Sul in Biorefinery Processes Natural Resources. 9**,** 175-187.
Guan, Y., et al., 2019. Pyrolysis kinetics behavior of solid leather wastes. Waste Management. 100**,** 122-127.
Gupta, G. K., Mondal, M. K., 15 - Bioenergy generation from agricultural wastes and enrichment of end products. In: R. P. Kumar, et al., Eds.), Refining Biomass Residues for Sustainable Energy and Bioproducts. Academic Press, 2020, pp. 337-356.
Hadiya, V., et al., 2022. Biochar production with amelioration of microwave-assisted pyrolysis: Current scenario, drawbacks and perspectives. Bioresource Technology. 355**,** 127303.
Haldorai, Y., et al., 2017. Electrochemical determination of tryptophan using a glassy carbon electrode modified with flower-like structured nanocomposite consisting of reduced graphene oxide and SnO 2. Sensors and Actuators B: Chemical. 239**,** 1221-1230.
Halim, S. A., Swithenbank, J., 2016. Characterisation of Malaysian wood pellets and rubberwood using slow pyrolysis and microwave technology. Journal of Analytical and Applied Pyrolysis. 122**,** 64-75.
Hansen, S., et al., 2020. A comprehensive state-of-technology review for upgrading bio-oil to renewable or blended hydrocarbon fuels. Renewable and Sustainable Energy Reviews. 118**,** 109548.
Hansirisawat, P., Srinophakun, T. R., 2020. Techno-Economic of 100 kW Power Plant from Microwave-Assisted Biodiesel Pyrolysis. International Journal of Renewable Energy Research. 10**,** 1021-1030.
Hao, L. C., et al., 2 - Natural fiber reinforced vinyl polymer composites. In: S. M. Sapuan, et al., Eds.), Natural Fibre Reinforced Vinyl Ester and Vinyl Polymer Composites. Woodhead Publishing, 2018, pp. 27-70.
Hasan, M. M., et al., 2021. Energy recovery from municipal solid waste using pyrolysis technology: A review on current status and developments. Renewable and Sustainable Energy Reviews. 145**,** 111073.

Hassan, M., et al., 2020. Influences of feedstock sources and pyrolysis temperature on the properties of biochar and functionality as adsorbents: A meta-analysis. Sci Total Environ. 744**,** 140714.
Hidalgo, P., et al., 2019. Synthesis of carbon nanotubes using biochar as precursor material under microwave irradiation. Journal of Environmental Management. 244**,** 83-91.
Hu, X., Gholizadeh, M., 2020. Progress of the applications of bio-oil. Renewable and Sustainable Energy Reviews. 134**,** 110124.
Huang, Y.-F., et al., 2015. Microwave pyrolysis of rice straw to produce biochar as an adsorbent for CO2 capture. Energy. 84**,** 75-82.
Huang, Y. F., et al., 2016a. Microwave pyrolysis of lignocellulosic biomass: Heating performance and reaction kinetics. Energy. 100**,** 137-144.
Huang, Y. F., et al., 2016b. A review on microwave pyrolysis of lignocellulosic biomass. Sustainable Environment Research. 26**,** 103-109.
Huber, G., et al., 2006. Synthesis of Transportation Fuels from Biomass: Chemistry, Catalysts, and Engineering. Chemical Reviews. 106**,** 4044-4098.
Hussain, K., et al., 2018. Production of highly upgraded bio-oil by microwave–metal interaction pyrolysis of biomass in a copper coil reactor. International Journal of Green Energy. 15**,** 758-765.
Idris, S. S., et al., 2022. Microwave-Assisted Pyrolysis of Oil Palm Biomass: Multi-Optimisation of Solid Char Yield and Its Calorific Value Using Response Surface Methodology. Frontiers in Chemical Engineering. 4.
Ifeanyi Michael Smarte, A., et al., Bioenergy Production: Emerging Technologies. In: S. Mohamed, (Ed.), Biomass, Biorefineries and Bioeconomy. IntechOpen, Rijeka, 2022, pp. Ch. 14.
Inayat, A., et al., 2022. Techno-Economical Evaluation of Bio-Oil Production via Biomass Fast Pyrolysis Process: A Review. Frontiers in Energy Research. 9.
J. Tang, F. P. R., 1 - Electromagnetic basis of microwave heating. In: P. S. P. Matthew W. Lorence, (Ed.), Development of Packaging and Products for Use in Microwave Ovens, Woodhead Publishing, 2009, pp. 3-38e.
J.Solar, et al., 2016. Influence of temperature and residence time in the pyrolysis of woody biomass waste in a continuous screw reactor. Biomass and bioenergy. 95**,** 416-423.
Jahirul, M. I., et al., 2012. Biofuels Production through Biomass Pyrolysis-A Technological Review. Energies. 5**,** 4952-5001.
Jayaprakash, K., et al., 2022. Agriculture Waste Biomass Repurposed into Natural Fibers: A Circular Bioeconomy Perspective. Bioengineering (Basel). 9.
Jennita Jacqueline, P., et al., 2022. Catalytic microwave preheated co-pyrolysis of lignocellulosic biomasses: A study on biofuel production and its characterization. Bioresource Technology. 347**,** 126382.
Jesus, M. S., et al., 2018. Energy and mass balance in the pyrolysis process of eucalyptus wood. CERNE. 24**,** 2317-6342.
Juan Camilo Solarte-Toro, Y. C.-P., Carlos Ariel Cardona-Alzate, 2018. Evaluation of biogas and syngas as energy vectors for heat and power generation using lignocellulosic biomass as raw material. Electronic Journal of Biotechnology. 33**,** 52-62.
K. Shi, T. W., J. Yan, H. Zhao and E. Lester, Microwave enhanced pyrolysis of gumwood. International Conference on Materials for Renewable Energy and Environment, 2013, pp. 223-227.
K.Sarkar, D., Chapter 3 - Fuels and Combustion. Thermal Power Plant, 2015, pp. 91-137.
K.Tanneru, S., H.Steele, P., 2015. Direct hydrocracking of oxidized bio-oil to hydrocarbons. Fuel. 154**,** 268-274.
Kadlimatti, H. M., et al., 2019. Bio-oil from microwave assisted pyrolysis of food waste-optimization using response surface methodology. Biomass and bioenergy. 123**,** 25-33.
Kalinke, C., et al., 2021. State-of-the-art and perspectives in the use of biochar for electrochemical and electroanalytical applications. Green Chemistry. 23**,** 5272-5301.

Kan, T., et al., 2016. Lignocellulosic biomass pyrolysis: A review of product properties and effects of pyrolysis parameters. Renewable and Sustainable Energy Reviews. 57**,** 1126-1140.
Karimi-Maleh, H., et al., 2014. A sensitive nanocomposite-based electrochemical sensor for voltammetric simultaneous determination of isoproterenol, acetaminophen and tryptophan. Measurement. 51**,** 91-99.
Karpagam, R., et al., 2021. Review on integrated biofuel production from microalgal biomass through the outset of transesterification route: a cascade approach for sustainable bioenergy. Science of The Total Environment. 766**,** 144236.
Kazim, A.-H. A.-O. R. A.-A. H., Production of fuel gases from reed by using downdraft gasifier. The 3rd International Conference on Buildings, Construction and Environmental Engineering, BCEE3-2017, Vol. 162, 2018.
Khan, A., et al., 2017. Low-Cost Carbon Fillers to Improve Mechanical Properties and Conductivity of Epoxy Composites. Polymers. 9**,** 642.
Khan, S. A., et al., 2021. Mutually trading off biochar and biogas sectors for broadening biomethane applications: A comprehensive review. Journal of Cleaner Production. 318**,** 128593.
Khelfa, A., et al., 2020. Microwave-Assisted Pyrolysis of Pine Wood Sawdust Mixed with Activated Carbon for Bio-Oil and Bio-Char Production. Processes. 8**,** 1437.
Khuenkaeo, N., et al., 2021. Production and characterization of bio-oils from fast pyrolysis of tobacco processing wastes in an ablative reactor under vacuum. PLoS One. 16**,** e0254485.
Kokab, T., et al., 2021. Electrochemical sensing platform for the simultaneous femtomolar detection of amlodipine and atorvastatin drugs. RSC Advances. 11**,** 27135-27151.
Kosakowski, W., et al., 2020. Biochars from Post-Production Biomass and Waste from Wood Management: Analysis of Carbonization Products. Materials (Basel). 13.
Koul, B., et al., 2022. Agricultural waste management strategies for environmental sustainability. Environmental Research. 206**,** 112285.
Kumar, R., Strezov, V., 2021. Thermochemical production of bio-oil: A review of downstream processing technologies for bio-oil upgrading, production of hydrogen and high value-added products. Renewable and Sustainable Energy Reviews. 135**,** 110152.
Kung, C.-C., et al., 2022. A review of biopower and mitigation potential of competing pyrolysis methods. Renewable and Sustainable Energy Reviews. 162**,** 112443.
Lam, S. S., et al., 2019a. Microwave vacuum pyrolysis of waste plastic and used cooking oil forsimultaneouswastereductionandsustainableenergyconversion:Recoveryof cleaner liquid fuel and techno-economic analysis. Renewable and Sustainable Energy Reviews. 115.
Lam, S. S., Chase, H. A., 2012. A Review on Waste to Energy Processes Using Microwave Pyrolysis. Energies. 5**,** 4209-4232.
Lam, S. S., et al., 2019b. Microwave vacuum pyrolysis of waste plastic and used cooking oil for simultaneous waste reduction and sustainable energy conversion: Recovery of cleaner liquid fuel and techno-economic analysis. Renewable and Sustainable Energy Reviews. 115**,** 109359.
Lam, S. S., et al., 2020. Engineering pyrolysis biochar via single-step microwave steam activation for hazardous landfill leachate treatment. Journal of Hazardous Materials. 390**,** 121649.
Lay, M., et al., 2020. Converting dead leaf biomass into activated carbon as a potential replacement for carbon black filler in rubber composites. Composites Part B: Engineering. 201**,** 108366.
Le Pera, A., et al., 2022. Composting food waste or digestate? Characteristics, statistical and life cycle assessment study based on an Italian composting plant. Journal of Cleaner Production. 350**,** 131552.
Lee, S. Y., et al., 2019. Waste to bioenergy: a review on the recent conversion technologies. BMC Energy. 1**,** 4.

Lei, P., et al., 2020. Gold nanoparticles decorated bimetallic CuNi-based hollow nanoarchitecture for the enhancement of electrochemical sensing performance of nitrite. Mikrochim Acta. 187**,** 572.
Leng, L., et al., 2021. An overview on engineering the surface area and porosity of biochar. Sci Total Environ. 763**,** 144204.
Li, H. Y., et al., 2022a. Microwave-assisted depolymerization of lignin with synergic alkali catalysts and a transition metal catalyst in the aqueous system. Reaction Chemistry & Engineering. 7**,** 1750-1761.
Li, J., et al., 2016. Biochar from microwave pyrolysis of biomass: A review. Biomass & Bioenergy. 94**,** 228-244.
Li, J., et al., 2022b. Wet wastes to bioenergy and biochar: A critical review with future perspectives. Science of The Total Environment. 817**,** 152921.
Li, P., et al., 2021. Bio-oil from biomass fast pyrolysis: Yields, related properties and energy consumption analysis of the pyrolysis system. Journal of Cleaner Production. 328**,** 129613.
Li, Q., et al., 2022c. Co-liquefaction of mixed biomass feedstocks for bio-oil production: A critical review. Renewable and Sustainable Energy Reviews. 154**,** 111814.
Li, S.-J., et al., 2013. Electrochemical detection of dopamine using water-soluble sulfonated graphene. Electrochimica Acta. 102**,** 58-65.
Li, S., et al., 2022d. Microwave pyrolysis of sludge: a review. Sustainable Environment Research. 32**,** 23.
Li, X., et al., 2018. White poplar microwave pyrolysis: Heating rate and optimization of biochar yield. BioResources. 13**,** 1107-1121.
Li, X., et al., 2022e. Microwave pyrolysis coupled with conventional pre-pyrolysis of the stalk for syngas and biochar. Bioresource Technology. 348**,** 126745.
Li, X., et al., 2019. Effects of root exudates on the sorption of polycyclic aromatic hydrocarbons onto biochar. Environmental Pollutants and Bioavailability. 31**,** 156-165.
Li, Y., et al., 2022f. Recent Advances of Biochar-Based Electrochemical Sensors and Biosensors. Biosensors (Basel). 12.
Lim, X. Y., et al., 2022. Engineered biochar produced through microwave pyrolysis as a fuel additive in biodiesel combustion. Fuel. 312**,** 122839.
Lin, B.-J., Chen, W.-H., 2015. Sugarcane Bagasse Pyrolysis in a Carbon Dioxide Atmosphere with Conventional and Microwave-Assisted Heating. Frontiers in Energy Research. 3.
Lin, B., W.Chen, 2015. Sugarcane bagasse pyrolysis in a carbon dioxide atmosphere with conventional and microwave-assisted heating. Front. Energy Res. 4.
Lin, F., et al., 2015. Relationships between Biomass Composition and Liquid Products Formed via Pyrolysis. Frontiers in Energy Research. 3.
Lin, J., et al., 2022. Comparison of microwave pyrolysis and conventional pyrolysis of Eupatorium adenophorum. Environmental Progress & Sustainable Energy.
Lin, J., et al., 2023. Scaled-up microwave pyrolysis of sludge for hydrogen-rich biogas and life cycle assessment: Parameters synergistic optimization, carbon footprint analysis and technology upgrade. Chemical Engineering Journal. 452**,** 139551.
Liu, C., et al., 2020. Preparation of Acid- and Alkali-Modified Biochar for Removal of Methylene Blue Pigment. ACS Omega. 5**,** 30906-30922.
Liu, H., et al., 2021a. Preparation of porous biochar based on pharmaceutical sludge activated by NaOH and its application in the adsorption of tetracycline. Journal of Colloid and Interface Science. 587**,** 271-278.
Liu, Q., et al., 2021b. Role of the biochar modified with ZnCl2 and FeCl3 on the electrochemical degradation of nitrobenzene. Chemosphere. 275**,** 129966.
Liu, R., et al., 2014. Influence of acetone addition on the physicochemical properties of bio-oils. Journal of the energy institute. 87**,** 127-133.
Liu, T., et al., 2022. Recent advances, current issues and future prospects of bioenergy production: A review. Science of The Total Environment. 810**,** 152181.

Liu, Y., et al., 2021c. Variations of GHG emission patterns from waste disposal processes in megacity Shanghai from 2005 to 2015. Journal of Cleaner Production. 295**,** 126338.
Liu, Y., et al., 2021d. Comparison between hydrogen-rich biogas production from conventional pyrolysis and microwave pyrolysis of sewage sludge: is microwave pyrolysis always better in the whole temperature range? International Journal of Hydrogen Energy. 46**,** 23322-23333.
Liyana, Z., et al., Investigation of sugar cane bagasse as alternative material for pyramidal microwave absorber design. 2012 IEEE Symposium on Wireless Technology and Applications (ISWTA), Bandung, 2012.
Lo, S. L., et al., 2017. Microwave pyrolysis of lignocellulosic biomass. 8th International Conference on Applied Energy (Icae2016). 105**,** 41-46.
Luk, H.-N., et al., 2021. Promotion Effect of Palladium on BiVO4 Sensing Material for Epinephrine Detection. Catalysts. 11**,** 1083.
Luo, S., et al., 2022. A Low Cost Fe(3)O(4)-Activated Biochar Electrode Sensor by Resource Utilization of Excess Sludge for Detecting Tetrabromobisphenol A. Micromachines. 13**,** 115.
Lyu, G., et al., 2015. Estimation and Comparison of Bio-Oil Components from Different Pyrolysis Conditions. Frontiers in Energy Research. 3.
M.Waqasa, et al., 2018. Development of biochar as fuel and catalyst in energy recovery technologies. Journal of Cleaner Production. 188**,** 477-488.
Macquarrie, D. J., et al., 2012. The microwave pyrolysis of biomass. Biofuels, Bioproducts and Biorefining. 6**,** 549-560.
Madhu, R., et al., 2014. Eco-friendly synthesis of activated carbon from dead mango leaves for the ultrahigh sensitive detection of toxic heavy metal ions and energy storage applications. RSC Advances. 4**,** 1225-1233.
Mahari, W. A. W., et al., 2018. Microwave co-pyrolysis of waste polyolefins and waste cooking oil:Influence of N2atmosphere versus vacuum environment. Energy Conversion and Management. 171**,** 1292-1301.
Mani, V., et al., 2014. Direct electrochemistry of myoglobin at reduced graphene oxide-multiwalled carbon nanotubes-platinum nanoparticles nanocomposite and biosensing towards hydrogen peroxide and nitrite. Biosens Bioelectron. 53**,** 420-7.
Manoj, D., et al., 2018. Towards green synthesis of monodisperse Cu nanoparticles: An efficient and high sensitive electrochemical nitrite sensor. Sensors and Actuators B: Chemical. 266**,** 873-882.
Martínez-Sánchez, C., et al., 2019. Electrochemical sensing of acetaminophen using a practical carbon paste electrode modified with a graphene oxide-Y2O3 nanocomposite. Journal of the Taiwan Institute of Chemical Engineers. 96**,** 382-389.
Mašek, O., et al., 2013. Microwave and slow pyrolysis biochar—Comparison of physical and functional properties. Journal of Analytical and Applied Pyrolysis. 100**,** 41-48.
Meng, R., et al., 2018. Development, modification, and application of low-cost and available biochar derived from corn straw for the removal of vanadium(v) from aqueous solution and real contaminated groundwater. RSC Advances. 8**,** 21480-21494.
Merlen, A., et al., 2017. A Guide to and Review of the Use of Multiwavelength Raman Spectroscopy for Characterizing Defective Aromatic Carbon Solids: from Graphene to Amorphous Carbons. Coatings. 7**,** 153.
Mierzwa-Hersztek, M., et al., 2019. Assessment of energy parameters of biomass and biochars, leachability of heavy metals and phytotoxicity of their ashes. Journal of Material Cycles and Waste Management. 21**,** 786–800.
Millati, R., et al., Chapter 1 - Agricultural, Industrial, Municipal, and Forest Wastes: An Overview. In: M. J. Taherzadeh, et al., Eds.), Sustainable Resource Recovery and Zero Waste Approaches. Elsevier, 2019, pp. 1-22.
Mishra, R. R., Sharma, A. K., 2016. Microwave–material interaction phenomena: Heating mechanisms, challenges and opportunities in material processing. Composites Part A: Applied Science and Manufacturing. 81**,** 78-97.

Moghadam, R. A., et al., 2014. Investigation on syngas production via biomass conversion through the integration of pyrolysis and air-steam gasification processes. Energy Conversion and Management. 87**,** 670-675.
Mohamed, B. A., et al., 2016. Microwave-assisted catalytic pyrolysis of switchgrass for improving bio-oil and biochar properties. Bioresour Technol. 201**,** 121-32.
Mohammed, I. Y., et al., 2015. Pyrolysis of Napier Grass in a Fixed Bed Reactor: Effect of Operating Conditions on Product Yields and Characteristics. Bioresources. 10**,** 6457-6478.
Mohan, J. M., et al., 2020. Highly Selective Electrochemical Sensing of Dopamine, Xanthine, Ascorbic Acid and Uric Acid Using a Carbon Fiber Paper. IEEE Sensors Journal. 20**,** 11707-11712.
Mohanty, A., et al., 2022. Sustainable utilization of food waste for bioenergy production: A step towards circular bioeconomy. International Journal of Food Microbiology. 365**,** 109538.
Mong, G. R., et al., 2021. Multivariate optimisation study and life cycle assessment of microwave-induced pyrolysis of horse manure for waste valorisation and management. Energy. 216**,** 119194.
Mong, G. R., et al., 2022. Environment impact and bioenergy analysis on the microwave pyrolysis of WAS from food industry: Comparison of CO2 and N2 atmosphere. Journal of Environmental Management. 319**,** 115665.
Monticelli, D. S. G. B. C. D. D., 2020. Biochar as an alternative sustainable platform for sensing applications: A review. Microchemical Journal. 159.
Moriarty, P., 2022. Can Bioenergy Once again Become a Major Global Energy Source? Encyclopedia. 2**,** 1357-1369.
Muhammad Hafiz, S., et al., 2014. A practical carbon dioxide gas sensor using room-temperature hydrogen plasma reduced graphene oxide. Sensors and Actuators B: Chemical. 193**,** 692-700.
Mullane, J., Average Electricity Costs per kWh. Canstar Blu, 2022.
Mullaney, H., et al., Technical, Environmental and Economic Feasibility of Bio-Oil. New Hampshire Industrial Research Center (NHIRC), Durham, 2002.
Mulu, E., et al., 2021. A review of recent developments in application of low cost natural materials in purification and upgrade of biogas. Renewable and Sustainable Energy Reviews. 145**,** 111081.
Mulyasuryani, A., et al., 2019. Simultaneous Voltammetric Detection of Acetaminophen and Caffeine Base on Cassava Starch—Fe3O4 Nanoparticles Modified Glassy Carbon Electrode. Chemosensors. 7**,** 49.
Muzyka, R., et al., 2018a. Characterization of Graphite Oxide and Reduced Graphene Oxide Obtained from Different Graphite Precursors and Oxidized by Different Methods Using Raman Spectroscopy. Materials. 11**,** 1050.
Muzyka, R., et al., 2018b. Characterization of Graphite Oxide and Reduced Graphene Oxide Obtained from Different Graphite Precursors and Oxidized by Different Methods Using Raman Spectroscopy. Materials (Basel). 11.
Najeeb, M. I., et al., 2021. Characterization of Lignocellulosic Biomass from Malaysian's Yankee Pineapple AC6 Toward Composite Application. Journal of Natural Fibers. 18**,** 2006-2018.
Nhuchhen, D. R., et al., 2018. Characteristics of biochar and bio-oil produced from wood pellets pyrolysis using a bench scale fixed bed, microwave reactor. Biomass & Bioenergy. 119**,** 293-303.
Nikkhah, H., et al., 2020. Investigating the influence of acid washing pretreatment and Zn/activated biochar catalyst on thermal conversion of Cladophora glomerata to value-added bio-products. Energy Conversion and Management. 225**,** 113392.
Nizamuddin, S., et al., 2018. An overview of microwave hydrothermal carbonization and microwave pyrolysis of biomass. Reviews in Environmental Science and Bio/Technology. 17**,** 813–837.

Nomanbhay, S., et al., 2017. Microwave pyrolysis of lignocellulosic biomass—a contribution to power Africa. Energy, Sustainability and Society 7.
Nozieana, K., et al., Nano-Cellulosic Fibers from Agricultural Wastes. In: S. Arpit, B. Sangita, Eds.), Cellulose Science and Derivatives. IntechOpen, Rijeka, 2021, pp. Ch. 3.
Nzediegwu, C., et al., 2021. Fuel, thermal and surface properties of microwave-pyrolyzed biochars depend on feedstock type and pyrolysis temperature. Bioresour Technol. 320**,** 124282.
Omar, R., Robinson, J. P., 2014. Conventional and microwave-assisted pyrolysis of rapeseed oil for bio-fuel production. Journal of Analytical and Applied Pyrolysis. 105**,** 131-142.
Osman, A. I., et al., 2021. Conversion of biomass to biofuels and life cycle assessment: a review. Environmental Chemistry Letters. 19**,** 4075-4118.
Özyuğuran, A., et al., 2018. Prediction of calorific value of biomass based on elemental analysis. International advanced researches and engineering journal. 2**,** 254-260.
P.M.Mortensen, et al., 2011. A review of catalytic upgrading of bio-oil to engine fuels. Applied Catalysis A: General. 407**,** 1-19.
Panwar, N. L., Paul, A. S., 2021. An overview of recent development in bio-oil upgrading and separation techniques. Environmental Engineering Research. 26**,** 200382-0.
Patella, B., et al., 2021. Electrochemical detection of dopamine with negligible interference from ascorbic and uric acid by means of reduced graphene oxide and metals-NPs based electrodes. Analytica Chimica Acta. 1187**,** 339124.
Peiris, C., et al., 2019. The influence of three acid modifications on the physicochemical characteristics of tea-waste biochar pyrolyzed at different temperatures: a comparative study. RSC Advances. 9**,** 17612-17622.
Pham, T. N., et al., 2013. Ketonization of Carboxylic Acids: Mechanisms, Catalysts, and Implications for Biomass Conversion. Acs Catalysis. 3**,** 2456-2473.
Pishvaee, M. S., et al., Biofuel supply chain structures and activities. In: M. S. P. S. M. S. Bairamzadeh, (Ed.), Biomass to Biofuel Supply Chain Design and Planning Under Uncertainty. Concepts and Quantitative Methods, 2021, pp. 21-36.
Prasad, S., Ingle, A. P., Chapter 12 - Impacts of sustainable biofuels production from biomass. In: M. Rai, A. P. Ingle, Eds.), Sustainable Bioenergy. Elsevier, 2019, pp. 327-346.
Prathiba, R., et al., 2018. Pyrolysis of polystyrene waste in the presence of activated carbon in conventional and microwave heating using modified thermocouple. Waste Management. 76**,** 528-536.
Qi, S., et al., 2015. Determination of ascorbic acid, dopamine, and uric acid by a novel electrochemical sensor based on pristine graphene. Electrochimica Acta. 161**,** 395-402.
Qian, C., et al., 2020. Prediction of higher heating values of biochar from proximate and ultimate analysis. Fuel. 265**,** 116925.
Qu, T. T., et al., 2011. Experimental Study of Biomass Pyrolysis Based on Three Major Components: Hemicellulose, Cellulose, and Lignin. Industrial & Engineering Chemistry Research. 50**,** 10424-10433.
Quillope, J. C. C., et al., 2021. Optimization of process parameters of self-purging microwave pyrolysis of corn cob for biochar production. Heliyon. 7**,** e08417.
Rafiq, M. K., et al., 2016. Influence of Pyrolysis Temperature on Physico-Chemical Properties of Corn Stover (Zea mays L.) Biochar and Feasibility for Carbon Capture and Energy Balance. PLOS ONE. 11**,** e0156894.
Raheem, A., et al., 2022. Evaluating performance of pyrolysis and gasification processes of agriculture residues-derived hydrochar: Effect of hydrothermal carbonization. Journal of Cleaner Production. 338**,** 130578.
Rajendran, K., et al., Influential Aspects in Waste Management Practices. In: M. J. T. K. B. J. W. A. Pandey, (Ed.), Sustainable Resource Recovery and Zero Waste Approaches, 2019, pp. 65-78.

Rajendran, N., et al., 2021. Recent advances in valorization of organic municipal waste into energy using biorefinery approach, environment and economic analysis. Bioresource Technology. 337**,** 125498.
Raji, F., Pakizeh, M., 2013. Study of Hg(II) species removal from aqueous solution using hybrid ZnCl2-MCM-41 adsorbent. Applied Surface Science. 282**,** 415-424.
Randviir, E. P., Banks, C. E., 2013. Electrochemical impedance spectroscopy: an overview of bioanalytical applications. Analytical Methods. 5**,** 1098-1115.
Riaz, A., et al., 2016. High-yield and high-calorific bio-oil production from concentrated sulfuric acid hydrolysis lignin in supercritical ethanol. Fuel. 172**,** 238-247.
Riva, L., et al., 2021. Considerations on factors affecting biochar densification behavior based on a multiparameter model. Energy. 221**,** 119893.
Robinson, J., et al., 2015. Microwave Pyrolysis of Biomass: Control of Process Parameters for High Pyrolysis Oil Yields and Enhanced Oil Quality. Energy & Fuels. 29**,** 1701-1709.
Rossignolo, J. A., et al., 2017. Improved interfacial transition zone between aggregate-cementitious matrix by addition sugarcane industrial ash. Cement and Concrete Composites. 80**,** 157–167.
Rover, M. R., Analysis of sugars and phenolic compounds in bio-oil. Vol. Doctor of philosophy. Iowa State University, 2013, pp. 134.
S, M. S., Paramasivan, B., 2021. Evaluation of influential factors in microwave assisted pyrolysis of sugarcane bagasse for biochar production. Environmental Technology & Innovation. 24**,** 101939.
S.Bharathiraja, et al., 2017. Production of Enzymes From Agricultural Wastes and Their Potential Industrial Applications. Advances in Food and Nutrition Research. 80**,** 125-148.
S.Mutsengerere, et al., 2019. A review of operating parameters affecting bio-oil yield in microwave pyrolysis of lignocellulosic biomass. Renewable and Sustainable Energy Review. 104**,** 328-336.
Sadh, P. K., et al., 2018. Agro-industrial wastes and their utilization using solid state fermentation: a review. Bioresources and Bioprocessing. 5**,** 1.
Sahoo, D., Remya, N., 2022. Influence of operating parameters on the microwave pyrolysis of rice husk: biochar yield, energy yield, and property of biochar. Biomass Conversion and Biorefinery. 12**,** 3447-3456.
Sainab Omar, S. A., Yang Yang, Jiawei Wang, 2019. Production of renewable fuels by blending bio-oil with alcohols and upgrading under supercritical conditions. Front. Chem. Sci. Eng. . 13**,** 702–717.
Sajjadi, B., et al., 2019. Chemical activation of biochar for energy and environmental applications: a comprehensive review. Reviews in Chemical Engineering. 35**,** 777-815.
Sakhiya, A. K., et al., 2020. Production, activation, and applications of biochar in recent times. Biochar. 2**,** 253-285.
Sant'Anna, M. V. S., et al., 2020. Electrochemical sensor based on biochar and reduced graphene oxide nanocomposite for carbendazim determination. Talanta. 220**,** 121334.
Santhoshkumar, A., Anand, R., 5 - Microwave-assisted fast pyrolysis of hazardous waste engine oil into green fuels. In: K. Azad, (Ed.), Advances in Eco-Fuels for a Sustainable Environment. Woodhead Publishing, 2019, pp. 119-155.
Sarangi, P. K., et al., 2022. Sustainable utilization of pineapple wastes for production of bioenergy, biochemicals and value-added products: A review. Bioresource Technology. 351**,** 127085.
Selvam S, M., Paramasivan, B., 2022. Microwave assisted carbonization and activation of biochar for energy-environment nexus: A review. Chemosphere. 286**,** 131631.
Senthilkumar, K., et al., 2021. Extraction of cellulosic fibres from agricultural waste and its applications. AIP Conference Proceedings. 2387**,** 040003.

Setter, C., et al., 2020. Slow pyrolysis of coffee husk briquettes: Characterization of the solid and liquid fractions. Fuel. 261**,** 116420.
Shahbeig, H., Nosrati, M., 2020. Pyrolysis of municipal sewage sludge for bioenergy production: Thermo-kinetic studies, evolved gas analysis, and techno-socio-economic assessment. Renewable and Sustainable Energy Reviews. 119**,** 109567.
Shanbhag, Y. M., et al., 2022. Direct and Sensitive Electrochemical Evaluation of Pramipexole Using Graphitic Carbon Nitride (gCN) Sensor. Biosensors. 12**,** 552.
Sharma, H. B., et al., 2020. Downstream augmentation of hydrothermal carbonization with anaerobic digestion for integrated biogas and hydrochar production from the organic fraction of municipal solid waste: A circular economy concept. Science of The Total Environment. 706**,** 135907.
Sheng, C. D., Azevedo, J. L. T., 2005. Estimating the higher heating value of biomass fuels from basic analysis data. Biomass & Bioenergy. 28**,** 499-507.
Shi, K., et al., 2020a. Production of H2-Rich Syngas From Lignocellulosic Biomass Using Microwave-Assisted Pyrolysis Coupled With Activated Carbon Enabled Reforming. Frontiers in Chemistry. 8.
Shi, K., et al., 2020b. Production of H2-Rich Syngas From Lignocellulosic Biomass Using Microwave-Assisted Pyrolysis Coupled With Activated Carbon Enabled Reforming. Frontiers in Chemistry 8**,** 1-12.
Shi, K., et al., 2020c. Production of H2-Rich Syngas From Lignocellulosic Biomass Using Microwave-Assisted Pyrolysis Coupled With Activated Carbon Enabled Reforming. Frontiers in Chemistry. 8**,** 1-12.
Shin Ying Foong, N. S. A. L., Rock Keey Liew, Peter Nai Yuh Yek, Su Shiung Lam, 2020. Production of biochar for potential catalytic and energy applications via microwave vacuum pyrolysis conversion of cassava stem. Materials Science for Energy Technologies. 3**,** 728-733.
Shukla, N., et al., 2019. Biochar from microwave pyrolysis of rice husk for tertiary wastewater treatment and soil nourishment. Journal of Cleaner Production. 235**,** 1073-1079.
Si, Z., et al., 2017. An Overview on Catalytic Hydrodeoxygenation of Pyrolysis Oil and Its Model Compounds. Catalysts. 7**,** 169.
Siddique, I. J., et al., 2022. Technical challenges in scaling up the microwave technology for biomass processing. Renewable and Sustainable Energy Reviews. 153**,** 111767.
Sieng-Huat Kong; Su Shiung Lam; Peter Nai Yuh Yek; Rock Keey Liew; Nyuk Ling Ma; Mohammad Shahril Osman; Chee Chung Wong, 2018. Self-purging microwave pyrolysis: an innovative approach to convert oil palm shell into carbon-rich biochar for methylene blue adsorption. Chemical Technology and Biotechnology. 94**,** 1397-1405.
Singh, A., et al., Chapter 7 - Recent advancement in microwave-assisted pyrolysis for biooil production. In: C. M. Hussain, et al., Eds.), Waste-to-Energy Approaches Towards Zero Waste. Elsevier, 2022, pp. 197-219.
Singh, Y. D., 2019. Comprehensive characterization of indigenous lignocellulosic biomass from Northeast India for biofuel production. Sn Applied Sciences. 1.
Sinha, A. K., et al., Agricultural Waste Management Policies and Programme for Environment and Nutritional Security. In: R. Bhatt, et al., Eds.), Input Use Efficiency for Food and Environmental Security. Springer Nature Singapore, Singapore, 2021, pp. 627-664.
Sluiter, A., et al., Determination of Ash in Biomass. Laboratory Analytical Procedure (LAP). National Renewable Energy Laboratory, 2008.
Spanu, D., et al., 2020. Biochar as an alternative sustainable platform for sensing applications: A review. Microchemical Journal. 159.
Sridhar, A., et al., 2021. Conversion of food waste to energy: A focus on sustainability and life cycle assessment. Fuel. 302**,** 121069.
Su, G., et al., 2022a. Pyrolysis of oil palm wastes for bioenergy in Malaysia: A review. Renewable and Sustainable Energy Reviews. 164**,** 112554.
Su, G., et al., 2022b. State-of-the-art of the pyrolysis and co-pyrolysis of food waste: Progress and challenges. Science of The Total Environment. 809**,** 151170.

Sudha, V., et al., 2019. Hierarchical porous carbon derived from waste amla for the simultaneous electrochemical sensing of multiple biomolecules. Colloids Surf B Biointerfaces. 177**,** 529-540.
Sukruansuwan, V., Napathorn, S. C., 2018. Use of agro-industrial residue from the canned pineapple industry for polyhydroxybutyrate production by Cupriavidus necator strain A-04. Biotechnol Biofuels. 11**,** 202.
Sun, J., et al., 2022a. A state-of-the-art review on algae pyrolysis for bioenergy and biochar production. Bioresource Technology. 346**,** 126258.
Sun, K., et al., 2018. Effect of ZnCl2-activated biochar on catalytic pyrolysis of mixed waste plastics for producing aromatic-enriched oil. Waste Manag. 81**,** 128-137.
Sun, Y., et al., 2022b. Tailoring wood waste biochar as a reusable microwave absorbent for pollutant removal: Structure-property-performance relationship and iron-carbon interaction. Bioresource Technology. 362**,** 127838.
Supramono, D., et al., Microwave Pyrolysis of Sugarcane Bagasse for Bio-Oil Production. Conference: Seminar Nasional Teknik Kimia Indonesia 2015. Sustainable Energy and Mineral Processing for National Competitiveness, Yogyakarta, 2015.
Suresh, A., et al., 2021a. Microwave pyrolysis of coal, biomass and plastic waste: a review. Environmental Chemistry Letters. 19**,** 3609-3629.
Suresh, A., et al., 2021b. Microwave pyrolysis of coal, biomass and plastic waste: a review. Environmental Chemistry Letters. 19**,** 3609-3629.
Suriapparao, D. V., et al., 2018. Selective production of phenolics from waste printed circuit boards via microwave assisted pyrolysis. Journal of Cleaner Production. 197**,** 525-533.
Suriapparao, D. V., et al., 2022a. Analysis of pyrolysis index and reaction mechanism in microwave-assisted ex-situ catalytic co-pyrolysis of agro-residual and plastic wastes. Bioresource Technology. 357**,** 127357.
Suriapparao, D. V., et al., 2022b. Microwave co-pyrolysis of PET bottle waste and rice husk: effect of plastic waste loading on product formation. Sustainable Energy Technologies and Assessments. 49**,** 101781.
Suriapparao, D. V., et al., 2021. Optimization of microwave power and graphite susceptor quantity for waste polypropylene microwave pyrolysis. Process Safety and Environmental Protection. 149**,** 234-243.
Suriapparao, D. V., et al., 2015a. Bio-Oil Production from Prosopis juliflora via Microwave Pyrolysis. Energy fuels. 29**,** 2571-2581.
Suriapparao, D. V., et al., 2015b. Bio-Oil Production from Prosopis juliflora via Microwave Pyrolysis. Energy & Fuels. 29**,** 2571-2581.
Suriapparao, D. V., et al., 2020a. Effective deoxygenation for the production of liquid biofuels via microwave assisted co-pyrolysis of agro residues and waste plastics combined with catalytic upgradation. Bioresour Technol. 302**,** 122775.
Suriapparao, D. V., et al., 2020b. Recovery of renewable aromatic and aliphatic hydrocarbon resources from microwave pyrolysis/co-pyrolysis of agro-residues and plastics wastes. Bioresource Technology. 318**,** 124277.
Suttibak, S., et al., 2012. Production of Bio-oil via Fast Pyrolysis of Cassava Rhizome in a Fluidised-Bed Reactor. Energy Procedia. 14**,** 668-673.
Suzanne Anouti, G. H., Maxime Deniel, Anne Roubaud, 2016. Analysis of Physicochemical Properties of Bio-Oil from Hydrothermal Liquefaction of Blackcurrant Pomace. Energy and Fuels, American Chemical Society. 30**,** 398-406.
Tamizhdurai, P., et al., 2017. Environmentally friendly synthesis of CeO2 nanoparticles for the catalytic oxidation of benzyl alcohol to benzaldehyde and selective detection of nitrite. Sci Rep. 7**,** 46372.
Tang, Y.-H., et al., 2020. Microwave-assisted production of CO2-activated biochar from sugarcane bagasse for electrochemical desalination. Journal of Hazardous Materials. 383**,** 121192.

Tawaf Ali, S., et al., Composition and Role of Lignin in Biochemicals. In: S. Associate Prof. Arpit, T. Dr. Jaya, Eds.), Lignin - Chemistry, Structure, and Application. IntechOpen, Rijeka, 2022, pp. Ch. 10.
Teo, E. Y. L., et al., 2019. One-step production of pyrene-1-boronic acid functionalized graphene for dopamine detection. Materials Chemistry and Physics. 231**,** 286-291.
Thiagarajan, S., Chen, S.-M., 2007. Preparation and characterization of PtAu hybrid film modified electrodes and their use in simultaneous determination of dopamine, ascorbic acid and uric acid. Talanta. 74**,** 212-222.
Tomar, Y. Z. M. G. V., 2019. Nanomechanical Raman Spectroscopy in Biological Materials.
Tomczyk, A., et al., 2020a. Biochar physicochemical properties: pyrolysis temperature and feedstock kind effects. Reviews in Environmental Science and Bio-Technology. 19**,** 191-215.
Tomczyk, A., et al., 2020b. Biochar physicochemical properties: pyrolysis temperature and feedstock kind effects. Reviews in Environmental Science and Bio/Technology. 19**,** 191-215.
Toscano Miranda, N., et al., 2021. Sugarcane bagasse pyrolysis: A review of operating conditions and products properties. Renewable and Sustainable Energy Reviews. 149**,** 111394.
Tripathi, M., et al., 2016. Effect of process parameters on production of biochar from biomass waste through pyrolysis: A review. Renewable and Sustainable Energy Reviews. 55**,** 467-481.
Ubiera, L., et al., 2021. Energy optimization of bio-oil production from biomass by fast pyrolysis using microwaves. Reaction Chemistry & Engineering. 6**,** 1884-1899.
Undri, A., et al., Microwave pyrolysis of polymeric materials. Microwave Heating. InTech, Italy, 2011, pp. 208-232.
Varjani, S., et al., 2022. Sustainable management of municipal solid waste through waste-to-energy technologies. Bioresource Technology. 355**,** 127247.
VenkataMohan, S., et al., Algal oils as biodiesel. Biofuels from Algae (Second Edition). Biomass, Biofuels, Biochemicals, 2019, pp. 287-323.
Venkatesh, G., et al., 2022. Characterization of Biochar Derived from Crop Residues for Soil Amendment, Carbon Sequestration and Energy Use. Sustainability. 14**,** 2295.
Villota, N., et al., 2019. Kinetic study of colored species formation during paracetamol removal from water in a semicontinuous ozonation contactor. Science of The Total Environment. 649**,** 1434-1442.
Von Cossel, M., et al., 2021. Comparison of thermochemical conversion and anaerobic digestion of perennial flower-rich herbaceous wild plant species for bioenergy production. Bioresource Technology. 340**,** 125724.
Wainaina, S., et al., 2020. Resource recovery and circular economy from organic solid waste using aerobic and anaerobic digestion technologies. Bioresource Technology. 301**,** 122778.
Wallace, C. A., et al., 2019a. Effect of feedstock and microwave pyrolysis temperature on physio-chemical and nano-scale mechanical properties of biochar. Bioresources and Bioprocessing. 6**,** 33.
Wallace, C. A., et al., 2019b. Effect of feedstock and microwave pyrolysis temperature on physio-chemical and nano-scale mechanical properties of biochar. Bioresources and Bioprocessing. 6.
Wan Mahari, W. A., et al., 2022. Microwave co-pyrolysis for simultaneous disposal of environmentally hazardous hospital plastic waste, lignocellulosic, and triglyceride biowaste. Journal of Hazardous Materials. 423**,** 127096.
Wang, J., et al., 2020a. Conductive Metal-Organic Frameworks for Amperometric Sensing of Paracetamol. Frontiers in Chemistry. 8.
Wang, J., et al., 2020b. Gold nanoparticles decorated biochar modified electrode for the high-performance simultaneous determination of hydroquinone and catechol. Sensors and Actuators B: Chemical. 306**,** 127590.

Wang, L., et al., Techno-Economic Analysis of Microwave-Assisted Pyrolysis for Production of Biofuels. In: Z. Fang, et al., Eds.), Production of Biofuels and Chemicals with Microwave. Springer Netherlands, Dordrecht, 2015, pp. 251-263.
Wang, L., et al., 2020c. Electrostatic repulsion strategy for high-sensitive and selective determination of dopamine in the presence of uric acid and ascorbic acid. Talanta. 210**,** 120626.
Wang, S., et al., 2012. Catalytic conversion of carboxylic acids in bio-oil for liquid hydrocarbons production. Biomass and Bioenergy. 45**,** 138-143.
Wang, W., et al., 2020d. High efficiency pyrolysis of used cigarette filters for ester-rich bio-oil through microwave-assisted heating. Journal of Cleaner Production. 257**,** 120596.
Wang, X., et al., 2021a. An electrochemical immunosensor for the detection of carcinoembryonic antigen based on Au/g-C3N4 NSs-modified electrode and CuCo/CNC as signal tag. Microchimica Acta. 188**,** 408.
Wang, X. Y., et al., 2018. High Quality Bio-oil Production from Catalytic Microwave-assisted Pyrolysis of Pine Sawdust. Bioresources. 13**,** 5479-5490.
Wang, Z., et al., 2021b. Co-pyrolysis of waste plastic and solid biomass for synergistic production of biofuels and chemicals-A review. Progress in Energy and Combustion Science. 84**,** 100899.
Wattanasilp, C., et al., 2021. Techno-Cost-Benefit Analysis of Biogas Production from Industrial Cassava Starch Wastewater in Thailand for Optimal Utilization with Energy Storage. Energies. 14**,** 416.
Wei, Y., et al., 2020. Simultaneous Detection of Ascorbic Acid, Dopamine, and Uric Acid Using a Novel Electrochemical Sensor Based on Palladium Nanoparticles/Reduced Graphene Oxide Nanocomposite. Int J Anal Chem. 2020**,** 8812443.
Welty.;, J., et al., 2007. Fundamentals of momentum, heat and mass transfer. John Wiley & Sons, Inc.
Wu, C., et al., 2014. Conventional and microwave-assisted pyrolysis of biomass under different heating rates. Journal of Analytical and Applied Pyrolysis. 107**,** 276-283.
Wu, H.-Y., et al., 2020a. Assessment of agricultural waste-derived activated carbon in multiple applications. Environmental Research. 191**,** 110176.
Wu, L., et al., 2023. Effects of variable amounts of volatiles in corncob on microwave co-pyrolysis of low-rank coal and corncob. Fuel. 332**,** 126133.
Wu, L., et al., 2022. Biomass hydrogen donor assisted microwave pyrolysis of low-rank pulverized coal: Optimization, product upgrade and synergistic mechanism. Waste Management. 143**,** 177-185.
Wu, P., et al., 2020b. Visualizing the emerging trends of biochar research and applications in 2019: a scientometric analysis and review. Biochar. 2**,** 135-150.
Wu, Z., et al., 2019. Design and optimization of a flexible water-based microwave absorbing metamaterial. Applied Physics Express. 12**,** 057003.
Xin, X., et al., 2021. Transforming biomass pyrolysis technologies to produce liquid smoke food flavouring. Journal of Cleaner Production. 294**,** 125368.
Xiqiang Zhao, J. Z., Zhanlong Song, Hongzhen Liu, Longzhi Li, Chunyuan Ma, 2011. Microwave pyrolysis of straw bale and energy balance analysis. Journal of Analytical and Applied Pyrolysis. 92**,** 43-49.
Xu, Q., et al., 2019. Characteristics and Applications of Sugar Cane Bagasse Ash Waste in Cementitious Materials. Materials. 12.
Xue, Y., et al., 2021. Comparative analysis for pyrolysis of sewage sludge in tube reactor heated by electromagnetic induction and electrical resistance furnace. Waste Management. 120**,** 513-521.
Y. Zhang, P. C., et al., Microwave-Assisted Pyrolysis of Biomass for Bio-Oil Production. Pyrolysis. Mohamed Samer, IntechOpen, 2017, pp. 129-166.
Yahya, S. A., et al., 2021. Techno-Economic Analysis of Fast Pyrolysis of Date Palm Waste for Adoption in Saudi Arabia. Energies. 14**,** 6048.

Yan, L., et al., 2020. ZnCl2 modified biochar derived from aerobic granular sludge for developed microporosity and enhanced adsorption to tetracycline. Bioresour Technol. 297**,** 122381.
Yan, Y., et al., 2021. Synthesis of graphene oxide and graphene quantum dots from miscanthus via ultrasound-assisted mechano-chemical cracking method. Ultrasonics Sonochemistry. 73**,** 105519.
Yang, Q.-L., et al., 2021. Performance of sesame straw cellulose, hemicellulose, and lignin biochars as adsorbents in removing benzo(a)pyrene from edible oil. Food Science and Technology.
Yang, Y., et al., 2018. A techno-economic analysis of energy recovery from organic fraction of municipal solid waste (MSW) by an integrated intermediate pyrolysis and combined heat and power (CHP) plant. Energy Conversion and Management. 174**,** 406-416.
Yaning Zhang, P. C., Shiyu Liu, Liangliang Fan, Nan Zhou, Min Min, Yanling Cheng, Peng Peng, Erik Anderson, Yunpu Wang, Yiqin Wan, Yuhuan Liu, Bingxi Li and Roger Ruan, Microwave-Assisted Pyrolysis of Biomass for Bio-Oil Production. In: M. Samer, (Ed.), Pyrolysis, ntechOpen, 2017.
Yek, P. N. Y., et al., 2020. Engineered biochar via microwave CO2 and steam pyrolysis to treat carcinogenic Congo red dye. Journal of Hazardous Materials. 395**,** 122636.
Yi, Y., et al., 2020. Hierarchically Porous Carbon Microsphere Doped with Phosphorus as a High Conductive Electrocatalyst for Oxidase-like Sensors and Supercapacitors. ACS Sustainable Chemistry & Engineering. 8**,** 9937-9946.
Yoshikawa, N., Mechanism of Microwave Heating of Matter. In: S. Horikoshi, N. Serpone, Eds.), RF Power Semiconductor Generator Application in Heating and Energy Utilization. Springer Singapore, Singapore, 2020, pp. 71-89.
Yu, H., et al., 2022a. Co-pyrolysis of biomass and polyvinyl chloride under microwave irradiation: Distribution of chlorine. Science of The Total Environment. 806**,** 150903.
Yu, X., et al., 2020. Corncob-derived activated carbon for roxarsone removal from aqueous solution: isotherms, kinetics, and mechanism. Environmental Science and Pollution Research. 27**,** 15785-15797.
Yu, Y., et al., 2016. Characterization of Pyrolytic Sugars in Bio-Oil Produced from Biomass Fast Pyrolysis. Energy & Fuels. 30**,** 4145-4149.
Yu, Y., et al., 2022b. Steam explosion of lignocellulosic biomass for multiple advanced bioenergy processes: A review. Renewable and Sustainable Energy Reviews. 154**,** 111871.
Zafar, M. A., et al., 2022. Electrochemical sensing of oxalic acid using silver nanoparticles loaded nitrogen-doped graphene oxide. Carbon Trends. 8**,** 100188.
Zaman, K., et al., 2018. Effect of Particle Size and Temperature on Pyrolysis of Palm Kernel Shell. International Journal of Engineering & Technology. 7**,** 118-124.
Zamfir, L. G., et al., 2020. Advances in Electrochemical Impedance Spectroscopy Detection of Endocrine Disruptors. Sensors (Basel). 20**,** 6443.
Zamorano Ulloa, R., et al., The Interaction of Microwaves with Materials of Different Properties. Electromagnetic Fields and Waves. Kim Ho Yeap and Kazuhiro Hirasawa, IntechOpen, 2019.
Zeng, Y., et al., 2022. Microwave catalytic co-pyrolysis of waste cooking oil and low-density polyethylene to produce monocyclic aromatic hydrocarbons: Effect of different catalysts and pyrolysis parameters. Science of The Total Environment. 809**,** 152182.
Zhang, D., et al., 2019a. Enhanced nitrobenzene reduction by modified biochar supported sulfidated nano zerovalent iron: Comparison of surface modification methods. Science of The Total Environment. 694**,** 133701.
Zhang, Q., et al., 2022a. Sustainable production of gluconic acid and glucuronic acid via microwave-assisted glucose oxidation over low-cost Cu-biochar catalysts. Green Chemistry. 24**,** 6657-6670.
Zhang, S., Xiong, Y., 2016. Washing pretreatment with light bio-oil and its effect on pyrolysis products of bio-oil and biochar. RSC Adv. 6**,** 5270-5277.

Zhang, W., et al., 2018. Electrochemical sensing platform based on the biomass-derived microporous carbons for simultaneous determination of ascorbic acid, dopamine, and uric acid. Biosensors and Bioelectronics. 121**,** 96-103.
Zhang, X., et al., 2022b. Microwave biochars produced with activated carbon catalyst: Characterization and sorption of volatile organic compounds (VOCs). Science of The Total Environment. 827**,** 153996.
Zhang, X. S., et al., 2017a. An overview of a novel concept in biomass pyrolysis: microwave irradiation. Sustainable Energy & Fuels. 1**,** 1664-1699.
Zhang, Y., et al., Microwave-Assisted Pyrolysis of Biomass for Bio-Oil Production. In: M. Samer, (Ed.), Pyrolysis. IntechOpen, 2017b, pp. 129-166.
Zhang, Y., et al., 2017c. Effects of feedstock characteristics on microwave-assisted pyrolysis – A review. Bioresource Technology. 230**,** 143-151.
Zhang, Y., et al., Gasification Technologies and Their Energy Potentials. In: M. J. T. o. W. i. B. A. Pandey, (Ed.), Sustainable Resource Recovery and Zero Waste Approaches, 2019b, pp. 193-206.
Zhang, Y., et al., 2020. Fast microwave-assisted pyrolysis of wastes for biofuels production – A review. Bioresource Technology. 297**,** 122480.
Zhang, Y., et al., 2022c. A review of biochar prepared by microwave-assisted pyrolysis of organic wastes. Sustainable Energy Technologies and Assessments. 50**,** 101873.
Zhang, Y., et al., 2022d. Influence of corn straw on distribution and migration of nitrogen and heavy metals during microwave-assisted pyrolysis of municipal sewage sludge. Science of The Total Environment. 815**,** 152303.
Zhao, L., et al., 2022. Advances in pretreatment of lignocellulosic biomass for bioenergy production: Challenges and perspectives. Bioresource Technology. 343**,** 126123.
Zhao, Z., et al., 2021. Selective Production of Phenol-Rich Bio-Oil From Corn Straw Waste by Direct Microwave Pyrolysis Without Extra Catalyst. Frontiers in Chemistry. 9.
Zhou, J., et al., 2018. Development and application of a continuous fast microwave pyrolysis system for sewage sludge utilization. Bioresource Technology. 256**,** 295-301.
Zhou, N., et al., 2021. Catalytic pyrolysis of plastic wastes in a continuous microwave assisted pyrolysis system for fuel production. Chemical Engineering Journal. 418**,** 129412.
Zhu, Q.-L., et al., 2021. Bioenergy from dairy manure: technologies, challenges and opportunities. Science of The Total Environment. 790**,** 148199.
Zi, W., et al., 2019a. Pyrolysis, morphology and microwave absorption properties of tobacco stem materials. Science of The Total Environment. 683**,** 341-350.
Zi, W., et al., 2019b. Pyrolysis, morphology and microwave absorption properties of tobacco stem materials. Sci Total Environ. 683**,** 341-350.

APPENDIX A

Figure A1: Actual microwave pyrolysis systems and their components.

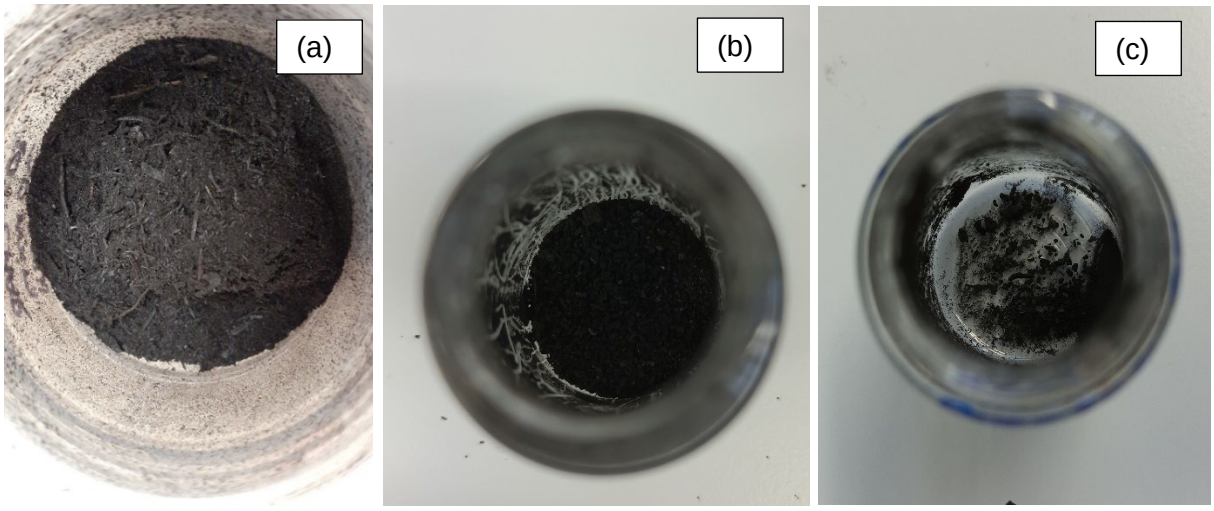

Figure A2: (a) H_2SO_4 activated SCB-biochar, (b) pineapple peel $ZnCl_2$- activated biochar, and (c) banana peel biochar-based graphene oxide.

Figure A3: Sugarcane bio-oil obtained from microwave pyrolysis in data chapter 3.

Figure A4: Sugarcane biogas collected in vacuum tubes from microwave pyrolysis in data chapter 3.